UM-HSRI-78-51

INVESTIGATION OF THE INFLUENCE OF VARIOUS BRAKING REGULATIONS ON ACCIDENT-AVOIDANCE PERFORMANCE

MVMA Project #4.31

Final Technical Report

M. Sayers

L. Segel

November 1978

Highway Safety Research Institute
The University of Michigan
Ann Arbor, Michigan 48109

Technical Report Documentation Page

1. Report No.	2. Government Accession No.	3. Recipient's Catalog No.
UM-HSRI-78-51		

4. Title and Subtitle	5. Report Date
Investigation of the Influence of Various Braking Regulations on Accident-Avoidance Performance	November 1978
	6. Performing Organization Code
7. Author(s) M. Sayers and L. Segel	8. Performing Organization Report No. UM-HSRI-78-51
9. Performing Organization Name and Address Highway Safety Research Institute The University of Michigan Huron Parkway & Baxter Road Ann Arbor, Michigan 48109	10. Work Unit No. 361512 11. Contract or Grant No. MVMA Proj. #4.31 13. Type of Report and Period Covered Final 7/1/77-10/31/78
12. Sponsoring Agency Name and Address Motor Vehicle Manufacturers Association 300 New Center Building Detroit, Michigan 48202	14. Sponsoring Agency Code

15. Supplementary Notes

16. Abstract Passenger car braking regulations promulgated by the United States and various European countries are analyzed to determine the incompatibilities in brake proportioning that derive from the performance requirements of the regulations. Two vehicles, one produced in the U.S. and the other in Europe, with extreme loading conditions (as derive from option selection and vehicle loading) were considered. The analysis shows that the European regulations require a larger forward bias in brake proportioning than FMVSS 105-75. Computer simulations were used to predict the differences in braking performance which result from proportioning the example vehicles to comply with the different regulations. Conditions of straight-line braking, braking in a turn, and three surface friction levels were considered. In general, both vehicles were capable of achieving shorter stopping distances when proportioned to meet FMVSS 105-75 than when proportioned to comply with the European regulations, but the differences were small and could be considered trivial when a car is driven by an ordinary driver. When proportioned to meet FMVSS 105-75, the rear wheels of the two study cars sometimes locked up first, a result that the European regulations are designed to prevent. Braking-in-a-turn test procedures (which have been discussed both in the U.S. and abroad) were also studied through computer simulations and found to be relatively insensitive to the fore-aft proportioning of brake torques.

17. Key Words	18. Distribution Statement
Braking, Standards, Braking in a Turn, Simulation, Stopping Distance, Impact Velocity, Friction	UNLIMITED

19. Security Classif. (of this report)	20. Security Classif. (of this page)	21. No. of Pages	22. Price
NONE	NONE		

TABLE OF CONTENTS

1.0 INTRODUCTION

The proliferation of vehicle performance regulations to the international community has resulted in a variety of braking performance requirements among North American and European countries. These regulations are influenced by different opinions on good braking and handling performance so that they are to some extent incompatible with each other. As a result, it may be necessary for some manufacturers to modify brake proportioning on vehicles intended for export. In addition to the problem with regulation of straight-line braking performance, the U.S. government and various European organizations (ISO) are actively pursuing methods for measuring and regulating braking-in-a-turn performance. Advocates of braking-in-a-turn requirements say that this is a more precise tool for controlling brake proportioning that may be somewhat more representative of a realistic driving situation. Some of the advocates perceive braking-in-a-turn requirements as a replacement for some of the straight-line braking tests; however, it is more likely that these maneuvers would be added to the present requirements rather than substituted.

This study provides a set of analyses which serve to illustrate the distinctions between braking performances implied by the various regulations over a broad range of conditions, covering vehicle configuration, loading, road surface, and braking maneuver types.

The study was divided into three main tasks, which are documented in Sections 2.0, 3.0, and 4.0 of this report.

Section 2.0 presents an overview of the various regulations in terms of their requirements on proportioning. Although each regulation covers several facets of braking performance and, frequently, is applicable to several vehicle types, only the requirements on the stopping or deceleration performance of passenger cars, with non-failed and partially failed systems, are considered here. Whereas radically different approaches towards certification have been

adopted in the various countries, we consider here only the technical aspects of the regulations. Two representative passenger cars, one domestic and one European, are selected to demonstrate the constraints on brake proportioning which are imposed by the various regulations. Available option packages and permissible loading conditions are considered for each vehicle in order to select two option/load combinations which will limit to the greatest degree the proportioning range allowed by each regulation. The range of proportioning permitted by each regulation is calculated by means of a quasi-static analysis. In order to compare the constraints imposed on proportioning selection by the different regulations, one proportioning value is picked to best satisfy the U.S. regulation, and another to best satisfy the various European regulations.

Section 3.0 attempts to answer the question "Which regulatory philosophy leads towards better accident-avoidance capability?" To this end, a computer simulation of braking maneuvers is used to calculate the braking performance of the two representative vehicles in each of the two most extreme option/load combinations (as determined by quasi-static analysis). The maneuvers include straight-line braking and braking in a moderate constant radius turn on three surfaces exhibiting high, medium, and low frictional properties. Each condition is simulated for the proportioning selected to best comply with FMVSS 105-75 and for the proportioning selected to satisfy the European regulations (as determined in Section 2.0). Results are presented in terms of the distance necessary to reduce the vehicle speed to an arbitrary velocity and in terms of the impact velocity which results if stopping distance is limited. Steady-state deceleration levels and the changes in reaction time needed to compensate for the differently proportioned vehicle in each case are also presented.

The activities of agencies within the United States and Europe towards developing a braking-in-a-turn regulation are reviewed and analyzed in Section 4.0. Testing procedures are hypothesized from

the previous work done by the agencies involved and, when necessary, further computer simulations are conducted to evaluate any further constraints on proportioning selection which might be imposed by a braking-in-a-turn regulation.

2.0 AN ANALYSIS TO COMPUTE BRAKE PROPORTIONING VALUES WHICH SATISFY EXISTING REGULATIONS

This section reviews the braking regulations used throughout the world, and quantifies the proportioning constraints which they impose on brake design for passenger cars. A quasi-static analysis is used to directly compare the range of proportioning which each standard permits for the case of two vehicles, one being a "typical" domestically-produced car and the other being a "typical" European car. When all possible option packages and loading conditions are considered, the braking standards of Europe require a slightly higher proportioning than the proportioning which would be selected to comply with the U.S. standard. The regulations are contrasted by selecting one proportioning value to maximize the likelihood of passing the U.S. standard and another value to best comply with the European standards. This is done for both representative passenger cars. The relative highway "safety" which results from the selection of a proportioning value to comply with each of the different regulations is then determined by conducting a large number of computer simulations of braking conditions not covered by the regulations. This activity is described in Section 3.0.

Throughout this report, the term "proportioning" refers to the ratio of the brake torque applied at the front axle to the total brake torque applied at both axles. The characteristics of the various components which comprise the total brake system are superfluous to the intent of this study. Accordingly, the various mechanicale components are considered to define a "black box," for which a given pedal force will repeatedly provide front and rear brake torques having known magnitudes.

The term "braking efficiency" is often used in this section, and in this context, efficiency is defined as the ratio of the limit (no locked wheels) deceleration to an ideal deceleration, where the car is "optimally" proportioned for a given surface, such that the

tires are all producing braking forces that are the maximum levels which can be obtained for the surface conditions. If the available friction were a constant, μ, the braking efficiency would simply be A_x/μ, where A_x = deceleration in g's.

2.1 An Overview of the Existing Regulations

The various world braking regulations have been reviewed, discussed, and compared extensively [1,2,3,4], so the focus of this study is on just two questions: "How do the various brake regulations restrict front/rear proportioning selection on typical passenger cars?" and "Which regulations lead to passenger cars with better accident-avoidance capabilities?" The various braking regulations will be discussed here only in the context of these two questions and thus we will be dealing with small portions of a few selected standards.

In a broad review of existing brake standards, Oppenheimer [1] categorizes the existing regulations into the braking standards of:

(a) United States
(b) Europe
(c) Sweden
(d) Japan
(e) Other

The braking regulation of the United States, FMVSS 105-75, has been a model for regulations in Canada and Australia. Most of the European regulations are modeled after the United Nations Economic Commission for Europe (ECE) Regulation 13, or are national approvals of a regulation that is nearly identical in technical content, the Common Market European Economic Community (EEC) Directive 71/320 (updated by Directives 75/524 and 74/132). Sweden has its own standard, Regulation F-18, and Japan is in the process of developing an independent national standard. According to Oppenheimer, all of

the major braking standards of the world are currently represented by the four regulations listed above, which comprise the first three categories.

The braking standards of the United States, Europe, and Sweden have many important similarities and contrasts, particularly within the scope of this study. The standards reflect different philosophies towards what kind of performance constitutes good braking and utilize some different means of implementation.

Many of the differences in the processes of achieving certification under the regulations FMVSS 105-75, ECE R.13, 71/320/ECE, and F-18 are discussed by Oppenheimer [1], with the details to be found in the regulations themselves [5,6,7,8]. It is useful here to simplify the situation by reducing the total number of certification processes to two types, namely, a "testing" type (in which a representative vehicle is tested by an authorized agency according to the provisions of the regulation) and a "non-test" type (wherein the manufacturer submits engineering data to the proper agency). "Testing" procedures are identified as being more demanding than "non-test" processes because, not only is the engineering design being checked, but also the manufacturing quality control and time-varying characteristics of vehicle components (such as brake lining properties). When designing for a regulation involving physical testing, a manufacturer typically allows for different sorts of imprecisions; in this study, a tolerance of 10% is used repeatedly.

The four braking standards all require stopping distance or deceleration limits which are verified by testing a candidate vehicle. The requirements of these standards are summarized in Table 1 which also shows 90% target stopping distances and equivalent decelerations for each regulation. The equivalent decelerations shown in the table were calculated after assuming that the vehicle deceleration starts at zero, increases linearly to a time Δt, then remains constant for the duration of the stop. The "equivalent deceleration" is the constant value reached after time Δt and is

Table 1. Target Stopping Distance and Deceleration Capabilities from the Collected Standards.

Standard	Test	Loading	Velocity (mph)	Stopping Distance (ft)	90% of Stopping Distance (ft)	Equivalent Deceleration (g's)
USA	2nd Effectiveness	GVWR	30 60 80	54 204 383	48.6 183.6 344.7	.795 .744 .678
	3rd Effectiveness	Lightly Laden	60	194	174.6	.787
	1st & 4th Effectiveness	GVWR	30 60 80 100	57 216 405 673	51.3 194.4 362.7 605.7	.746 .697 .641 .587
EEC & ECE	Type 'O'	Lightly Laden & GVWR	49.7	166.2	149.6	.628
EEC, ECE, Sweden	Retardation	Lightly Laden & GVWR	49.7	.592 g's specified, + 10% =		.651

calculated via the relationship

$$A_x = \frac{V \cdot \Delta t/2 - S + \sqrt{S^2 \mp V \cdot \Delta t \cdot S + V^2 \cdot \Delta t^2/3}}{g \cdot \Delta t^2/12} \qquad (2.1)$$

where V is the initial velocity (ft/sec), S is the specified stopping distance (ft), and g is the gravitational constant (ft/sec^2). To prepare the table, the rise time, Δt, was defined to be 0.5 second.

The stopping distance and deceleration performance measures of the four standards can be directly compared by referring to Table 1, although the effects of differing surface conditions and testing procedures are not accounted for. The deceleration levels calculated from FMVSS 105-75, the U.S. regulation, are clearly the most demanding.

Although the European regulations are seen to require less deceleration capability, they contain additional provisions aimed at preserving the stability of the vehicle and thus reflect a different philosophy as to what constitutes "good braking." In general, comparing the different regulations is like comparing "apples and oranges" and cannot be done unless specific vehicles are used as examples. The remainder of this section outlines the methodology developed to do this comparison, which is then demonstrated for a typical U.S. and European passenger car.

2.2 A Quasi-Static Analysis of Braking

As indicated, the braking standards of the U.S., ECE, EEC, and Sweden have sufficiently different formats and philosophies that they cannot be directly compared. On the other hand, a quasi-static analysis of braking can be used to calculate proportioning constraints for a particular vehicle, based on the provisions of any of the four standards. A quasi-static analysis involves only the fore/aft load transfer in a vehicle during braking to give adhesion utilization values for the front and rear axles for a given deceleration

level and a given proportioning. The adhesion utilization values, K_F and K_R, for the front and rear axles represents the braking forces between the tire and the road, normalized by the vertical loads on the tires and are calculated as:

$$K_F = \frac{p \cdot A_x}{(1 - a/\ell + h/\ell \cdot A_x} \tag{2.2}$$

$$K_R = \frac{(1-p) \cdot A_x}{(a/\ell - h/\ell \cdot A_x)} \tag{2.3}$$

where p is proportioning (as defined earlier), A_x is deceleration (in g's), a/ℓ is the longitudinal distance between the center of gravity (c.g.) of the vehicle and the front axle divided by the wheelbase, and h/ℓ is the ratio of the height of the c.g. of the vehicle divided by the wheelbase of the vehicle. It is assumed in Equations (2.2) and (2.3) that none of the wheels are locked, that the braking force at each axle is equal to the brake torque divided by the rolling radius of the tire, and that the rolling radii of all of the tires are equal. Equations (2.2) and (2.3) can be used to compare all of the braking standards in the case of a particular vehicle if it is assumed that the brakes on the vehicle are sufficiently powerful and fade resistant to lock up any wheel on dry pavement with a reasonable pedal force application. If this is the case, the only variable is the front/rear proportioning, p, which must be set to keep K_F and K_R within limits specified, or implied, by the various braking standards. When K_F and K_R are not specified, but a deceleration level or stopping distance is specified, the implied constraint is that K must be less than the available traction, as expressed by the friction coefficient between the tire and the road.

Accordingly, the four main braking regulations are summarized below in terms that make use of Equations (2.2) and (2.3) and in terms of figures which graphically show the proportioning constraints imposed by the separate regulations. On these figures, deceleration

constitutes the abscissa, since it is specified directly much of the time and when it is not, stopping distance (which depends on initial velocity) can be used to calculate an equivalent deceleration with the aid of Equation (2.1).

2.3 Summaries of the Various Regulations

The following summaries deal only with those portions of the regulations which pertain to the required performance of the vehicle when braked with the service brake fully operational, or to the performance required during a partial failure (divided circuit test). Other aspects of braking system performance such as fade, water recovery, and power-boost failure, to name a few, are beyond the scope of this study but can, in general, be easily compared by referring directly to the regulations.

2.3.1 FMVSS 105-75. The United States regulation [5] requires stopping distance tests to be performed on "a 12-foot-wide, level roadway having a skid number of 81." For a non-antilock-equipped vehicle, "stops are made without lockup of any wheel at speeds greater than 10 mph." All of the non-failed stopping distance requirements were listed in Table 1, along with the "equivalent deceleration" levels calculated for 90% stopping distances and a .5-second build-up time for the deceleration. This type of test result is influenced primarily by the maximum torque levels supplied by the brakes and by the available tire traction. Assuming that the brakes are capable of providing high torque levels, the traction capabilities of the tires directly limit the performance of the vehicle, although the proportioning determines the braking efficiency.

The adhesion utilization, K, of the front and rear axle is shown as a function of deceleration and proportioning in Figure 1 for the case of an American intermediate-sized car which is in the 105-75 "lightly-loaded" condition, where

> "Lightly loaded vehicle weight" means: For vehicles with a GVWR of 10,000 lb or less, unloaded vehicle weight plus 300 lb (including driver and instrumentation)..."

The curves of constant K are used to locate proportioning boundaries for various possible levels of tire-road frictional capabilities, as indicated by the friction coefficient, μ. For example, if $\mu = .80$, the proportioning must be very close to 73% to achieve a deceleration of .79 g (see Table 1) with no lockup. If the proportioning were set at p = 70%, we can see that K_F (the adhesion utilization of the front axle) would be .75 but that K_R would be .90. The rear axle would try to generate more longitudinal force than is available with $\mu = .8$, and the wheels would lock up. If, however, $\mu = .95$, the 70% proportioning would be permissible. With $\mu = .95$, the quasi-static analysis defines a "proportioning window," extending from p = 68% to p = 88%, such that any proportioning within this "window" will yield a .79 g deceleration with no wheel lockup.

Tire traction limits are known to be sensitive to the vertical load on the tire. Consequently, assuming that μ_F (friction available at the front tires) equals μ_R (friction available at the rear tires) can lead to errors in choosing the correct values of K_F and K_R. For example, the dry-asphalt traction data compiled for the tires installed on the American intermediate car (Table 3 on page 27) give values of $\mu_F = 1.03$ and $\mu_R = 1.11$, at the normal loads produced by this car in a .79 g deceleration. Thus, on dry asphalt the applicable proportioning "window" is indicated in Figure 1 by the heavy black lines. This window, as shown, is for one option package and loading condition. Since the standard is applied to all possible option packages at both GVWR and light loading, the proportioning "windows" must be considered for each combination. The final "window" for the car model is defined by the overlap of all of the "windows" applicable to specific option and loading combinations.

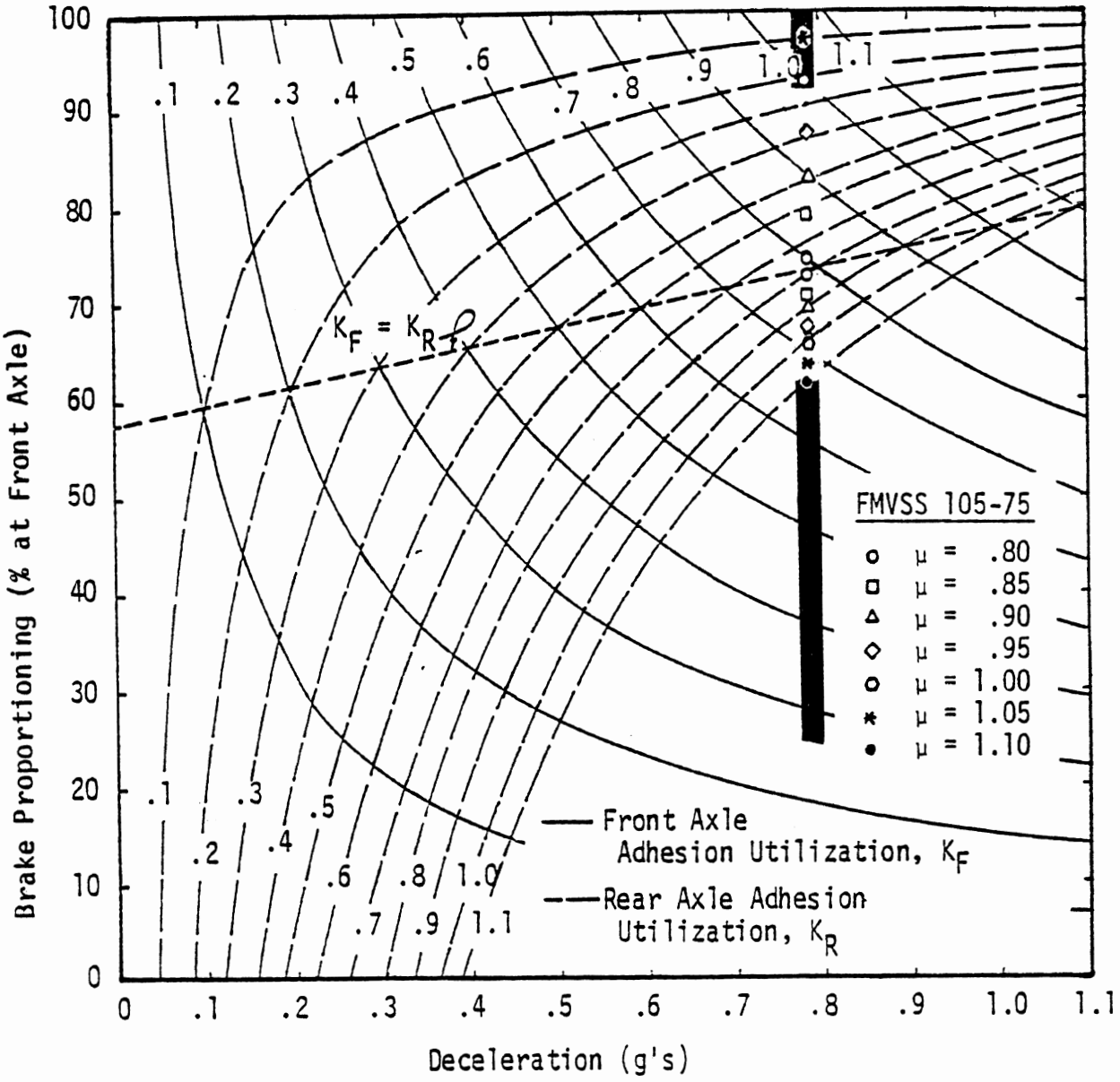

Figure 1. The use of adhesion utilization curves to determine the "proportioning window" imposed by FMVSS 105-75 for the case of a particular vehicle-loading condition.

The partial failure test, namely, one circuit is disabled, is performed on the same surface at both load conditions, but wheel lockup is allowed. The stopping distance must not exceed 456 feet. A 90% target stopping distance is thus 410.4 feet, and the "equivalent deceleration," calculated from Equation (2.1), is 0.31 g's. The adhesion utilization required for the case of a front/rear brake circuit split can easily be seen in Figure 1, for when the rear circuit is failed, the proportioning is 100% and when the front circuit is failed, the proportioning is 0%. For the example vehicle under discussion, we see that when the rear circuit is failed, the value of K_F at p = 100% should be about .49 and when the front circuit is failed, $K_R \cong .82$. Both of these utilizations apparently do not exceed the friction available on a surface having a skid number of 81, thus a front/rear split should be adequate for meeting the partial failure requirements of 105-75.

2.3.2 Europe: ECE R.13 and 71/320/EEC. The Common Market regulation 71/320 [7] is nearly identical to the United Nations ECE R.13 [6] in the technical aspects, and unless noted otherwise, terms and phrases cited below are excerpted from 71/320/EEC. The European regulations specify stopping distances given that "the road shall possess a surface having good adhesion." They further require that during the test, the required stopping distance "must be obtained without the wheels locking, without the vehicle leaving its path and without abnormal vibrations." The light loading condition is defined as the "unladen vehicle with only the driver on board and possibly one other person seated, if possible, on the front seat..."

A proportioning "window" based on a target deceleration level of 0.65 g's (see Table 1) is shown in Figure 2 for the same vehicle and loading condition considered in Figure 1. This "window" has been determined and plotted in the same manner as the "window" for FMVSS 105-75 (see Figure 1). The bounds on proportioning applicable to the European stopping distance requirement are, clearly, much wider than is the case for the U.S. requirement, in view of the lower deceleration requirement called out in 71/320/EEC.

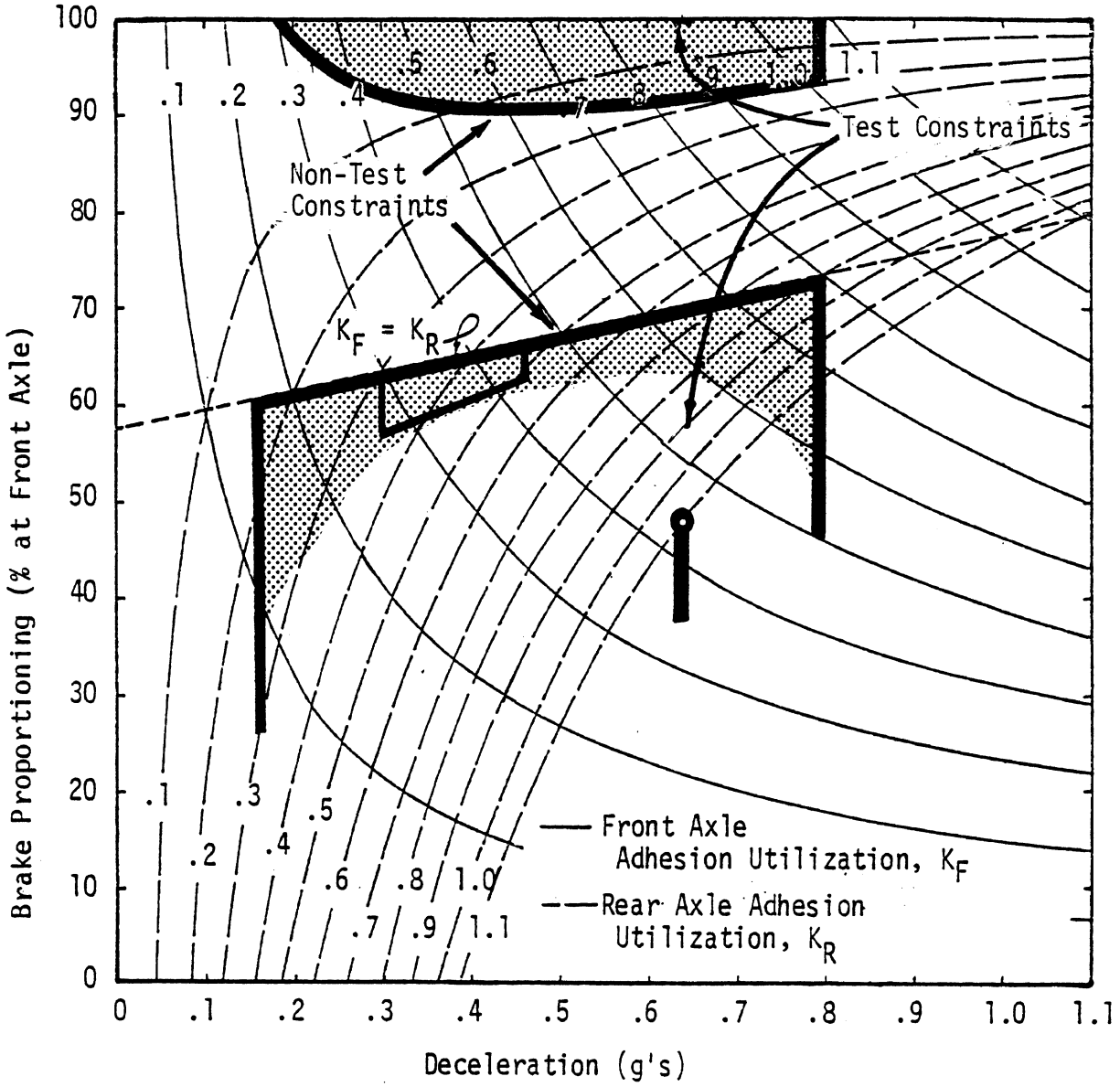

Figure 2. Proportioning constraints imposed by 71/320/EEC, for the case of a particular vehicle-loading condition.

Although the U.S. and the European regulations both include a specification on wheels-unlocked stopping distance, a significant departure from the form of 105-75 is found in 71/320/EEC—namely, the latter also contains a "nontest" requirement which is satisfied by the submission of engineering data by the vehicle manufacturer. These data consist of plots of adhesion utilization (K) versus deceleration (A_x) which are calculated according to Equations (2.2) and (2.3). The regulation requires that these curves meet the following two conditions, which conditions are plotted in Figure 3 as they appear in the regulation, namely:

1) $A_x \geq 0.1 + .85(K_F - .2)$

2) $K_F > K_R$

Note that the second condition implies that $K_R < A_x$ (as shown in the figure), since Equations (2.2) and (2.3) require that if K_R is less than A_x, K_F must be greater than A_x, and vice-versa. In the regulation the first condition technically refers to K in general, but since $K_F > K_R$, the limit is for K_F as shown.

For purposes of this study, we must ask how these "nontest" conditions (or limits) act as constraints on proportioning. In order to transform these "nontest" limits on adhesion utilization into constraints in the proportioning/deceleration space, we combine these constraints with Equations (2.2) and (2.3) to obtain the following relationships:

$$p > 1 - a/\ell + h/\ell \cdot A_x \qquad (2.4)$$

$$p < \left(\frac{A_x - 1}{.85} + .2\right) \cdot (1 - a/\ell + h/\ell \cdot A_x)/A_x \qquad (2.5)$$

where again a/ℓ is the longitudinal distance between the front axle and the center of gravity (c.g.) of the vehicle, divided by the wheelbase, and h/ℓ is the height of the c.g. of the vehicle divided by

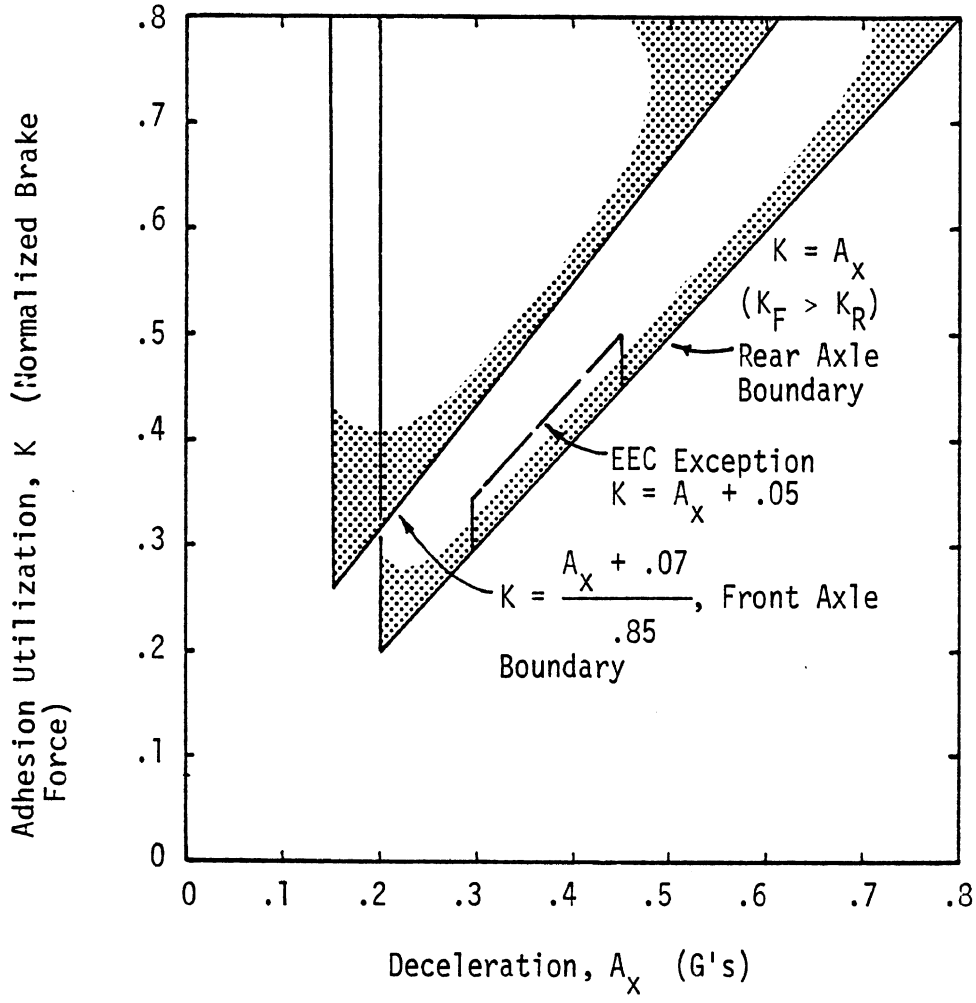

Figure 3. Adhesion Utilization Boundaries for the ECE and EEC Brake Regulations.

the wheelbase. The proportioning boundaries yielded by Equations (2.4) and (2.5) have been plotted on Figure 2 and we see that the "nontest" constraints restrict the allowable proportioning much more than the stopping distance criterion.

The dashed line in Figure 3 indicates the only applicable difference between the EEC and ECE regulations, namely, the former regulation permits the adhesion utilization of the rear axle to be greater than that of the front (although K_R is still limited by the function $A_x + .05$) over the range $.03 < A_x < .45$. This difference between 71/320/EEC and ECE R.13, in terms of proportioning requirements, is also shown in Figure 2. It should be noted that this small difference is unimportant in the context of this study. It is mentioned only for reasons of completeness.

The adhesion utilization limits are calculated per the regulations with a quasi-static analysis using Equations (2.4) and (2.5). In order to provide the engineering curves per the regulation, the manufacturer must define proportioning as a function of deceleration, and thus assume a value for the braking force/line pressure gain at each axle. But this gain depends on the brake lining friction which is known to vary significantly under different operating conditions. Thus differing curves could be prepared for one vehicle by making different (yet valid within proper contexts) assumptions regarding the lining friction. Nevertheless, the "paper regulation" is treated as real, for this study, to help establish in an ideal sense which of the various regulations leads to better highway safety.

The partial failure test is identical to the service brake test with respect to initial speed, road surface, and vehicle loading. The required stopping distance, however, is 306.2 feet rather than 166.2 feet. Thus the 90% target distance is 275.6 feet and for an initial velocity of 49.7 mph and an assumed time delay of .5 second, the equivalent deceleration, A_x, is .32 g's. This requirement is seen to be slightly more demanding than the requirement in 105-75, but again, the required stopping distance should be physically realizable, given normal tire traction capabilities on dry surfaces.

2.3.3 Sweden, F-18. The Swedish regulation F-18 [8] is a test-oriented regulation, as is 105-75, but there the similarities end. The performance requirement to be met by the non-failed service brakes is written as follows:

> 4.1.12.1 The brake system shall be so arranged that with any loading condition within the framework of the total permitted load or guaranteed axle pressure, and with the load uniformity distributed over the loading area, no wheel will lock at retardations lower than those prescribed in 4.1.15.1 and 4.1.16.1, when braking on a carriageway having a coefficient of friction of 0.8. For vehicles with a total weight of maximum 3,500 Kg, there is also the condition that at a retardation between 5.8 and 8.0 in/sec^2 the rear wheels shall not lock before the front wheels.

The required retardation (deceleration) with no wheels locked is .592 g's for a passenger car.

There are several interesting features in F-18 which warrant discussion. For example, regulation F-18 allows the test agency to test the vehicle "with any loading condition within the framework of the total permitted load....with the load uniformly distributed over the loading area" instead of limiting the tests to a light and a GVWR loading, as do the other regulations. However, this provision should not amount to much actual difference, as the loading condition which results in the lowest braking efficiency is typically one of the two extreme conditions, namely, driver only (light loading when the rear axle has the greatest tendency to lock) and GVWR (when the front axle has the greatest tendency to lock).

The second departure of F-18 from other regulations is the specification of a "carriageway having a coefficient of friction of .8." This specification is not a theoretical assumption, but an actual test condition. The procedure involves wetting the track (this act, in itself, is a major departure from the other regulations, which call for testing on dry pavement), measuring the tire-road friction

coefficient, μ_p, at optimal slip (found by varying the brake torque on the test wheel until the maximum μ value is measured), and if necessary, changing the water depth until the μ_p readings are within .05 of the specified value of .8. (Readings are taken at 5-meter intervals, and the reference tire used to establish the specified test condition is the ASTM E249-14 tire which is no longer the standard tire in the U.S.) On one hand, this condition gives the best idea of what to expect in terms of available friction since it is peak friction, μ_p, that is physically measured. On the other hand, the correlation between measurements made with the ASTM tire and those made with a normal passenger car tire is usually not very good. The problem at hand is to estimate the maximum friction (μ_p) available for a passenger car tire, given that μ_p = .8 for an ASTM E249-14 tire. This estimation is not possible unless tire tests are designed and conducted with the intent of answering this particular question. For lack of any data, we will assume below that μ_p = .8 for the tires on the vehicle being tested. We shall also assume that the tire-road friction coefficient is not load sensitive (not true, but the nature of the load sensitivity varies considerably with tires and operating conditions), and that the effect of velocity on friction coefficient is negligible. (This latter assumption can be justified by noting that if the wheels do not lock, the frictional limits are not exceeded and braking force is limited by the applied brake torque. While tire traction on a wet surface is very sensitive to velocity, the friction is the lowest at the velocity at which the stop is initiated and will only go up as the vehicle slows. If a wheel locks because too much pedal force is applied, the lockup should occur shortly after the stop is initiated when the velocity has not decreased significantly. Thus the friction coefficient which exists at the initial velocity should be adequate to predict lockup and thus determine the brake torque levels which define the "limit" condition.)

The third important condition in the Swedish standard is that the order of wheel lockup is as much a criterion for certification as

deceleration capability. Since the order of wheel lockup is found through road testing, manufacturing tolerances should be considered. Brake proportioning, defined by the relationship

$$p = \frac{T_F}{T_F + T_R} \tag{2.6}$$

(where T_F and T_R are the front and rear brake torques which result from a given pedal force) can be thought of as a design proportioning subject to error as a result of actual torques being different from the desired torques. Thus, we can write that

$$p(1+\varepsilon_p) = \frac{T_F(1+\varepsilon_F)}{T_F(1+\varepsilon_F) + T_R(1+\varepsilon_R)} \tag{2.7}$$

where T_F, T_R, and p are now the design values of front torque, rear torque, and proportioning, and ε_F, ε_R, and ε_p are the corresponding errors. By rewriting Equation (2.7), the proportioning error can be expressed as:

$$\varepsilon_p = \frac{(\varepsilon_F-\varepsilon_R)(1/p - 1)}{\varepsilon_F - \varepsilon_R + (1+\varepsilon_R)/p} \tag{2.8}$$

The final difference between F-18 and the other standards is that F-18 does not specify stopping distances, but instead specifies a deceleration level. Therefore, the reaction time of the vehicle is not critical and, clearly, there is no need to calculate any "equivalent decelerations."

The proportioning boundaries imposed by F-18 on the example American intermediate-sized car (at light loading) are sketched in Figure 4. The error tolerances for the front and rear brake torque gains were set ±10% with the signs set to the worst case for each boundary. (That is, if braking performance is limited by impending lockup of the front axle, ε_F is assumed to be +10%, while ε_R is

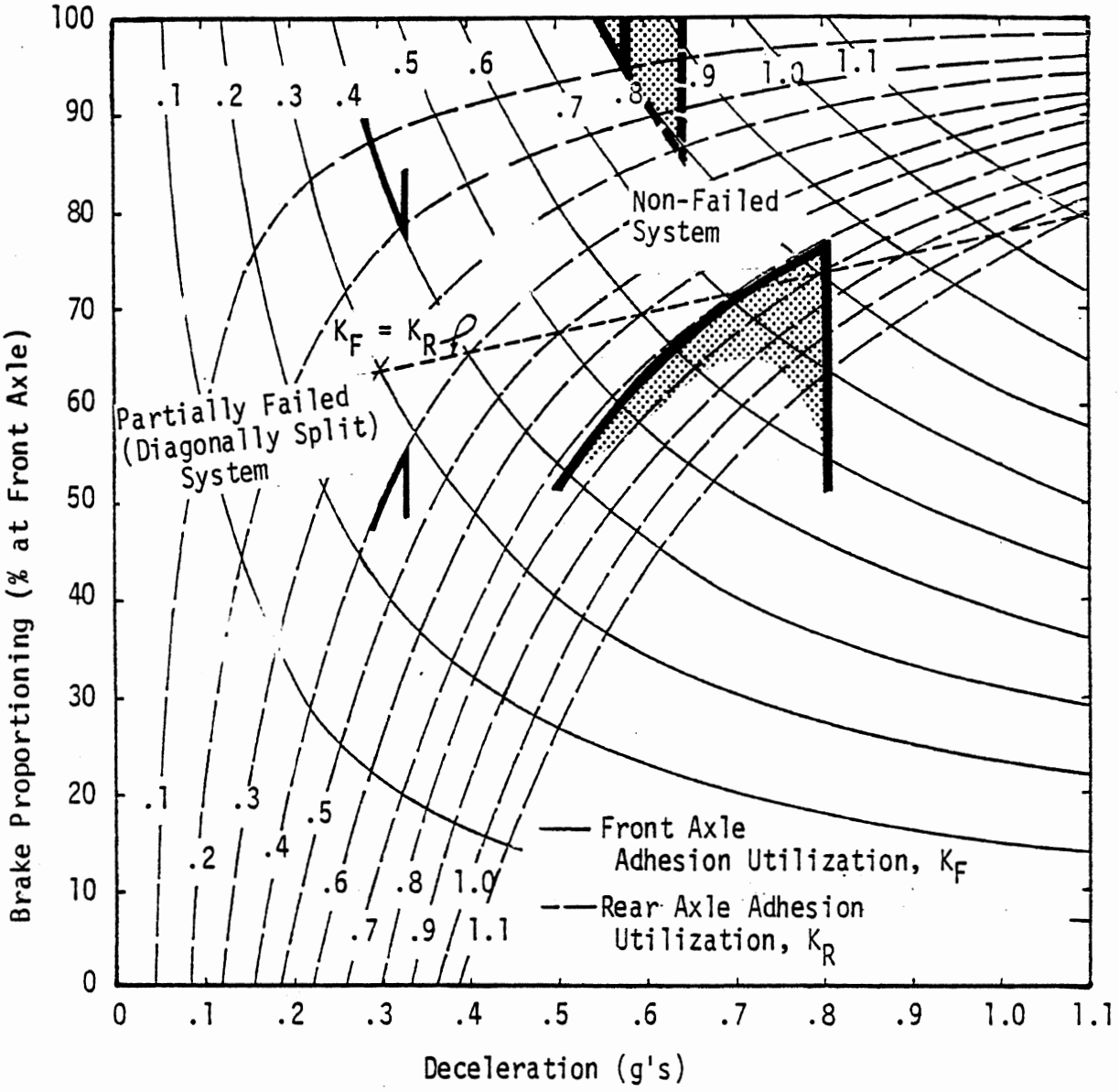

Figure 4. Proportioning constraints imposed by the Swedish regulation, F-18, for a particular vehicle-loading condition.

assumed to be -10%. The actual proportioning is then greater than the design proportioning by the amount ε_p, calculated from Equation (2.8). And if performance is limited by impending rear axle lockup, the signs are reversed to ε_F = -10% and ε_R = +10%.) Without tolerances on torque gain, the lower boundary would follow the K_R = .8 adhesion utilization curve exactly to satisfy the requirement that the rear axle not lock first. When the error tolerances are included via Equation (2.8), the boundary falls above the K_R = .8 curve. The upper boundary similarly follows the K_F = .8 curve, with an adjustment for the proportioning tolerance up to the deceleration which is specified for no wheel lockup. The solid line is for the limit A_X = .59, which is the value given in the standard, and the dashed line is for A_X = .65, which is the target value that includes a 10% margin of safety, as per Table 1. Note that, in deriving the proportioning boundaries required to satisfy F-18, two tolerances are employed: a 10% increase in A_X and assumed ±10% errors in the brake torque gains. In discussing FMVSS 105-75, we only used one tolerance since the order in which wheels lock is not specified by the standard. Since F-18 requires that the rear wheels not lock before the front wheels at decelerations between 5.8 and 8.0 m/sec^2, the lower proportioning boundary is extended to A_X = .82 g's. If, however, the available friction is only μ_p = .80, as we have assumed, this lower boundary need only be extended to A_X = 0.8.

A comparison of Figures 1, 2, and 4 reveals the proportioning constraints imposed by F-18 to be more restrictive than those imposed by 105-75 or 71/320/EEC (ECE R.13), but it must be emphasized that the assumptions which are behind Figure 4 are more numerous than the assumptions behind the other two figures, and often somewhat arbitrary as noted in the preceding discussions.

The partial failure test requires a retardation to be achieved which is 50% that of the full service system. No mention, however, is made of wheel lockup. Thus, the required deceleration is A_X = .296, which, with a 10% margin, becomes A_X = .326. This deceleration level

is only slightly higher than the requirements of 105-75 and 71/320/EEC. However, F-18 is a much tougher performance standard because the surface is wetted to achieve a .8 coefficient of friction, whereas the other tests are conducted on dry surfaces likely to exhibit higher values of μ_p.

The performance of a front/rear circuit split is estimated from Figure 4 by considering p = 0% (front circuit failure) and p = 100% (rear circuit failure), as was done earlier in the examination of 105-75. At p = 100%, Figure 4 shows that at A_x = .33 the adhesion utilization, K_F, of the front tires is .5, which is well under the available friction, namely, μ_p = .8. However, when p = 0%, the necessary adhesion utilization of the rear tires is .9, a level higher than μ_p. Thus, the vehicle manufacturer must either (1) install tires capable of achieving an adhesion of .9 on the test surface prescribed in F-18, (2) use a different type of split for the emergency hydraulic circuit, or (3) be willing to forego the assumed 10% safety margin, since at A_x = .30, the required utilization is only 0.8, a utilization that should be attainable.

The performance of a diagonally split hydrualic brake circuit can also be estimated from Figure 4. The adhesion utilization curves shown were prepared by dividing the braking force at each wheel by the normal force when fore-aft load transfer is due to a constant deceleration. Since the normal forces depend only on deceleration, the same curves apply to the condition of only one wheel per axle applying braking force if the values of adhesion utilization which are shown in the figure are doubled to account for the fact that the braking wheels must apply twice as much force to reach a deceleration level than they do during a non-failed stop. The proportioning boundaries for this type of brake line split when partially failed are shown in Figure 4, at $A_x \leq .33$, along the line labeled K = .4, to correspond to the friction coefficient value of .8. If one of the two braking wheels is allowed to lock, a higher deceleration level

might be achievable if the loss in braking force due to lockup is less than the increase in braking force at the unlocked wheel, which is due to the higher pedal force.

2.4 Proportioning Constraints Which are Imposed by the Various Regulations on Two Representative Vehicles

Two "representative" vehicles, namely, a typical American passenger car and a typical European car, were selected in this study to evaluate the limits on those proportioning values which satisfy the various regulations. The methodology employed is that outlined in the preceding section.

The representative American vehicle is the 1978 Chevrolet Monte Carlo and the representative European vehicle is the Volkswagen Golf.

For each of the two representative vehicles, there are two combinations of options and loading for which the braking efficiency is the most compromised. These are:

1) A lightly loaded car equipped with many options which add weight to the front end. The front brakes cannot be fully utilized because the relatively unloaded rear wheels would lock prematurely.

2) A heavily loaded car equipped such that the gross axle weight rating (GAWR) for the rear axle is highest relative to that of the front axle.

Overall vehicle weight is also a factor in deceleration performance since tire traction decreases with increasing load.

The selection of options for the Golf was straightforward since there are few of them and only one set of gross axle weight rating (GAWR) exists. In the case of the Monte Carlo, the GAWR are unique for each option combination, so several candidate combinations were chosen and GAWR data were obtained from the manufacturer for each one.

After receiving the GAWR data, the "worst case" was identified. The "worst cases," as determined for the two representative passenger cars, are indicated in Table 2.

Table 3 presents data which define the limit traction exhibited by the tires that are installed on the Monte Carlo and the Golf. The peak friction coefficient, μ_p, is shown as a function of load. Appendix A contains a discussion of these data and their sources.

The proportioning boundaries imposed by each of the regulations discussed above are given in Figure 5 for the intermediate-sized American car. All of the lower boundaries apply to one of the "worst case" option/load combinations, while the upper boundaries are for the other "worst case." A comparison of Figure 5 with Figures 1 through 4 reveals the extent to which the "proportioning windows" become smaller when "worst cases" are considered.

The "window" defined by FMVSS 105-75 depends on the available traction, which is a function of the tire and road surface properties. Figure 5 shows limits for various μ values, so that the tire data can be used to determine the proportioning value which would do the bst job of insuring that the car can pass the road tests required by 105-75. The load on each front wheel during a .79 g deceleration would be 1380 lbs for the car with no options at GVWR loading, while the load on each rear wheel, for the lightly loaded car with all of the front-end options, would be 500 lbs at the same deceleration. Table 3 does not list any loads lower than 800 lbs, but a large amount of data compiled for this size and construction of tire [9] indicates that the difference in μ for loads of 500 lbs and 1400 lbs would be about .12. A proportioning value of p = 68% would be optimal if the friction coefficient at the rear axle is higher than that of the front axle by .12, and thus 68% was selected as the "American Proportioning" to be used for subsequent computer simulations.

Table 2. Parameter Values for Two Representative Passenger Cars.

Origin	Domestic				European			
Options	None, Base Vehicle		5.0 V8, A/C, Auto, Power Windows, Console, AM/FM/TP, Power Seat, etc.		4 dr., Sun Roof, R. Window Washer		Auto, Passive Seat Belts	
Loading	300 lb	GVWR	300 lb	GVWR	300 lb	GVWR	300 lb	GVWR
Static Front Load (lb)	1894	2069	2143	2344	1333	1454	1285	1454
Static Rear Load (lb)	1547	2249	1597	2245	752	1302	830	1302
c.g. height/wheelbase (h/ℓ)	.20	.20	.20	.20	.22	.23	.22	.23
Normalized Front Axle Load ($1-a/\ell$)	.55	.48	.57	.51	.64	.53	.61	.53
"Worst Case"	No	Yes	Yes	No	No	Yes	Yes	Yes

Table 3. Friction Coefficients on Dry Asphalt for Tires Installed on the Two Representative Vehicles.

Vehicle	Tire Size	Load (lbs)	μ_p
Domestic	P205/70R-14	800	1.11
		1368	1.03
		1716	.99
		2060	.89
Foreign	155SR-13	384	1.00
		588	.94
		793	.88
		994	.83
		1195	.81

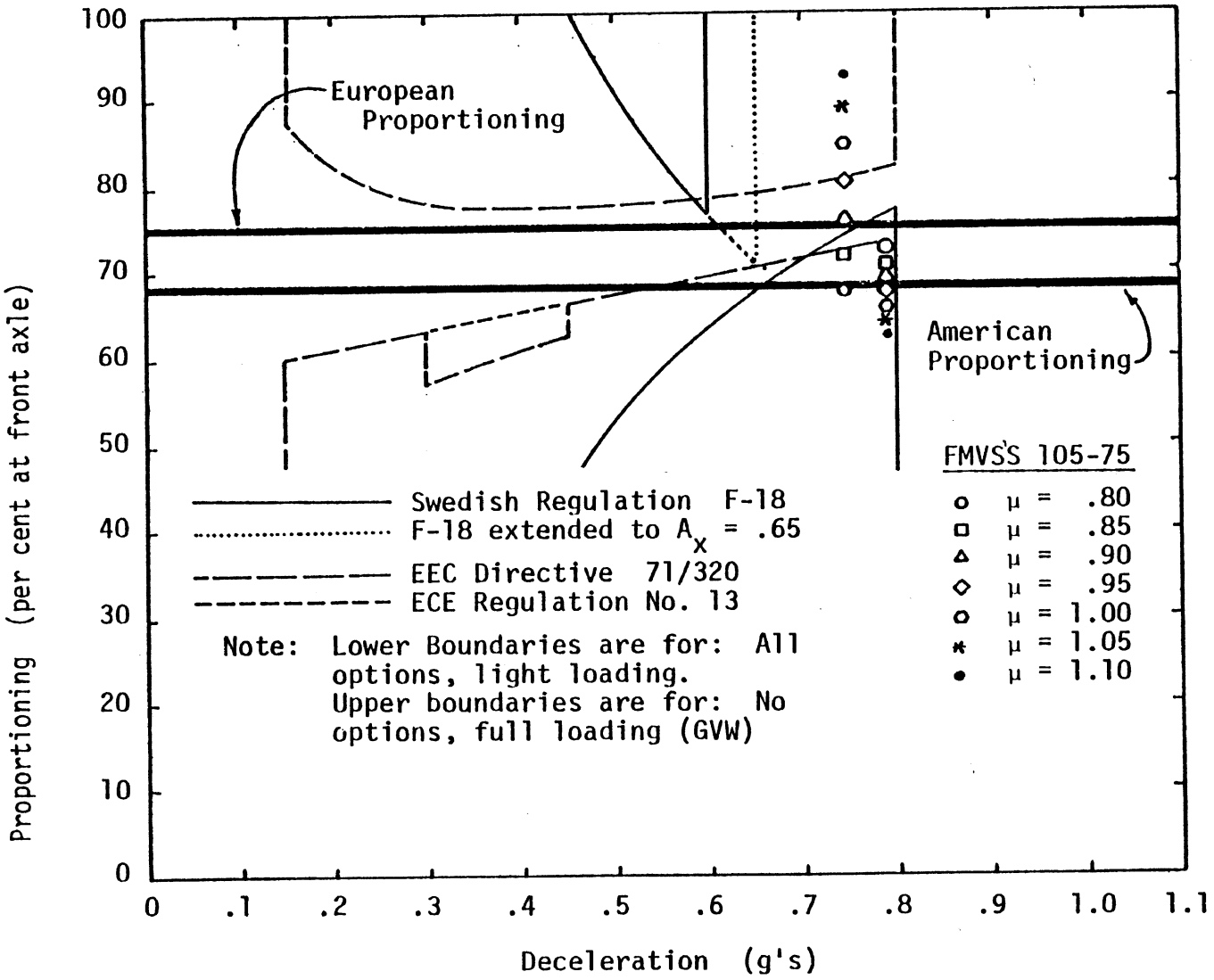

Figure 5. Proportioning Boundaries Imposed by Various Braking Regulations on an American Intermediate Sized Passenger Car.

The European regulation 71/320/EEC (ECE R.13) is best satisfied by a proportioning value of p = 75%. The boundaries due to the Swedish regulation F-18 overlap, as shown in the figure, with p = 75% being a value that minimizes the degree to which the proportioning boundaries are violated.

The partial failure condition was discussed in Section 2.3 for the "most severe case," which is the car equipped with many options and lightly laden. It was noted that a front/rear split might not be adequate to pass F-18 because the available friction at the rear axle during the failed-fronts test must be μ_p = .80 to achieve the deceleration level required by F-18 and must be μ_p = .90 to achieve 110% of the required level. If a diagonal split were employed in the circuit, the proportioning could not be greater than p = 67% for the adhesion utilization of the front tire to be 0.80 (for the car with no options and loaded to the GVWR). If the pedal force is increased until the front wheel locks, the rear wheel can provide more braking force up to a limit determined by μ_p. The deceleration, A_x, is then

$$A_x = \frac{a/\ell(\mu_p-\mu_s) + \mu_s}{2 - 2 \cdot h/\ell(\mu_p-\mu_s)} \tag{2.8}$$

If A_x is specified, Equation (2.8) can be rewritten as

$$\mu_s = \frac{2 \cdot A_x - \mu_p(a/\ell - h/\ell \cdot A_x)}{1 - a/\ell + h/\ell \cdot A_x} \tag{2.9}$$

For the case at hand, A_x = .33, μ_p = .8, a/ℓ and h/ℓ are given in Table 2, and we have the condition that if μ_s > .54, a reasonable assumption, the F-18 partial failure test can be passed.

Figure 6 illustrates the proportioning constraints applicable to the European subcompact car. All of the preceding discussion of the non-failed requirements for the domestic car also apply here.

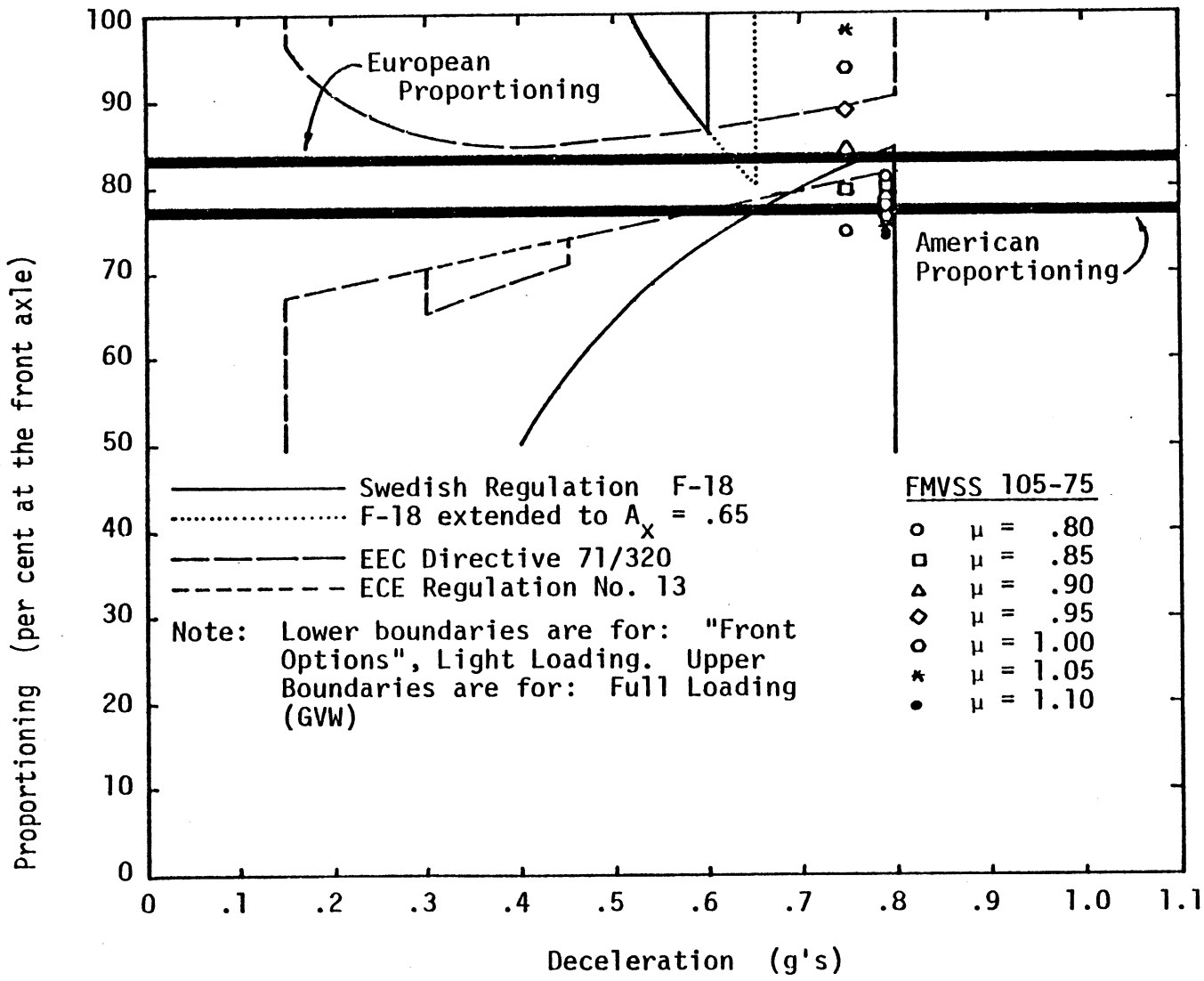

Figure 6. Proportioning Boundaries Imposed by Various Braking Regulations on a European Subcompact Passenger Car.

Regarding the partial-failure test condition, it turns out (again) that only the Swedish test imposes much of a restriction. For the diagonal split of the European car, the most severe condition is that of GVWR loading when, to keep the adhesion utilization of the front wheel less than .80, the proportioning must be less than 74%. To achieve the required .33 g deceleration, the front could be locked and must have a sliding friction coefficient of μ_s = .55. (Note that a front/rear split would not be adequate for passing any of the regulations with the front brakes disabled because the extremely forward position of the c.g. in the lightly loaded condition would require an unrealistically high traction capability from the rear tires.)

Although the regulations of the U.S. and Europe reflect different philosophies towards what constitutes "good" braking performance, they actually impose similar constraints on proportioning selection. FMVSS 105-75 requires a proportioning which gives a high braking efficiency, for either light or GVWR loading, on a high friction surface (and deceleration levels near .8 g's). Efficiency is at a maximum for the lightly loaded vehicles at a deceleration level lower than .8 g's, and at a maximum for the GVWR loaded vehicle at a deceleration level that is higher than .8 g's. But on lower friction surfaces, where high deceleration levels are impossible because of the low tire traction capabilities, braking efficiency is much lower for either loading condition because the adhesion available at the rear axle is not well utilized. The European regulations require a slightly higher proportioning in order to prevent lockup of the rear axle at any deceleration up to .8 g's. (Thus the adhesion available at the rear axle is always under-utilized.) Braking efficiency would be at a maximum for the lightly loaded vehicle at a deceleration level near .8 g's and at a higher deceleration level for the GVWR loading. Efficiency on low friction surfaces is lower, slightly more so than for the proportioning selected to best comply with 105-75.

One might justifiably argue that the differences between the United States and European regulations which affect the resulting proportioning constraints are not significant enough to require a separate proportioning for vehicles sold in the U.S. and Europe. Reasons might be given for raising the value of the "American Proportioning" and for lowering the "European Proportioning" level, although the selection of one proportioning value would certainly reduce the probability of passing each regulation by some margin. Since the overall purpose of this study is to investigate the effect that the different regulations (and the philosophies behind them) have on braking performance and safety, two values of proportioning are used for making a comparison.

At this point, it should be noted that more complicated proportioning functions were considered than the constant proportioning discussed up until now. These proportioning functions were still "fixed," in that they did not vary with load, but did vary with pedal force. Figure 7 illustrates a general, non-constant function. Although the curves shown are those of braking torque versus line pressure, the line pressure magnitude is not needed to define the proportioning function if the y-axis intercept, T_0, and the ratio of the two slopes, a/b, are known for the portion of the curve which is being considered. The weight of the vehicle, W, defines the total braking force needed to achieve a given deceleration, and the rolling radius of the tires, R, translates the force levels into braking torque levels (assuming no locked wheels). The proportioning is then calculated from the total torque needed to achieve the given deceleration and the parameters T_0 and a/b according to the relation

$$p(A_x) = \frac{W \cdot R \cdot A_x - T_0}{W \cdot R \cdot (1+a/b) \cdot A_x} \qquad (2.10)$$

If a/b is less than unity, the proportioning function is "progressive" because the proportioning increases with A_x.

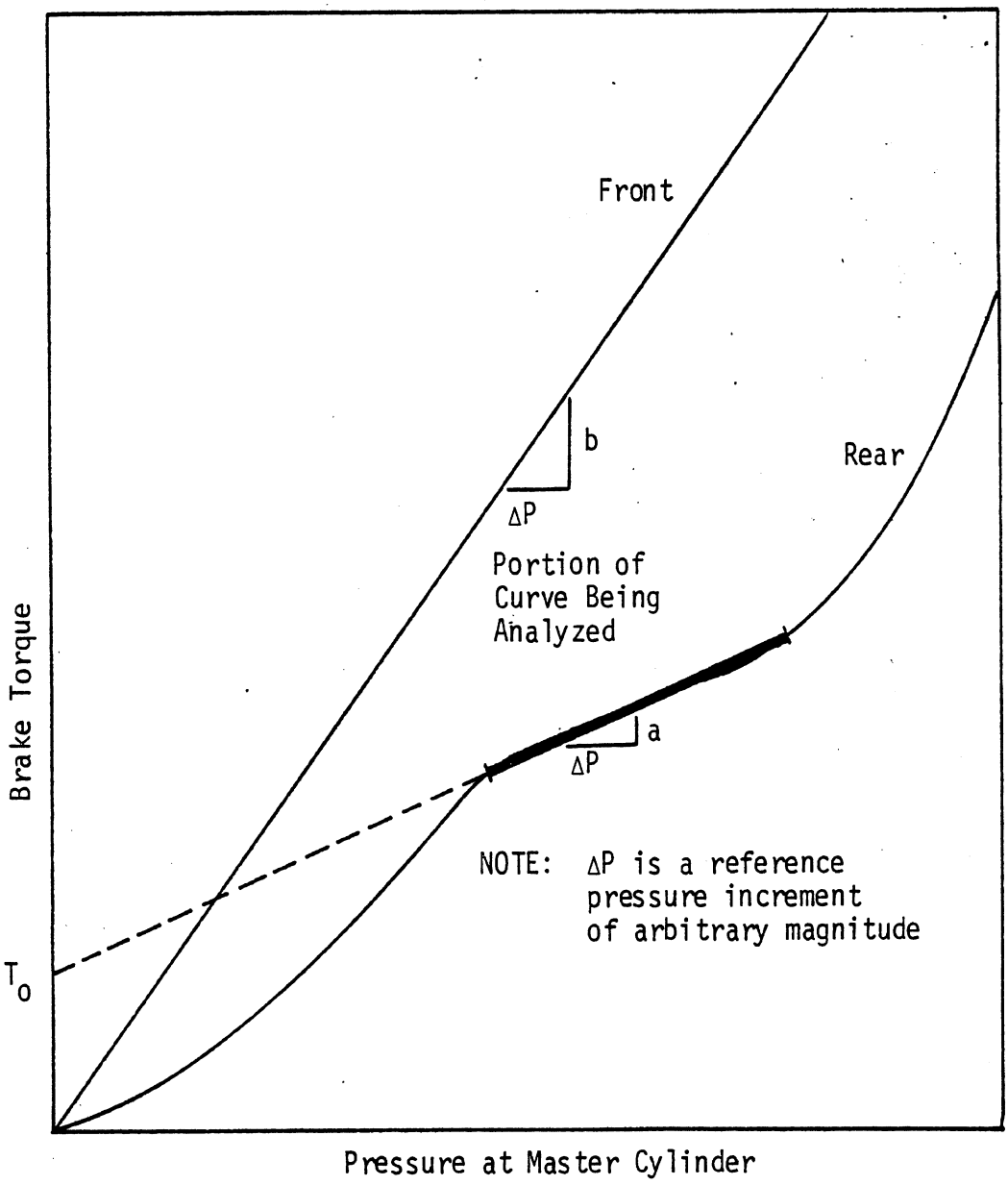

Figure 7. Analytic representation of a fixed, but non-constant, proportioning function.

The "progressive" proportioning system undoubtedly results in higher braking efficiency over a range of decelerations when a particular loading condition is considered. These gains are mitigated when a variety of loading conditions are considered, however, because increasing the payload (in either representative car) increases the brake torque levels needed to achieve a given deceleration, resulting in a higher proportioning (see Eq. (2.10)), and at the same time, shifts the c.g. to the rear of the vehicle such that the proportioning should be lowered to maintain constant braking efficiency.

For example, with the representative domestic car and the most "progressive" case of a/b = 0, where the torque on the rear axle is held constant for increasing pressure, T_o can be set for the p and A_x values that define the lower limit on proportioning imposed by F-18. This point is A_x = .82, p = 77%. For R = 12 in., W = 3740 lb (car with many options, lightly loaded), Equation (2.10) gives a value of T_o = 8464 in·lb. Using this value at A_x = .65, where the upper constraint occurs, we have p = 71%. However, since the upper boundary is for GVWR load, the value of W = 4318 lb should be used to calculate p and the resulting value is p = 75%. Thus the use of a more sophisticated hydraulic set-up to utilize a progressive proportioning system only gains 2% in the allowable proportioning range between the lower constraint for the lightly laden, heavily equipped car at A_x = .82, and the GVWR loaded vehicle, with no options, at A_x = .65. Constant values of proportioning (i.e., T_o = 0) were used in this study because:

1) The progressive proportioning function would reduce to a constant value at lower deceleration levels and there would be no justification for using a different value for the U.S. and European regulations over the lower-to-mid deceleration levels. A comparison of the relative safety resulting from the different regulations would not be possible.

2) The increase in the allowable proportioning range, 2% for the domestic car at best (a/b = 0), is not enough to justify the added complexity when the only design goal is assumed to be certification under a braking regulation.

3.0 A STUDY OF BRAKING PERFORMANCE UNDER CONDITIONS NOT ADDRESSED IN EXISTING REGULATIONS

In the previous section, the braking standards existing within the United States and Europe were found to make conflicting demands on the fore-aft proportioning of brake torque. Further, an examination of the European and U.S. standards showed that different regulatory philosophies underly their respective development. Having addressed the topic of their basic incompatibility, the purpose of this section is to seek answers pertaining to the question, "Which regulatory philosophy leads to overall better accident-avoidance capability?"

To facilitate the calculations (simulations) performed to address the above stated question, two proportioning settings were selected for each vehicle which would maximize the likelihood of each to comply with the U.S., European, and Swedish standards. For assumed conditions of loading and surface, straight-line and in-a-turn braking simulations are conducted. Each vehicle is simulated with each of the selected proportioning values, thereby facilitating direct comparisons. This procedure requires a large number of simulations which employ tire-vehicle system models that have been previously mechanized into a computer code.

3.1 Methodology of Study

The braking conditions selected for simulation are listed in Table 4. Each condition includes a number of runs because (1) two proportionings are used and (2) the brake line pressure must be varied by trial and error in order to establish limit conditions. Note that the loading conditions are identical to hose analyzed in Section 2.0. Three surfaces with high, medium, and low frictional properties are assumed to be representative of the friction conditions to be encountered in the real world. The straight-line and in-a-turn braking conditions are defined by the values of initial lateral acceleration

Table 4 Matrix of Non-Test Braking Conditions to be Simulated

Surface Condition	Vehicle Type	Loading Condition	Initial Lateral Acceleration For Constant Radius Turn (g's)
High friction (dry asphalt	Domestic	Light (Many options)	0 .2 .4
		GVWR (base-no options)	0 .2 .4
	European	Light (some front end options)	0 .2 .4
		GVWR	0 .2 .4
Medium friction (wet asphalt)	Domestic	Light	0 .2 .4
		GVWR	0 .2 .4
	European	Light	0 .2 .4
		GVWR	0 .2 .4
Low (polished, wet surface)	Domestic	Light	0 .2
		GVWR	0 .2
	European	Light	0 .2
		GVWR	0 .2

given in the table. A steering controller (see below) is added to the simulation since it is assumed that the driver is braking on a turn with a fixed radius. The initial velocity is 40 mph, although stopping distances which would be accrued at speeds other than 40 mph can be calculated from other variables that are calculated during the simulations.

The computer program used in this study was developed at HSRI during an earlier study of vehicle behavior [10]. It is based on a fourteen-degree-of-freedom model of the motor car and includes a pneumatic tire model of sufficient complexity that accurate predictions of shear forces can be generated under combined cornering and braking conditions. Both models are reviewed, in qualitative terms, in Appendix A which also lists and discusses the sources of the parameter data which are required as input.

As noted above, a simulation of braking on a constant-radius path requires that an automatic controller be added to the vehicle model. Since the braking performance, as simulated, depends to a large degree on the characteristics of the controller, these characteristics are discussed here in some detail.

The findings to be discussed below relate to vehicle behavior, as opposed to the driver control behavior. Thus, the automatic controller adopted to implement the simulation is in no way intended to simulate the actions of a driver, but rather to evaluate the braking-in-a-turn performance of the vehicle when navigating a constant-radius turn. The controller added to the vehicle model is conceptually simple and easy to implement. It employs a feedback signal, as illustrated in Figure 8, which is the path deviation of a point lying on the longitudinal axis of the vehicle located C_ℓ feet in front of the c.g. of the car body. A proportional-integral-derivative (PID) control scheme is used such that the intended steer angle (that is, not including deflection-steer or compliance-steer effects) at the road can be expressed as:

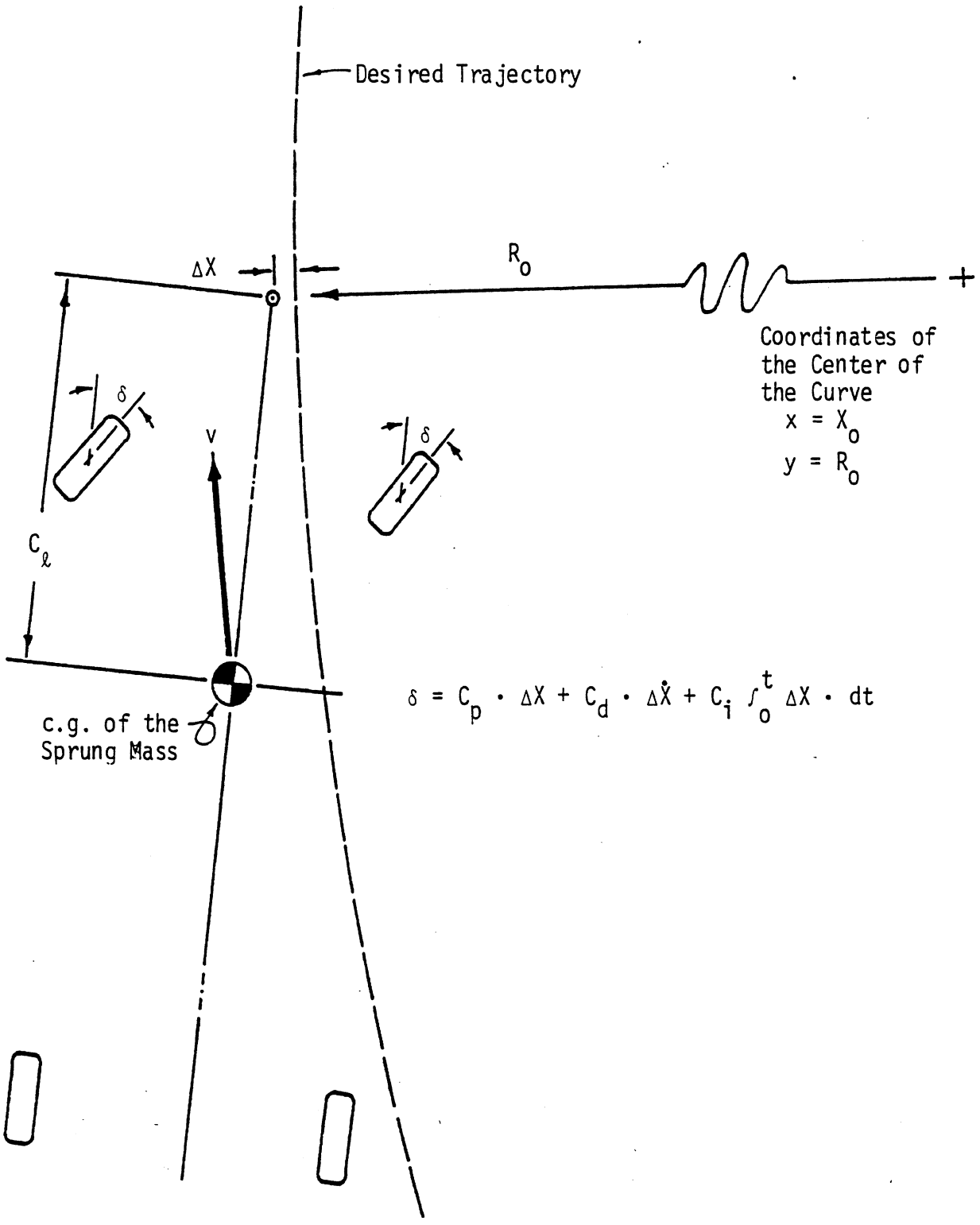

Figure 8. Geometry of the automatic controller which was adopted to maintain a constant radius turn.

$$\delta = C_p \cdot \Delta x + C_d \cdot \Delta \dot{x} + C_i \cdot \int_0^t \Delta x \cdot dt \qquad (3.1)$$

where Δx is the path deviation as shown in the figure, and C_p, C_d, and C_i are feedback gains. In general, derivative feedback is used to speed up the response of a system, at the expense of steady-state accuracy, while integral control is used to improve the steady-state accuracy, at the expense of response time and stability. It was found that the steady-state errors were small during simulated cornering maneuvers, so C_i was set at zero.

This controller scheme exhibits both advantages and disadvantages when it is compared to the human controller. On one hand, a human driver can predict the behavior of the vehicle and steer it by considering both its total current state and the expected transient response to a particular steering effort. The degree to which the driver can predict the vehicle response, and sense its current state, reflects the skill and experience of the driver. The automatic controller works with very limited input—only the deviation and its derivative (and possibly its integral) of a single point from the correct path—and then processes the information in a crude and simple fashion. These drawbacks in the automatic controller are somewhat mitigated because the controller is very fast (with no limit on the steer rate), accurate, and absolutely repeatable. On noting that the braking-in-a-turn simulations are not to establish precise magnitudes of vehicle performance indices, but rather to compare the performance of two differently proportioned vehicles, we can be reasonably assured that the controller is adequate to maintain desired vehicle trajectories within the context of this study.

A study of limit braking performance requires precise definitions of the term "limit." For physical testing activities, the limit condition is reached in straight-line braking when an increase in pedal force would result in lockup of the wheels on one axle. When braking in a turn, the limit is reached when an increase in pedal force would result in an uncontrollable vehicle which plows out or spins out.

However, it was found that simulated limit conditions were easily identified by the above criteria only when braking on the assumed medium or low friction surfaces. In these latter two cases, a wheel would reach a large longitudinal slip ratio and the longitudinal shear force decreased sufficiently for the wheel to lock and stay locked. On the high friction surface, however, the identification of the "limit" condition is not so clear. The drop in longitudinal force with large slip ratios was not as pronounced and the shear force often remained large enough to keep the wheel from locking completely, or if it did lock, to subsequently unlock and return to a moderate slip ratio. During straight-line stops, it was noted that an increase in line pressure caused an increase in the maximum slip ratio at one axle, right up to a short lockup. Further increases in line pressure would result in a lengthier time of lockup, but at no pressure levels were dramatic changes in performance noted. Regarding the braking-in-a-turn simulations, it was noted that an increased line pressure caused an increased maximum deviation of the vehicle from the intended path, and thus an increase in the maximum steer angle produced by the controller.

In general, the transition from a condition which was clearly sublimit to one where an axle remained locked for one second or more was smooth and gradual on the high friction surface. Thus it was necessary to set more or less arbitrary conditions to distinguish the limit condition, viz.:

1) The limit condition for straight-line braking is an axle lockup lasting .2 second.

2) Two criteria are employed for braking in a turn.

   a) The controller output was limited to an angle of 8° at the road. If the output stayed at 8° for .2 second, the run was defined as a "limit condition."

b) The "limit condition" was also defined as being reached if the deviation of the vehicle from the intended path exceeded .10 feet. (In the context of the automatic controller, an error of .10 feet was a good indication that the vehicle was becoming uncontrollable, although this is obviously not a reasonable limit for a slower (but much more sophisticated) human controller.)

3.2 Discussion of Results

The simulation matrix outlined in Section 3.1 yields predictions of braking performance which can be described by many different indices, some of which are summarized in Tables 5, 6, and 7. The longitudinal deceleration levels represent the steady-state values found at each limit condition. The stopping distances applicable to an initial velocity of 40 mph were obtained directly from the simulation, whereas the stopping distances from 60 mph were calculated as described below.

Stopping distances which result when the initial velocity is other than 40 mph can be calculated from the data presented in Tables 5-7 if it is assumed that

1) the velocity sensitivity of the tire-road friction is negligible, so that the friction available at an arbitrary velocity is equal to the friction available at 40 mph, and

2) understeer/oversteer effects are negligible for the braking-in-a-turn maneuver, such that the slip angles of the tires at the initiation of the braking input are mainly a function of the lateral acceleration which prevails prior to braking.

Each braking simulation contains a transient response to the brake input, during which time the vehicle state fluctuates with time.

Table 5. A Summary of Limit Stopping Distances Achieved on a High Friction Surface.

Vehicle	Loading Condition	Initial A_y (g's)	Proportioning	$A_{xs.s.}$ (g's)	S.D. (ft) V_o=40 mph	S.D. (ft) V_o=60 mph	ΔV (mph)	ΔS.D. (ft)
U.S.	Light, Many Options	0	U.S.	.91	64.6	140	-28.1	-28.8
			European	1.00	60.7	131	-30.1	-30.7
		.2	U.S.	1.02	58.7	129	-30.7	-31.4
			European	1.00	60.9	133	-29.5	-30.0
		.4	U.S.	.98	64.0	137	-28.5	-29.1
			European	.88	67.8	146	-26.9	-27.4
	GVWR, Base Vehicle	0	U.S.	.98	62.0	134	-29.4	-29.9
			European	.86	69.0	150	-26.0	-26.6
		.2	U.S.	.92	66.9	142	-27.6	-28.2
			European	.84	71.9	154	-25.4	-26.0
		.4	U.S.	.96	65.4	140	-27.9	-28.2
			European	.80	74.5	161	-24.1	-24.5
European	Light, Front-End Options	0	U.S.	.86	67.4	148	-26.8	-27.4
			European	.81	71.6	157	-25.0	-25.7
		.2	U.S.	.87	69.4	149	-26.3	-27.0
			European	.81	72.4	156	-25.2	-25.9
		.4	U.S.	.84	71.8	157	-24.7	-25.1
			European	.80	74.4	163	-23.7	-24.1
	GVWR	0	U.S.	.72	80.0	176	-22.1	-22.7
			European	.66	86.6	191	-20.3	-20.8
		.2	U.S.	.73	78.8	175	-22.2	-22.9
			European	.67	84.4	188	-20.6	-21.2
		.4	U.S.	.69	85.0	186	-20.5	-21.1
			European	.63	91.1	201	-19.1	-19.6

Table 6. A Summary of Limit Stopping Distances Achieved on a Medium Friction Surface.

Vehicle	Loading Condition	Initial A_y (g's)	Proportioning	$A_{xs.s.}$ (g's)	S.D. (ft) V_o=40 mph	S.D. (ft) V_o=60 mph	ΔV (mph)	ΔS.D. (ft)
U.S.	Light, Many Options	0	U.S.	.62	91.5	202	-19.3	-19.7
			European	.55	102.2	226	-17.1	-17.6
		.2	U.S.	.66	89.6	193	-19.8	-20.4
			European	.61	94.5	205	-18.8	-19.9
		.4	U.S.	.66	88.1	193	-19.9	-20.6
			European	.59	92.9	207	-19.1	-19.8
	GVWR, Base Vehicle	0	U.S.	.53	106.1	234	-16.5	-16.9
			European	.48	115.7	257	-15.1	-15.4
		.2	U.S.	.57	95.7	217	-18.0	-18.5
			European	.49	109.4	250	-15.7	-16.6
		.4	U.S.	.57*	82.7*	216	-18.2	-18.9
			European	.51*	92.2*	241	-16.3	-16.9
European	Light, Front-End Options	0	U.S.	.56	98.7	219	-17.9	-18.5
			European	.51	109.4	241	-16.1	-16.7
		.2	U.S.	.58	96.1	216	-17.9	-18.7
			European	.51	102.7	231	-17.6	-18.4
		.4	U.S.	.53	100.7	231	-16.9	-18.2
			European	.49	107.5	247	-16.1	-17.2
	GVWR	0	U.S.	.47	117.9	261	-14.9	-15.4
			European	.44	126.2	278	-14.0	-14.4
		.2	U.S.	.51	108.2	244	-15.8	-16.5
			European	.46	118.3	268	-14.5	-15.2
		.4	U.S.	.42	124.5	285	-14.1	-15.0
			European	.41	129.9	295	-13.4	-14.0

*V_o = 54.1 ft/sec for straight-line run, results were:

U.S. proportioning, $A_{xs.s.}$ = .53, S.D. = 90.5

European proportioning, $A_{xs.s.}$ = .48, S.D. = 98.7

Table 7. A Summary of Limit Stopping Distances Achieved on a Low Friction Surface.

Vehicle	Loading Condition	Initial A_y (g's)	Proportioning	$A_{xs.s.}$ (g's)	S.D. (ft) V_o=40 mph	S.D. (ft) V_o=60 mph	ΔV (mph)	ΔS.D. (ft)
U.S.	Light, Many Options	0	U.S.	.39	142.1	315	-12.2	-12.5
			European	.35	154.9	348	-11.2	-11.5
		.2	U.S.	.34	159.5	357	-11.0	-11.3
			European	.29	182.3	415	- 9.6	-10.0
	GVWR, Base Vehicle	0	U.S.	.34	160.9	360	-10.8	-11.0
			European	.30	182.7	407	- 9.5	- 9.7
		.2	U.S.	.26	210.2	465	- 8.4	- 8.7
			European	.24	228.2	504	- 7.8	- 8.1
European	Light, Front-End Options	0	U.S.	.39	140.5	314	-12.4	12.8
			European	.35	160.1	349	-11.1	-11.4
		.2	U.S.	.33	168.4	368	-10.7	11.0
			European	.29	191.4	418	- 9.4	- 9.8
	GVWR	0	U.S.	.32	172.4	380	-10.2	-10.5
			European	.30	183.5	405	- 9.6	- 9.9
		.2	U.S.	.27	206.5	448	- 8.8	- 9.1
			European	.26	220.6	467	- 8.3	- 8.5

Eventually, the transient response diminishes and the vehicle brakes in a quasi-static fashion with the longitudinal tire forces and the longitudinal deceleration having fairly constant values. It was observed that the transient response always had diminished by the time t=1.5 seconds. Thus, if the velocity and accumulated stopping distance at 1.5 seconds are known, the distance required to reach zero velocity can be calculated as:

$$S.D.(final) = S.D.(t=1.5) + \frac{V^2(t=1.5)}{2 \cdot g \cdot A_{xs.s.}} \tag{3.2}$$

It remains to calculate the distance traveled and the velocity at t=1.5 seconds. On noting that

$$\dot{x}(t) = \int_0^t \ddot{x}(t)dt + V_0 \tag{3.3}$$

and

$$x(t) = \int_0^t \dot{x}(t)dt = V_0 t + \int_0^t dt \int_0^t \ddot{x}(t)dt \tag{3.4}$$

we can identify the influence of the initial velocity, V_0, and isolate it by re-writing the above equations for t=1.5 seconds as

$$V(t=1.5) = V_0 + \Delta V$$

$$\Delta V = \int_0^{t=1.5} x(t)dt \tag{3.5}$$

$$S.D.(t=1.5) = V_0 \cdot 1.5 + \Delta S.D.$$

$$\Delta S.D. = \int_0^{t=1.5} dt \int_0^{t=1.5} \ddot{x}(t)dt \tag{3.6}$$

The values of ΔV and $\Delta S.D.$ are included in Tables 5-7. To illustrate the use of these tables, we can calculate the stopping distance to be expected for the lightly loaded, U.S.-proportioned domestic vehicle on the high friction surface with an initial velocity of 60 mph. At t=1.5 seconds, the velocity would be 60 - 28.1 = 31.9 mph = 46.8 ft/sec. The distance traveled in 1.5 seconds would be

$$60 \text{ mph} \cdot (1.47 \text{ ft/sec/mph}) \cdot 1.5 \text{ sec} - 28.8 \text{ ft} = 103 \text{ ft}$$

The stopping distance to reach zero speed is then

$$103 + \frac{(46.8)^2}{2 \cdot 32.2 \cdot .91} = 140 \text{ ft}$$

This procedure was followed in order to calculate the 60-mph stopping distances shown in the tables.

Adhesion utilization at the two axles becomes a dynamic variable during the transient portion of a braking run. Table 8 lists the steady-state and peak values of the adhesion utilization of both axles on the medium and high friction surfaces for purposes of comparison with the quasi-static calculations from Section 2.0 and the general European regulatory philosophy that the utilization of the front axle should be higher than that of the rear. Δp indicates the difference between the proportioning calculated from instantaneous longitudinal tire forces and the design value, based on the brake torques. The order of axle lockup is also indicated.

The simulated braking runs have also been used to prepare plots which show velocity as a function of stopping distance. Two example plots are included here as Figures 9 and 10 for the lightly loaded domestic car braked on the high-friction and low-friction surfaces, respectively. (All of the velocity/distance plots obtained in this study have been included in Appendix B.) These figures can be

Table 8. Data Pertaining to the Simulated Adhesion Utilization of the Two Axles on the Medium and High Friction Surfaces.

Surface Condition	Vehicle	Loading Condition	Proportioning	$A_{xs.s.}$	K_F		K_R		ΔP			First Axle to Lock
					S.S.	Max.	S.S.	Max.	Min.	S.S.	Max.	
High (Dry Asphalt)	U.S.	Light	U.S.	.91	.84	1.03	1.09	1.12	-3	+2	+4	Rear
			European	1.00	1.00	1.05	.95	1.11	-2	+2	+6	Front
		GVWR	U.S.	.98	1.00	1.04	.90	1.11	-16	+2	+19	Front
			European	.86	1.01	1.05	.60	1.11	-2	+1	+5	Front
	European	Light	U.S.	.86	.83	.87	.98	.99	-3	+2	+9	Rear
			European	.81	.85	.87	.61	.83	0	+2	+3	Front
		GVWR	U.S.	.72	.83	.85	.47	.54	-1	+2	+4	Front
			European	.66	.82	.86	.30	.34	0	+1	+2	Front
Medium (Wet Asphalt)	U.S.	Light	U.S.	.62	.62	.67	.61	.68	+1	+1	+4	Front
			European	.55	.62	.67	.41	.48	0	+1	+2	Front
		GVWR	U.S.	.53	.62	.67	.40	.43	-1	+1	+2	Front
			European	.48	.63	.67	.28	.30	-1	0	+1	Front
	European	Light	U.S.	.56	.58	.60	.47	.53	0	+2	+3	Front
			European	.51	.57	.59	.30	.32	0	+1	+2	Front
		GVWR	U.S.	.47	.58	.60	.27	.30	-1	+1	+2	Front
			European	.44	.59	.60	.19	.20	-1	+1	+2	Front

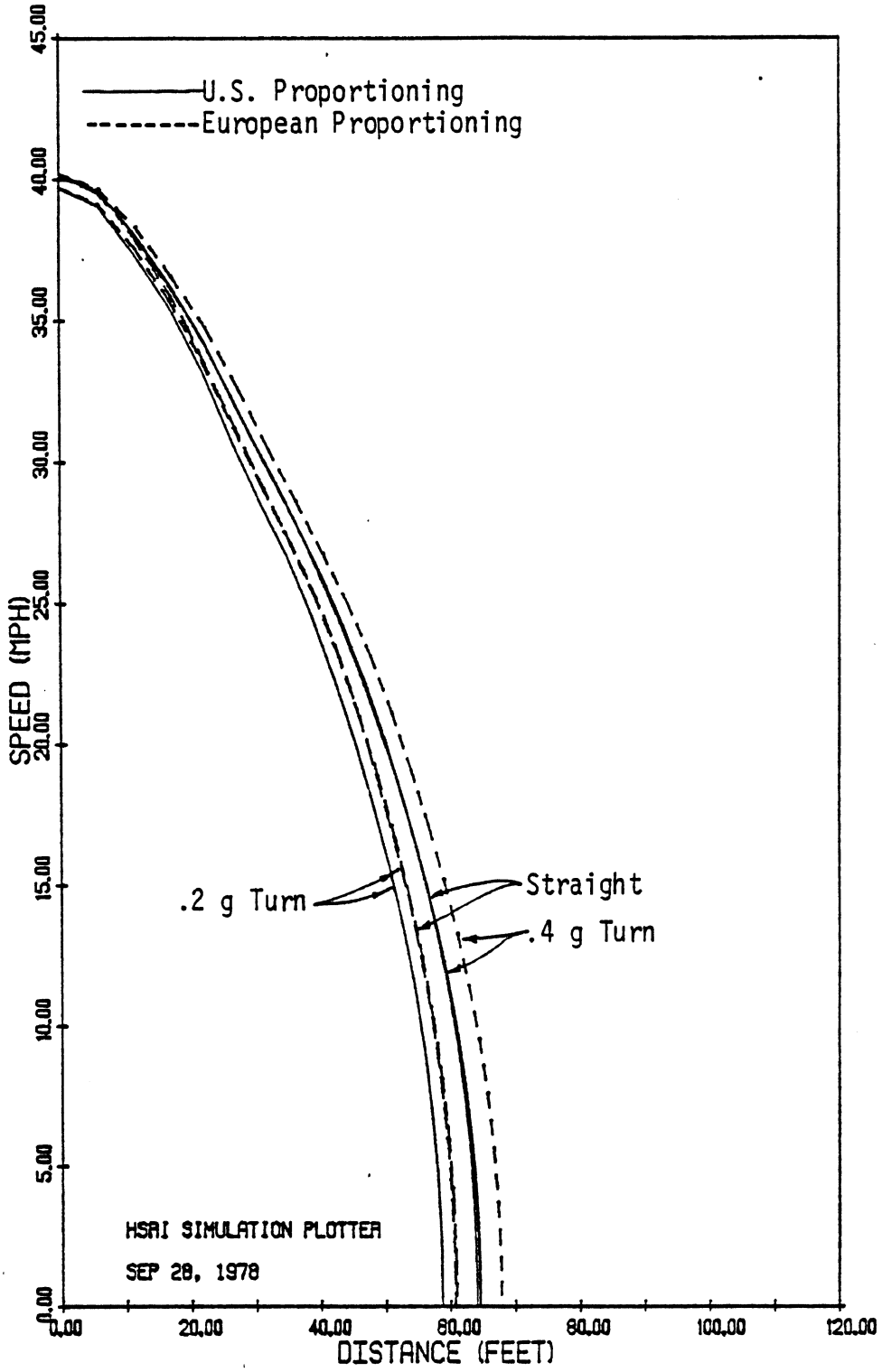

Figure 9. Speed vs. distance curves for the domestic intermediate, lightly loaded, on the high friction surface.

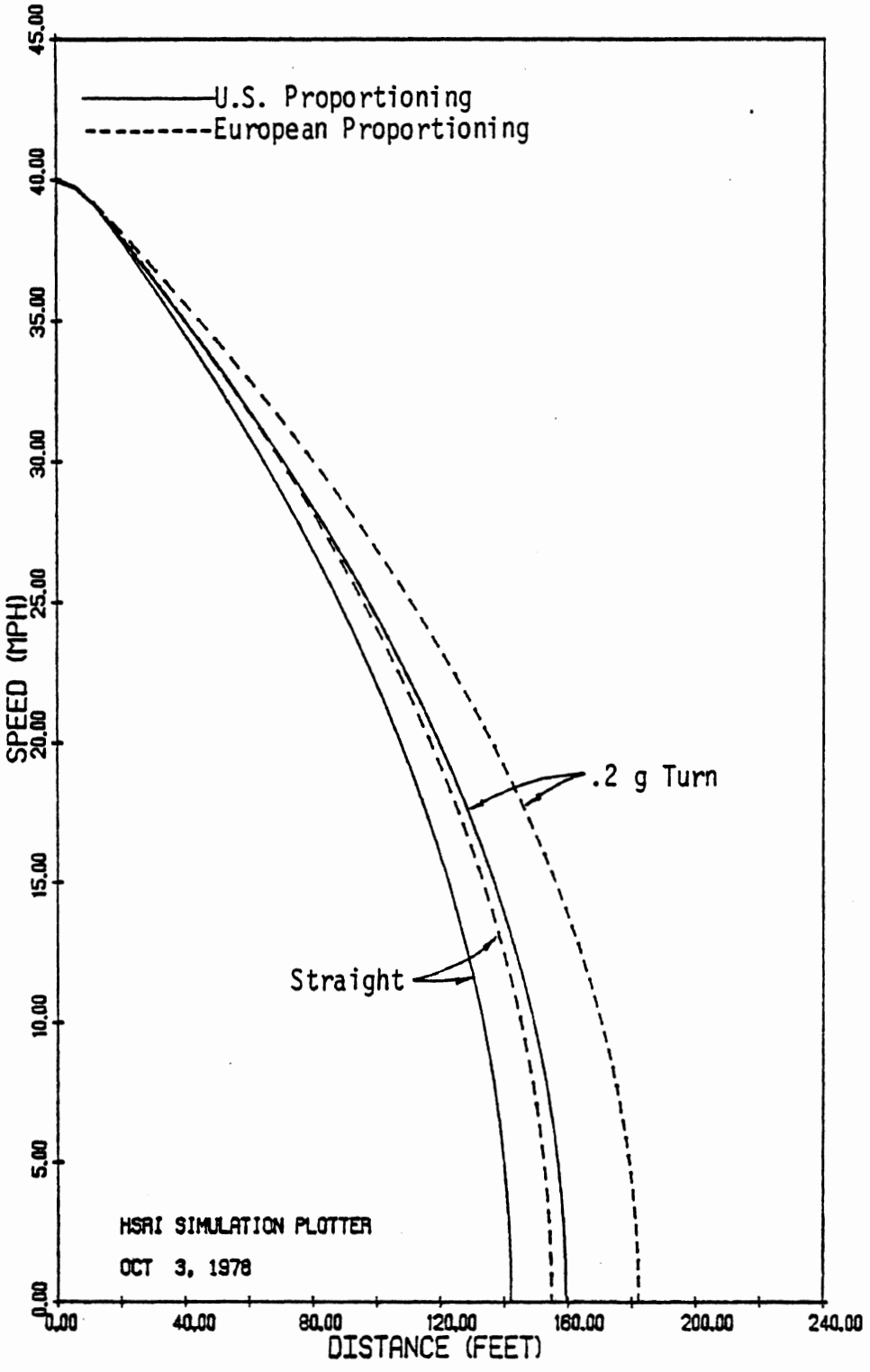

Figure 10. Speed vs. distance curves for the domestic intermediate, lightly loaded, on the low friction surface.

utilized to indicate the impact velocity which results if a limited stopping distance is available; for instance, if a distance of 60 feet is available to stop on the high-friction surface, the impact velocities would be:

- U.S. proportioning, straight line, 11 mph
- U.S. proportioning, .2 g turn, 0 mph
- U.S. proportioning, .4 g turn, 11 mph
- European proportioning, straight line, 5 mph
- European proportioning, .2 g turn, 5 mph
- European proportioning, .4 g turn, 14 mph

Thus the differences between the impact velocities exhibited by the differently proportioned vehicles are 6 mph for the straight-line stop, 5 mph for the stop in which $A_y(t=0) = .2$ g, and 3 mph for the stop in which $A_y(t=0) = .4$ g. It might be argued that kinetic energy, proportional to V^2, is more indicative of the damage to expect. The differences in V^2 are 96 $(mph)^2$ for the straight-line stop, 25 $(mph)^2$ for the .2 g's initial A_y stop, and 75 $(mph)^2$ for the .4 g's initial A_y stop. If the available distance is shorter, the differences in impact velocity fall more quickly than the differences in kinetic energy. For example, at 40 feet, the differences in velocity are only 1 mph, but the differences in V^2 are 67 $(mph)^2$ for the straight-line stop, 61 $(mph)^2$ for the .2 g initial A_y stop, and 48 $(mph)^2$ for the .4 g's initial A_y stop. In general, however, it appears that irrespective of whether V or V^2 is compared, the biggest difference is found at the distance at which the better proportioned vehicle comes to a complete stop.

The reaction time of the driver, namely, the time required to (a) notice an obstacle, (b) decide to brake, and (c) move the foot to the brake pedal, is clearly an important factor when braking to avoid a collision. The speed versus distance plots can be used to estimate

the additional reaction time which is gained or lost for the driver by the use of a different brake system. For example, in Figure 9 we see that if 60 feet are available to stop after the driver has reacted, and the condition is that of a straight stop, the impact velocity would be 5 mph for the European proportioned vehicle. From the figure, we see it would take the U.S. proportioned vehicle 64 feet to reach 5 mph and thus the extra "safety" in the European proportioning, for this condition, is 4 feet. The interpretation here is that the driver of the European vehicle has an additional .07 second at 40 mph to react and hit the obstacle at 5 mph compared to the time available to the driver of the U.S. proportioned car. The differences in the distance needed to reach a given speed are again the largest when the final speed is V=0 mph. The maximum values of Δt, the difference in reaction time which is needed to compensate for improved or decreased performance that results from a different proportioning, have been calculated and are presented in Table 9. For each condition the U.S. proportioned vehicle is taken as the baseline, and the Δt value indicates the extra time available to the driver to react to an emergency situation that would not be available if the vehicle were proportioned to comply with the European standards. Suppose that at 40 mph, on the medium friction surface, a situation presented itself where a stop must be made in 300 feet by the domestic passenger car nagivating a .2 g turn under GVWR loading. From Table 6 the limit stopping distance capability is 109.4 feet with European proportioning which requires a reaction time of 3.25 seconds. With the U.S. proportioning, the limit stopping distance capability is 95.7 feet, leaving 3.48 seconds for the driver to react. The difference is .23 second, which can be found in Table 9.

The data presented in Tables 5-9 lead to some general observations on the effects that the different proportioning values have on performance, namely:

Table 9. Extra Reaction Time That Derives from Proportioning the Representative Vehicles to Meet FMVSS 105-75 Instead of the European Regulations.

Surface Condition	Vehicle Type	Loading Condition	Initial Lateral Acceleration for Constant Radius Turn	Δt, "Extra Reaction Time" from U.S. Proportioning	
				V_o=40 mph	V_o=60 mph
High Friction (Dry Asphalt)	Domestic	Light (Many Options)	0 (g's)	-.07 (sec)	-.10 (sec)
			.2	.04	.05
			.4	.06	.10
		GVWR (Base - No Options)	0	.12	.18
			.2	.09	.14
			.4	.16	.24
	European	Light (Some Front-End Options)	0	.07	.10
			.2	.05	.08
			.4	.04	.07
		GVWR	0	.11	.17
			.2	.10	.15
			.4	.10	.17
Medium Friction (Wet Asphalt)	Domestic	Light	0	.18	.27
			.2	.08	.14
			.4	.08	.16
		GVWR	0	.16	.26
			.2	.23	.38
			.4	.16	.28
	European	Light	0	.18	.25
			.2	.11	.17
			.4	.12	.18
		GVWR	0	.14	.19
			.2	.17	.27
			.4	.09	.11
Low Friction (Polished Wet Surface)	Domestic	Light	0	.22	.38
			.2	.39	.66
		GVWR	0	.37	.53
			.2	.31	.44
	European	Light	0	.33	.40
			.2	.39	.57
		GVWR	0	.19	.28
			.2	.24	.22

1. For nearly every condition, the U.S. proportioning (that is, the proportioning value selected to best comply with the U.S. standard FMVSS 105-75) leads to better deceleration and stopping distance performance than does the European proportioning. Of course, this is exactly what should be expected from the analyses presented in Section 2.0. Deceleration capability is maximized when the adhesion utilization at each axle just reaches the frictional limit of the tire-road interface. The lower "U.S. proportioning" value selected to meet 105-75 is nearer to an optimal proportioning value for most conditions than is the higher "European proportioning" value, and thus greater deceleration is possible.

2. The U.S.-proportioned vehicles lock the rear wheels first on a high coefficient surface when the loading is such that the c.g. is in an extreme forward position. The deceleration achieved prior to rear-wheel lockup is very high for both the American-produced and the European-produced vehicle, in fact, higher than the deceleration capability required by any of the standards.

3. When proportioning is calculated as a function of the longitudinal tire forces produced under dynamic conditions, the resulting average value is always higher than the design value of proportioning as created by the torque ratio of the front and rear brakes. This is because the front tires are compressed due to the fore-aft load transfer and, with a reduced rolling radius, greater force is needed to balance the brake torque. For the same reason, less force is created at the rear tires. The design value of proportioning might be lowered to compensate for this effect in the case of the Swedish and U.S. standards, which are test oriented. However, the lower limit imposed by ECE R.13 and 71/320/EEC is a "paper regulation," and testing considerations are not applicable.

4. The adhesion utilization of the rear axle is often much greater than that of the front on the high friction surface for both proportionings. Due to the load sensitive behavior of pneumatic tires, however, there is much greater traction available at the relatively lightly loaded rear axle than at the heavily loaded front axle. When the rear axle does lock before the front, the difference between the steady-state values of K_F and K_R is .15 for the European vehicle and .25 for the domestic vehicle.

5. Limit deceleration for the braking-in-a-turn condition is sometimes greater, sometimes less than that found in straight-line braking. Only on the low friction surface is a trend evident—the limit deceleration in a turn is always less than that achievable during a straight-line stop.

6. Tire properties influence stopping performance much more than proportioning. The tire data for the two representative vehicles (see Appendix A) indicate that greater adhesion is available on the high and medium friction surfaces to the tires mounted on the domestic car. For all of the different maneuvers simulated on these surfaces, the difference in achievable deceleration between similarly proportioned, but differently tired, vehicles is greater than for differently proportioned but otherwise identical vehicles.

7. All of the performance comparisons deriving from stopping distance, such as differences in impact velocity, differences in impact velocity squared, increases in available reaction time, and, of course, stopping distance, are magnified at higher initial speeds and on surfaces with reduced traction.

8. Differences in deceleration capability are largest on the high friction surface, where the differences average .1 g, and smallest on the low friction surface, where they average about .03 g. When the differences in limit deceleration are normalized by the magnitude of the limit deceleration, the percentage change is always about 10%.

With respect to the measure of stopping distance, the U.S. regulation clearly leads to shorter stopping distances. The additional "safety" is relatively small, however, and unless the driver is skilled enough to exploit this additional "safety," as derives from a difference in brake proportioning, the differences must be considered to be negligible. The driver must react quickly to an emergency situation on a high friction surface to take advantage of a difference in stopping distance capability which amounts to .1 second or less at the initial traveling speed. On a low friction surface, the differences in stopping distance which are due to proportioning are more significant, but the driver must apply a pedal force precisely enough to utilize differences in deceleration capability which amount to several hundredths of a g. This can only be achieved if the driver is able to perceive the front wheels beginning to lock, and then decrease the pedal force to the level which gives the limit deceleration on the existing road surface. The driver who overbrakes and locks the front axle, the driver who is too cautious and underbrakes, and the driver who "pumps" the brake pedal through cycles of no braking to total lockup would, of course, realize negligible benefit from a slight difference in proportioning.

On the other hand, if one adopts the European view of "safety," the European proportioning would be identified as leading to "safer" braking because the rear axle can lock up on either of the two representative vehicles proportioned to meet 105-75, but not when they are proportioned to comply with the European regulations. It appears that the proportioning constraints imposed by the "non-test" provisions of 71/320/EEC and ECE R.13 are conservative in that they do not account for the effective increase in proportioning which is due to the spring rates of the tires (noted above) or for the greater adhesion available at the rear axle relative to the front axle. (On the other hand, manufacturing inaccuracies are not accounted for.)

4.0 THE INFLUENCE OF A BRAKING-IN-A-TURN REGULATION ON BRAKE PROPORTIONING

The U.S. Department of Transportation, the International Standards Organization (ISO), and other organizations in Europe have been actively pursuing methods for measuring (and perhaps regulating) braking-in-a-turn performance. The purpose of this section is to review the efforts made by these organizations towards developing braking-in-a-turn regulation, and through computer simulation, to evaluate whether further constraints on brake proportioning would accrue from the additional regulation. The past and current activities of the U.S. government and the ISO towards this goal are reviewed and discussed in Section 4.1, the methodology for studying the repercussions of proposed regulations is described in Section 4.2, and the results of the study are discussed in Section 4.3.

4.1 A Review of Proposed Braking-in-a-Turn Regulations

Test procedures which are designed to measure the performance of a passenger car which is braking in a turn fall into two broad categories, which will be discussed separately. One category, which is termed open-loop testing, consists of tests which do not allow the driver to steer or modulate the force on the brake pedal. (In control terms, such a system is an open-loop system.) Typically, the steering wheel is displaced and after the car has responded and is executing a constant-radius turn, pedal force (or brake line pressure) is applied. (The steering and brake inputs may be applied by specially designed machines or applied by a driver who may be aided by physical stops on the steering wheel and brake pedal.) In the second category, the driver attempts to make the shortest stop possible while steering to stay within a specified lane. Technically, both the car and driver are being tested as a closed-loop system, where modulation of the steering and/or braking control derives from feedback of the vehicle performance through the driver.

Open-loop tests of braking-in-a-turn performance have been used extensively in several projects supported by the NHTSA. HSRI developed and refined a braking-in-a-turn test as part of a larger vehicle handling program [11]. The performance of a car was measured by two methods, one of which is more suited for cars which spin out as a limit condition and the other which is better for cars which lose their steering at the limit. The first measure is a plot of the rate of the vehicle sideslip angle, $\dot{\beta}$, as a function of longitudinal deceleration, A_x. The second measure is a plot of "normalized path curvature," defined as

$$R_o \cdot \frac{1}{T} \int_0^{T=1 \text{ sec}} \rho(t)dt \quad ,$$

where $\rho(t)$ is the inverse of the instantaneous radius of curvature and R_o is the initial radius of curvature. These two performance measures are evaluated from digitized time histories of A_x, A_y, r (yaw rate), V (fifth wheel velocity), and a control channel. The test procedure is complicated to implement, but is conceptually straightforward and has been used to catalogue a wide range of passenger cars in a number of NHTSA-sponsored studies.

Another open-loop braking-in-a-turn test was developed by Calspan Corporation [12]. In this procedure, a constant radius turn is marked on a skid pad. The driver brings the car into the turn and adjusts the steering-wheel angle until the vehicle is following the path with no steering correction. The brakes are then applied and the steering-wheel angle is held constant. After the vehicle has stopped, the lateral deviation from the intended path and the heading error (yaw angle, relative to the tangent of the curve) are measured. Subsequent to this Calspan study, NHTSA has not sponsored any further research which utilizes this particular test procedure.

More recently, several European groups have been actively pursuing the development of a braking-in-a-turn test procedure for the ISO Committee on Road Vehicles, TC 22/SC 9. Two procedures are being considered, namely, an open-loop and closed-loop procedure. It appears that the open-loop procedure is further along and has been receiving more attention. The Italian delegation submitted a candidate procedure [13] which is identical to the test method developed by Calspan, although the performance measures differ from Calspan's. The procedure was tried in the field by Italy and the results were reported [14] to serve as a basis of discussion by other delegations. After several modifications [15, 16, 17, 18], the test procedure has gained substance and can be summarized in Table 10 in terms of initial conditions and physical quantities which might be measured. Conditions not given in the table are set in accordance with the straight-line test procedure given in ECE R.13. The candidate performance indices listed in the table seem to represent the least defined portion of the procedure and it is noted in all of the documents that they need clarification.

Closed-loop testing has been proposed by France [19] and some preliminary testing was conducted. However, most of the developmental work for a closed-loop braking-in-a-turn test has been performed in the United States under NHTSA sponsorship [20, 21, 22]. The most recent of these studies was conducted at HSRI and, at NHTSA's request, considered several candidate test additions to FMVSS 105-75, namely,

1) braking in a turn
2) low-friction surfaces
3) split-friction surfaces.

Two large testing programs were conducted and various analyses were performed to examine the candidate test methods and conditions. It was concluded that insufficient deficiencies existed in the vehicle population to justify the proposed extensions and that only the low friction, straight-line braking condition constitutes a viable extension of the stopping distance requirements of 105-75. It was also

Table 10. Summary of the ISO Braking-in-a-Turn Test Procedure (Document ISO/TC 22/SC 9, #143).

Radius of Turn:	R_o = 40 m (131 ft), 100 m (328 ft)
Load:	light loading, GVWR
Initial Speed:	R_o = 40 m, V_o = 49 Km/h (30 mph) R_o = 100 m, V_o = 62 Km/h (39 mph)
Instrumentation: (Must be Recorded Continuously)	A_x = longitudinal deceleration A_y = lateral acceleration β = slip angle r = yaw rate θ = pitch angle ϕ = roll angle Δ_s = steering-wheel angle P = front brake circuit pressure
Other Conditions Which are Noted:	V = vehicle speed tire inflation pressures wheel lockup
Brake Application Time:	.2 second or less
Candidate Performance Indices:	ΔS = change in stopping distance due to cornering. Plotted as a function of pedal force. A_{ymax} = maximum lateral acceleration r_{max} = maximum yaw rate $A_y(1)$ = lateral acceleration 1 second after brake application r(1) = yaw rate 1 second after brake application $\beta(1)$ = slip angle 1 second after brake application Δ = lateral deviation of the vehicle c.g. from the ideal (constant radius) path

found that stopping distances in a turn do not differ significantly from stopping distances measured during straight-line braking.

It appears that a braking-in-a-turn regulation is not imminent in the U.S. and that a consensus standard for a braking-in-a-turn test procedure will most likely be developed by ISO. An ISO standard is likely to fit one of two categories, namely:

1. An open-loop test, using the test procedure developed at Calspan [12], in which performance is measured in terms of one or more physical variables which would characterize the change in path curvature which results from braking.

2. A closed-loop test nearly identical to the candidate test addition to FMVSS 105-75 which was recently investigated by HSRI for NHTSA [22].

4.2 Methodology of Study

Of the many simulations run for the study presented in Section 3, closed-loop braking in a turn on a high friction surface (dry asphalt) was one of the conditions considered. Since two proportioning values were used, the results (see Appendix B and Section 3.2) can be studied to determine the effect of proportioning on stopping distance when braking in a turn, or, conversely, they can be studied to determine the limits that a stopping distance requirement would place on proportioning selection.

The consequences of an open-loop braking-in-a-turn regulation were studied by performing a special set of simulations. This set covered the following conditions:

1. two vehicle types (the two representative cars used throughout the project),

2. two loading conditions (the two extreme option and load combinations for each vehicle, as defined in Section 2.4),

3. two sets of initial conditions, as noted in Table 10,

4. three values of brake proportioning which were selected to extend over and slightly beyond the ranges permitted by the existing standards, and

5. various levels of brake line pressure (resulting in decelerations which ranged from about 0.5 g up to a level where either spin-out occurred or where steering was totally lost).

4.3 Discussion of Results

4.3.1 Closed-Loop Tests. The results of the simulations tend to reinforce earlier experimental findings [22] that stopping distances achieved in a turn do not vary much from those achieved during straight-line braking. Through all of the simulated maneuvers, the resulting limit stopping distances were close to each other, and were sometimes better, sometimes worse when in a turn than when in a straight line. In general, the straight-line stopping distance performance gives a good first-order estimate of the curved-path stopping distance. Based on the most recent braking-in-a-turn study sponsored by the NHTSA, it is difficult to envision a braking-in-a-turn regulation being promulgated in the U.S.

4.3.2 Open-Loop Tests. The open-loop testing procedure for braking in a turn that is being developed by the ISO does not yet address the question of how to measure performance. As Table 10 indicates, many possibilities are being considered. Accordingly, a broad range of possible performance indices has been prepared from the simulations. There have been arguments for using the instantaneous values at t = 1 second and arguments for using time averages, thus both are seen as possible measures and are included in the tabulated results. The numerics are listed for one example in Table 11, and defined as follows:

Table 11. Unweighted Numerics Resulting from Simulations of Open-Loop, Braking-in-a-Turn Maneuvers with an Initial Radius of 100 Meters (A_y = .3 g).

Prop. (%)	Pressure (psi)	$\tilde{A}_x$ (g's)	A_xs.s. (g's)	$\tilde{A}_y$ (g's)	$A_y(1)$ (g's)	$\tilde{r}$ (deg/sec)	r(1) (deg/sec)	$\tilde{\beta}$ (deg)	β(1) (deg)
70	250	.47	.51	.27	.21	9.0	8.7	- .7	- .3
	300	.55	.60	.26	.20	8.9	8.6	- .7	- .1
	350	.64	.69	.23	.16	7.5	6.3	- .8	.1
	400	.70	.76	.20	.09	6.2	3.5	- .9	.0
	450	.76	.82	.14	.02	3.7	-1.0	- .9	- .2
	500	.78	.85	.09	.01	2.1	-3.3	-1.3	- .4
80	300	.49	.53	.26	.20	8.7	8.6	- .7	- .2
	350	.56	.61	.22	.16	6.9	6.3	- .6	- .0
	400	.62	.67	.15	.04	4.2	1.3	- .5	.0
	450	.65	.69	.10	-.01	2.2	- .4	- .5	- .3
90	300	.44	.48	.26	.20	8.6	8.4	- .7	- .3
	350	.51	.55	.21	.14	6.7	5.2	- .6	- .2
	400	.55	.60	.13	.01	3.6	.3	- .5	- .0
	450	.56	.60	.09	-.01	1.9	- .1	- .4	0.0

1. Proportioning - the percent of the total brake torque which acts on the front axle.
2. Pressure - a brake line pressure which is input to the computer program.
3. $\tilde{A}_x$ - the longitudinal deceleration, averaged over the first one second after the brake application.
4. $A_{x_{s.s.}}$ - the steady-state longitudinal decleration.
5. $\tilde{A}_y$ - the lateral acceleration, averaged over the first one second after the brake application.
6. $A_y(1)$ - the instantaneous lateral acceleration at t=1 second.
7. $\tilde{r}$ - the yaw rate, averaged over the first one second.
8. r(1) - the instantaneous yaw rate, at t=1 second.
9. $\tilde{\beta}$ - the vehicle sideslip angle, averaged over the first one second.
10. $\beta(1)$ - the instantaneous vehicle sideslip angle at t=1 second.

A simple examination of the data presented in Table 11 does not indicate whether a low value of A_y or r is due to a change in path curvature or simply due to the fact that the vehicle is slowing down. If the rate of change of sideslip angle is zero, A_y and r depend on velocity as follows:

$$A_y = \frac{1}{g}\frac{V^2}{R_o} \tag{4.1}$$

$$r = V/R_o \tag{4.2}$$

where g is the gravitational constant and R_o is the radius of the turn. A better indication of the changes in path curvature caused by braking is given by normalizing the lateral acceleration, A_y, and

the yaw rate, r, by the right-hand sides of Equations (4.1) and (4.2). Table 12 was prepared accordingly. When average values are needed, the velocity or the velocity squared is averaged to use Equations (4.1) and (4.2). The actual normalized path curvature (see Reference [11]) is also indicated as an idealized reference, both for the average over the first one second and the instantaneous value at t=1 second. For the last six columns of Table 12, a value of 1.0 indicates that the path curvature is essentially unchanged, a value greater than 1.0 indicates increased curvature, that is, a tendency towards spinout, and a value less than 1.0 indicates a loss of steering which results in a loss of curvature.

In order to illustrate the effect which an open-loop type of braking-in-a-turn regulation might have on proportioning selection, plots were prepared showing constant values of normalized path curvature, averaged over one second, in the space defined by proportioning and deceleration. Figures 11 and 12 consist of two such plots for the representative European vehicle. The initial radius of turn is 100 meters and the lateral acceleration is 0.3 g's at t=0.

Figures 11 and 12 illustrate behavior whose explanation requires that we first consider the combined traction characteristics of the pneumatic tire. For example, data showing the manner in which lateral (side) and longitudinal force depend on combined lateral and longitudinal slip are plotted in Appendix A for the tires used on the Golf and the Monte Carlo. As has been noted elsewhere, the side force at a given slip angle decreases and falls to a very small value as longitudinal slip is increased from the free-rolling state to the "lockup" condition. We must next observe that a vehicle executing a steady turn requires side forces between the tires and the road. In the simplest sense, the front tires try to turn the vehicle, the rear tires try to restore the vehicle to a straight-line path, and the actual path curvature depends on the balance between the front and rear tire forces as well as on the instantaneous value of the total side force being generated by the tires.

Table 12. Normalized Numerics Resulting from Simulations of Open-Loop Braking-in-a-Turn Maneuvers, with an Initial Radius of 100 Meters (A_y = .3 g's).

Prop. (%)	Pressure (psi)	A_xs.s. (g's)	$\frac{\tilde{A}_y \cdot R_o}{\tilde{V}^2}$	$\frac{A_y(1) \cdot R_o}{V(1)^2}$	$\frac{\tilde{r} \cdot R_o}{\tilde{V}}$	$\frac{r(1) \cdot R_o}{V(1)}$	$R_o\tilde{\rho}$	$R_o\rho(1)$
70	250	.51	1.14	1.31	1.04	1.21	1.13	1.30
	300	.60	1.18	1.40	1.06	1.29	1.18	1.40
	350	.69	1.08	1.34	.91	1.01	1.03	1.46
	400	.76	.96	.86	.77	.60	.87	1.05
	450	.82	.68	.17	.47	-.18	.50	.19
	500	.85	.50	.06	.26	-.60	.24	.14
	600	.86	.46	.50	.52	.41	.14	.11
80	300	.53	1.12	1.29	1.01	.82	1.10	1.29
	350	.61	.98	1.19	.83	.95	.92	1.25
	400	.67	.69	.31	.51	.20	.56	.32
	450	.69	.47	-.06	.27	-.06	.30	-.10
90	300	.48	1.08	1.10	.98	1.14	1.06	1.22
	350	.55	.91	.90	.78	.75	.85	.88
	400	.60	.60	.10	.42	.05	.47	.11
	450	.60	.42	-.04	.22	-.01	.26	-.06

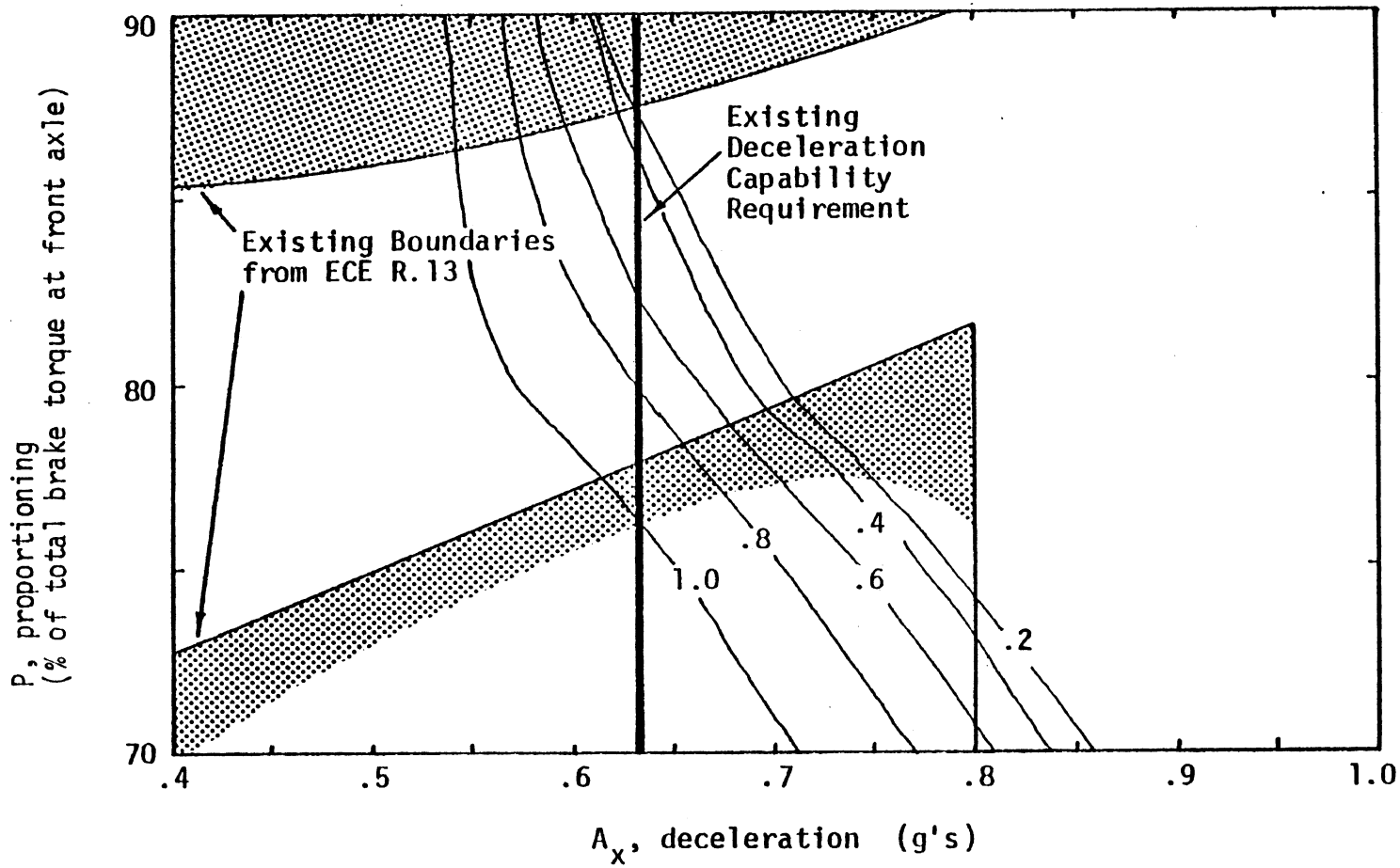

Figure 11. Lines of constant normalized path curvature for the European car, loaded to the GVWR condition, braking in a turn with an initial lateral acceleration of .3 g's.

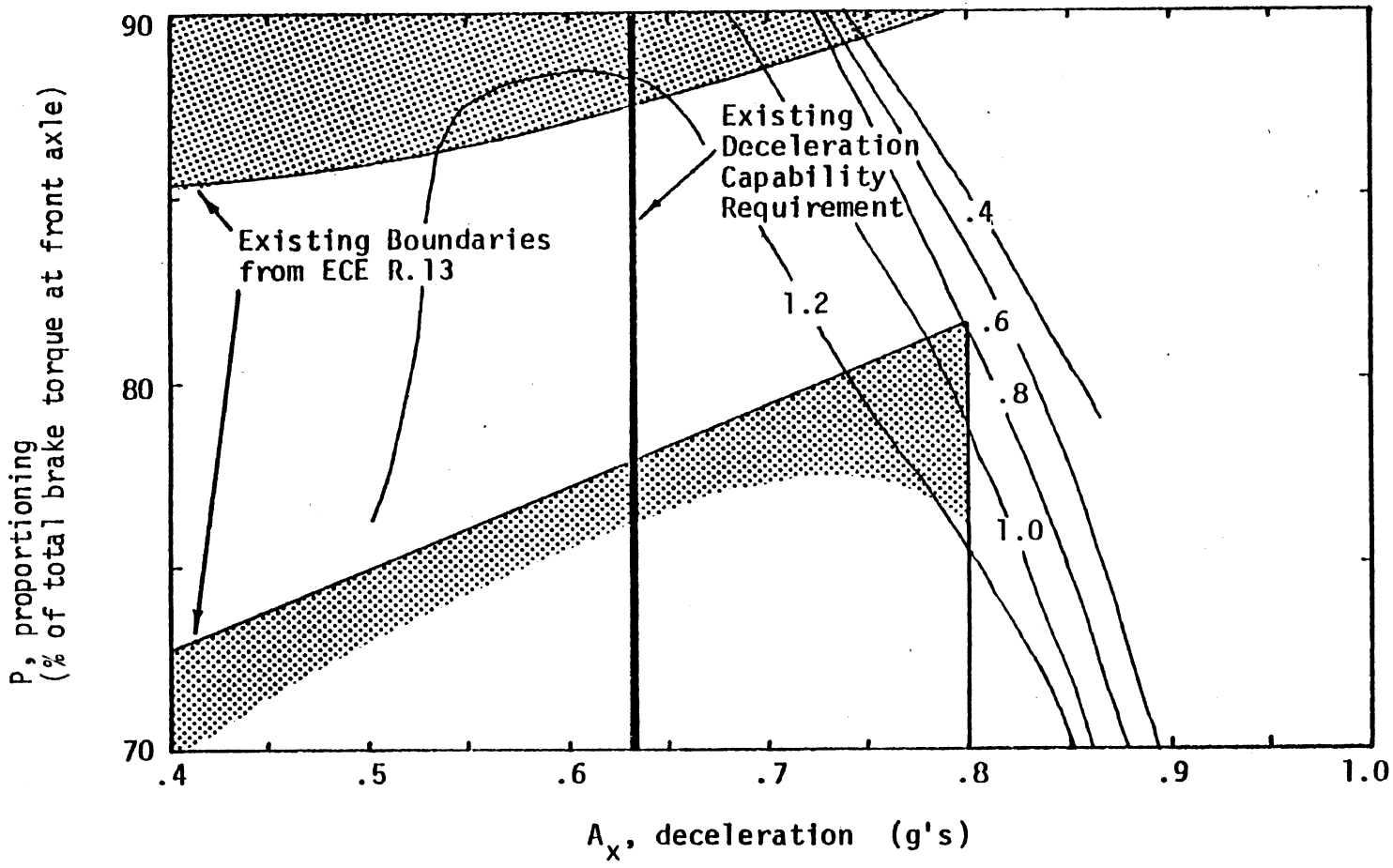

Figure 12. Lines of normalized path curvature for the European car, lightly loaded, braking in a turn with an initial lateral acceleration of .3 g's.

In light of these fundamentals, time histories of vehicle motions and tire forces, as generated during a simulation, were studied to identify the various effects which braking has on the path curvature of a passenger car during an open-loop braking-in-a-turn maneuver. Four distinct mechanisms, or stages in the time history, were identified, viz.:

1. During the period in which the brakes are being applied (the first .3 second), the sprung mass has not responded fully to the longitudinal forces and fore/aft load transfer is minimal. At the medium to high deceleration levels which were being simulated, adhesion utilization of the front axle is higher than the eventual steady-state utilization. Therefore, the slip ratios for the front tires increase, the side forces produced by the front tires decrease, and there is a loss of steering and path curvature.

2. Subsequently, the sprung mass responds to the deceleration by pitching forward, and overshoots the steady-state position at about t=.4 second. The load on the front axle is higher than the steady-state condition, while the rear axle load is lower. The slip ratios decrease at the front axle and increase at the rear, resulting in more steering force and less restoring force. The result is an increase in path curvature. It was noted that this "second stage" behavior nearly always has a larger effect than the "first stage," so after the first .5 second, the path curvature is usually greater than it was before brake application. Rear-wheel lockup, if it occurs at all, begins during this stage.

3. The body rebounds somewhat from "stage 2" and reaches a pitch angle which again unloads the front axle and loads the rear, producing an effect similar to "stage 1." This stage is often negligible, but can be significant when the

vehicle is loaded to the GVWR, as the damping ratio is then lower.

4. Finally, the vehicle settles into a more-or-less steady-state condition, in which the normal loads on the tires do not change very much. Curvature is now affected primarily by the understeer/oversteer characteristics of the vehicle and by the reduction in tire side forces resulting from longitudinal slip as influenced by the proportioning of the brake torques.

Having noted these four stages, we can now discuss Figures 11 and 12 more thoroughly.

When the vehicle is loaded to the GVWR condition, the center of gravity is at the most rearward location, and the selected values of proportioning result in a much higher adhesion utilization at the front axle than at the rear. From Figure 11, we note that at low and moderate decelerations, the path curvature is relatively insensitive to either deceleration or proportioning. But at higher deceleration levels, the path curvature decreases with increased deceleration and increased proportioning. The curvature decreases with deceleration because the front axle is always utilized more than the rear, and as the overall brake torque levels are increased to achieve the higher deceleration, the front tires lose their side force capabilities more quickly than the rear tires. Also, the third stage of the response to braking, described earlier, has a significant effect. The curvature decreases with proportioning because a higher brake torque is needed at the front axle to maintain a given deceleration level. Note that when the proportioning and deceleration are limited to the area permitted by regulation ECE R.13, the lines of constant path curvature are more sensitive to the deceleration level than to the proportioning. The deceleration has a large influence on the three stages of the braking transient, and these stages dominate the behavior exhibited during the first one second of braking.

The same vehicle, with options and light loading (see Section 2.4), maintains a much higher path curvature during the first one second of the braking transient than the case considered above. As is shown in Figure 12, there is a strong increase in path curvature at moderate deceleration levels, which increase is mostly due to the mechanism described as "stage two." At low proportionings, the steady-state behavior (stage four) is so strongly towards increased curvature that the high curvature lines extend to high decleration levels. The eventual loss of curvature at the highest deceleration levels is due to a loss of side force at all of the tires. Once again, we note that the curvature lines are more sensitive to deceleration than to proportioning because of the transient behavior (particularly, stage two).

A regulatory limit on the change in path curvature (irrespective of which variables are actually used to characterize curvature) will clearly be the most demanding for the GVWR loading case in which the vehicle c.g. is the most rearward. Europeans seem to be more concerned with a loss of path curvature than an increase in curvature. (This concern probably exists because their regulations lead to high proportionings which lead to a loss of steering under severe braking.) Thus a European regulation based on the ISO test procedure would most likely limit the loss of curvature, with the effect of encouraging a lower proportioning selection.

Figure 13 is comparable to Figure 11 except that the lines of constant path curvature apply to the domestic vehicle in the GVWR loading condition. We see, however, that the loss of path curvature occurs at much higher deceleration levels than occurred in the case of the European vehicle. This behavior is predicted because the tire data given in Appendix A indicate that the tires used on the Monte Carlo are characterized by traction levels that are significantly higher than that of the tires used on the Golf. It appears that tire selection has a much greater effect on the performance exhibited in this type of brake test than does proportioning.

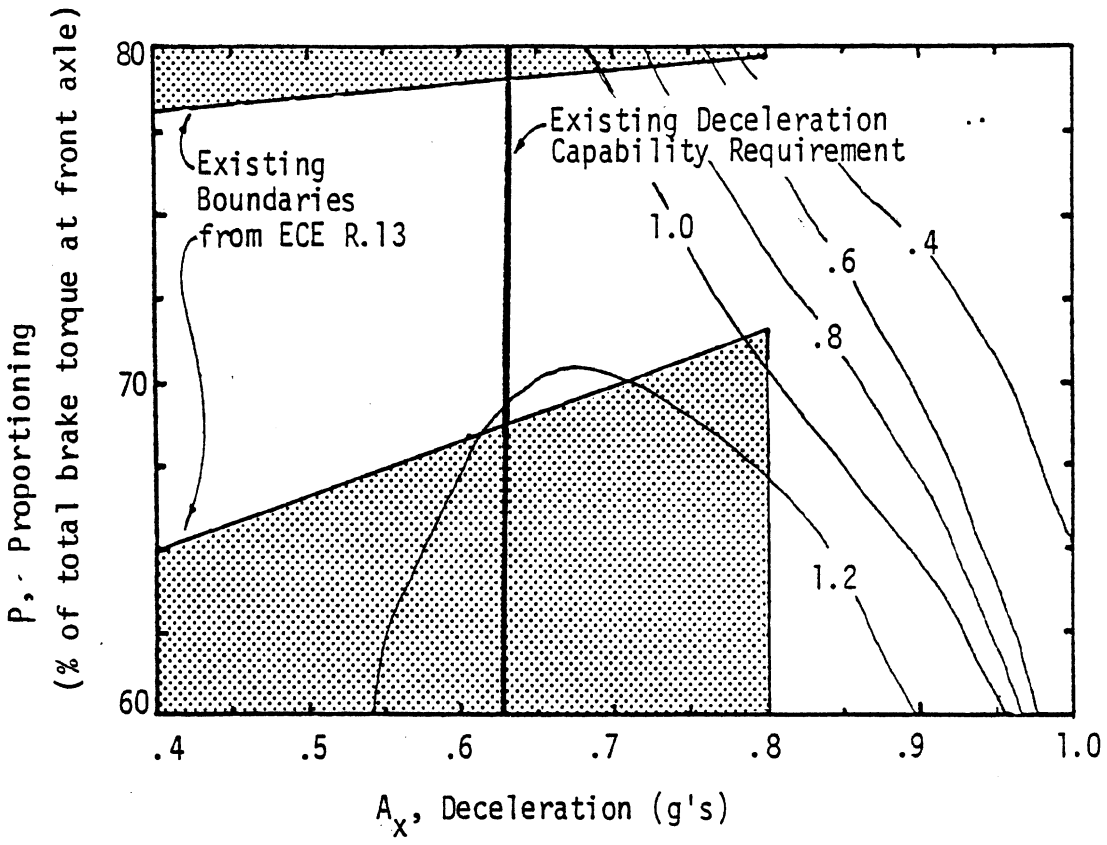

Figure 13. Lines of constant normalized path curvature for the domestic car, loaded to the GVWR condition, braking in a turn with an initial lateral acceleration of .3 g's.

The tabulated results of all of the open-loop simulations are included in Appendix C, together with figures showing lines of constant normalized path curvature, as determined for each test condition.

5.0 SUMMARY AND CONCLUSIONS

Nearly all of the braking regulations and standards which are now in use throughout the free world are based on one of two prototypes, the U.S. standard, FMVSS 105-75, and the United Nations' ECE Regulation 13, which is often implemented in a nearly identical regulation adopted by the common market, directive 71/320/EEC.

ECE R.13 requires straight-line braking tests on a dry, smooth surface which offers "good adhesion." The vehicle loading is set at driver plus instrumentation for one test and the maximum rated loading (GVWR) for another. The regulation requires a deceleration capability of about .6 g's, which is significantly below the frictional limits of most passenger car tires on dry surfaces. The test serves to insure that the brakes installed on the vehicle are sized properly and that the required pedal forces are not excessive, but the range of brake proportionings which can be used to achieve the necessary deceleration is rather wide. ECE R.13 also contains a "paper regulation," which requires the manufacturer to submit curves indicating the adhesion utilization (braking force divided by vertical force) existing at each axle for decelerations ranging from .15 g's to .80 g's. These curves must be prepared according to a simple analysis contained in the regulation, and do not account for dynamics in the transient response of the vehicle, nonlinearities inherent in the geometry of drum brakes, effects of velocity, temperature, and work history on brake lining friction coefficients, or for normal manufacturing imprecision. The "paper regulation" imposes explicit constraints on allowable proportioning, within the context of the analysis. The lower limit on proportioning is the value at which the front and rear axles have equal adhesion utilization when the vehicle is loaded such that the center of gravity (c.g.) is in the most forward position possible for the vehicle and the fore/aft load transfer is due to a constant deceleration of .8 g's. The partial failure

condition is tested in the same manner as the non-failed deceleration capability of the vehicle, but the deceleration requirement should not impose any proportioning constraints if the brakes are of sufficient size and the tires have moderate adhesion on the test surface.

ECE R.13 derives from a philosophy that the rear axle should never lock up before the front axle during a braking maneuver, thus maintaining stability. The braking efficiency (that is, the actual limit wheels-unlocked deceleration divided by the available tire-road friction) is very high on a high friction surface because the large fore/aft load transfer allows large braking forces to be generated at the heavily braked front axle, but the efficiency is less on lower frictional surfaces where less deceleration and thus less load transfer is possible.

Sweden is the only country with a significant braking regulation that is not based on ECE R.13 or FMVSS 105-75. The philosophy towards "good braking performance" is identical to that behind ECE R.13, but different methods are used to evaluate this performance. The Swedish regulation, F-18, requires brake tests on a surface with a peak friction coefficient of .8, as measured with an ASTM E249-14 test tire. Under GVWR and lightly loaded conditions (and technically, any condition in between), the vehicle must be capable of achieving a deceleration of .6 g's with no axle lockup, and furthermore, at higher deceleration levels, up through .8 g's, the front axle must always lock before the rear. When the requirements are made 10% more stringent, to allow for manufacturing tolerances, the allowable proportioning range is much narrower than that allowed by R.13, and a proportioning selected to satisfy F-18 easily satisfies ECE R.13. The partial failure test might be difficult to pass because of the limited available friction, but the partial-failure deceleration requirement does not impose further constraints on the proportioning of the non-failed brake system. It is difficult to predict the performance of a specific vehicle in the F-18

tests because the tire-road friction is a first-order influence and there is little information which serves to relate the peak friction measured on the ASTM tire to the peak friction available to a specific passenger car tire. Also, the surface is usually wetted to establish the proper friction coefficient, which compounds the task of correlating the traction capability of the ASTM tire with that of another tire.

The U.S. standard reflects a different definition of "good braking," which is that of good stopping distance performance on a high friction surface. FMVSS 105-75 requires nearly .8 g's of deceleration (when target stopping distances are set to be 90% of the required distances) on a smooth, dry surface with an ASTM skid number of 81. The required deceleration is specified in terms of stopping distance at several initial velocities. The required stopping distances must be achievable with no axle lockup, although, unlike the European standards, no constraints are placed on the order in which the axles lock at higher decelerations. FMVSS 105-75 requires indirectly that the tires installed on the vehicle have good adhesion and that the brakes are sized properly. Because the U.S. regulation requires significantly higher deceleration capability than the European regulations, it is conceivable that vehicles equipped to comply with the European regulations could have tires with less adhesion or brakes with less torque capability than a similar vehicle equipped to satisfy the U.S. regulation. Nonetheless, this study assumed that the same brakes and tires would be used on vehicles irrespective of whether they were intended to meet a U.S. or European braking standard. Only the brake proportioning would be altered to comply with a different standard.

The different concepts of "good braking" behind the U.S. and European regulations lead to brake proportionings which are more notable for their similarities than for their contrasts. The high decelerations required by 105-75 lead to a proportioning selection which is a tradeoff

between an "optimal" proportioning (where the braking forces generated at both axles reach the frictional limits at the same time and braking efficiency is nearly 100%) for the unloaded vehicle and an "optimal" proportioning for the vehicle loaded to GVWR. The European regulations lead to a slightly higher proportioning value, so on lower frictional surfaces vehicles proportioned to meet either type of regulation will have reduced braking efficiency.

To obtain some specific findings, two vehicles were selected as being representative passenger cars subject to these regulations—a domestically-produced intermediate sized car and a European subcompact car. Vehicle parameter values and tire data were gathered for each. Two option and loading conditions were identified for each vehicle as constituting extreme constraints on the proportioning needed to satisfy the various regulations. A value of fore-aft proportioning was selected for each of the two vehicles which would optimize the performance in the 105-75 tests with different values of proportioning being selected to optimize the performance in Sweden's F-18 tests. The proportionings selected to pass F-18 were also optimum for passing ECE R.13. For the domestic car, the European proportioning was .07 higher than the U.S. proportioning, and for the European car the difference was .06.

As a means of assessing differences in safety quality as it derives from the different proportioning levels required to satisfy the U.S. and the European standard, a variety of braking conditions were simulated utilizing detailed mathematical models of the vehicle and tire. These conditions covered (1) two extreme option/load combinations, (2) high, medium, and low friction surfaces, (3) straight-line braking, and (4) braking in a constant radius turn, with initial lateral accelerations of .2 and .4 g's. For each condition, the limit deceleration was found for the vehicle proportioned to meet the U.S. standards

and then found for the vehicle proportioned to meet the European standards. In nearly every case, the braking efficiency and the deceleration and stopping distance capabilities were better for the vehicle which was proportioned according to the demands of the U.S. standard. Plots of velocity as a function of stopping distance were prepared (see Appendix B) which illustrate (graphically) differences in braking performance as derive from different proportioning. It is possible to see the differences in "impact velocity" which would result if the available stopping distance is limited or the differences in required stopping distance if the vehicle is to be slowed to an arbitrary velocity. The most extreme contrasts exist for either interpretation when the final speed is V = 0 mph. (The differences in achievable stopping distance are tabulated for this condition in Section 3.0.) When differences in stopping distance are divided by the initial velocity, the result is the extra amount of time available to the driver before the brakes must be applied. (These times are also calculated and tabulated in Section 3.0.)

The computer simulations of the differently proportioned vehicles serve to quantify the "safety quality" (in the braking context) which results from the two proportionings. The conclusions on "safety quality" as derived from the proportioning implemented to meet the different standards are as follows:

1. In nearly every case, the vehicle proportioned to meet the U.S. standard achieves a shorter stopping distance than the vehicle proportioned to meet the European standard.

2. No trends are apparent from the braking-in-a-turn simulations on the medium or high friction surfaces. Performance is sometimes better, sometimes worse, than for straight-line braking.

3. Stopping distances are always longer when braking in a turn on the low friction surface than when braking in a straight line, but the computed change in performance is not dependent on the proportioning.

4. Differences in deceleration capability due to proportioning are about .1 g's on the high coefficient surface. When stopping distances are used to calculate "extra reaction time," the differences average about .07 seconds when the initial speed is 40 mph, and .11 seconds when the initial velocity is 60 mph.

5. Differences in stopping distance are magnified on lower friction surfaces, with the "extra reaction times" averaging .31 seconds for an initial velocity of 40 mph on the low friction surface and .44 seconds for an initial velocity of 60 mph. The average difference in limit deceleration is about .03 g's.

6. The tires installed on the domestic car had higher levels of traction on high and medium friction surfaces than the tires installed on the European car. On these surfaces, the available tire traction was clearly more influential with respect to stopping distance performance than was proportioning.

The outcome of a situation in which an accident is avoided or reduced in severity by braking depends on three general factors, namely,

1) the reaction time, which in this context, is the delay between the time at which the obstacle to be avoided interrupts the driver's line of vision and the time when the driver's foot hits the brake pedal,

2) the ability of the driver to apply the correct brake pedal force needed to achieve limit deceleration, and

3) the limit deceleration capability of the vehicle.

The differences in vehicle braking performance which result from the different proportionings are always small enough that great demands are placed on the driver if he is to benefit from the level of incremental vehicle performance due to proportioning. On a high friction surface, the driver must notice the obstacle, decide that braking is the best option, and then apply the brakes in a time short enough for a difference of .1 second (the difference in reaction time needed by the two differently proportioned vehicles to stop within the same distance) to be significant. With the other extreme, a low friction surface, the driver must take great care not to apply too much pedal force as this would cause the front axle to lock, resulting in a complete loss of steering and a significant loss in deceleration. Yet the driver must still be able to come close enough to the limit pedal force that the differences of several hundreths of a g in deceleration capability between the differently proportioned vehicles are significant.

Regarding the question "Which regulatory philosophy leads to greater accident-avoidance capability?", the tentative conclusion is that the U.S. regulation forces a proportioning selection that results in a marginally better stopping distance performance than does a proportioning selection intended to comply with the European regulations. The difference in proportioning is not as significant as the choice of tires with which the vehicle is equipped. The difference in performance capability would not be significant to "safety quality" unless extremely skilled drivers are assumed to be in control.

It should be noted that when a so-called "U.S. proportioning" is assumed, the rear wheels locked before the front when a vehicle in the unloaded condition is braked on a high friction surface. However, the decelerations achieved before lock up occurred were about .9 g's, a value well above the deceleration levels covered in any regulation.

Although the adhesion utilization of the rear axle was much higher than that of the front, the friction available at the rear axle was always higher than the friction at the front axle due to load sensitivities of the pneumatic tire.

Activities conducted by NHTSA towards extending the current regulations to include the braking-in-a-turn condition were reviewed. Although the NHTSA has been pursuing the topic for several years, the most recent study [22] concluded that no justification existed for supplementing 105-75 with braking-in-a-turn tests. Not withstanding this finding, the ISO is actively pursuing a braking-in-a-turn test standard.

The ISO is concurrently developing two braking-in-a-turn test procedures. The first, suggested by France, consists of measuring stopping distances accrued while braking in a constant-radius turn, with continual driver correction allowed (thus placing the test into the category of closed-loop testing). The results of the computer simulations of closed-loop braking-in-a-turn maneuvers on a high friction surface, which were carried out in Section 3.0, indicate that variations between straight-line stopping distance and in-a-turn stopping distance are not systematically influenced by proportioning. Thus the addition of a closed-loop braking-in-turn test to ECE R.13 should not impose any further constraints on the selection of proportioning for a passenger car. The second test procedure is an open-loop type test, where steering correction by the driver is not permitted after the brakes are applied. This latter test has undergone a great deal of developmental activity resulting in the test maneuver being fairly well established in terms of initial speed, surface type, and initial lateral acceleration. However, the index used to gauge performance has not been clarified. Presumably, the purpose of the test is to measure the change in path curvature which is due to braking in a steady turn. Suggested performance indices are lateral acceleration, yaw rate,

vehicle slip angle, and longitudinal deceleration, measured either one second after the time of brake application or averaged over some period of time.

The additional constraints imposed by the proposed open-loop braking-in-a-turn test cannot be quantified until the required performance levels have been decided upon. Simulations of the open-loop braking-in-a-turn maneuver were carried out, covering the two extreme load conditions of the two representative vehicles, using steer angles set to achieve the two different initial lateral accelerations being considered by the ISO. Proportioning and deceleration (through the brake line pressure) were varied and all of the proposed performance indices were tabulated. Thus, if one of the indices is given a value, the tables can be used to derive the proportioning boundary for various deceleration levels. The actual path curvature, normalized by the initial radius of the turn and averaged over the first one second following brake application, was also calculated from the simulations to present the "ideal" performance measure. Plots were prepared which show lines of constant normalized curvature in the space defined by proportioning and deceleration. (These plots, and the aforementioned tables, are all included in Appendix C.)

There appears to be a concern within Europe that passenger cars might be proportioned so heavily towards the front axle that steering could be lost prematurely when braking in a turn. A braking-in-turn regulation, as might come to pass in Europe, would probably limit the loss of path curvature during the first one second after brake application. The results obtained in this study indicate that a loss of path curvature is much more sensitive to deceleration than to proportioning. This is because the path curvature of the vehicle in the early period of the braking-in-a-turn process is a function of the transient response to the braking input and the deceleration level affects the

transient behavior much more than proportioning. The simulations conducted in this study involved a high friction surface, and it was noted that the deceleration level had to be very high in order for any amount of path curvature to be lost over proportioning ranges which extended slightly beyond those imposed by the United Nations regulation ECE R.13. It appears that this type of regulation would mainly influence tire selection, but if the tires were marginal regarding their frictional limits, a lower proportioning would increase the likelihood of compliance.

REFERENCES

1. Oppenheimer, Paul. "Braking Regulations in Europe." SAE Paper No. 740313, February-March, 1974.

2. Oppenheimer, Paul. "Braking Regulations for Passenger Cars." SAE Paper No. 770182, February-March, 1977.

3. Seiffert, U.W., Marks, H.-G., and Ziwica, K.-H. "Hydraulic Brake System U.S. Versus Common Market." SAE Paper No. 760219, February, 1976.

4. Aoki, Kazuhiko. "A Comparison of World Braking Standards with Reference to the Development of Japanese Braking Standards." SAE Paper No. 720030, January, 1972.

5. Braking Standard #105-75. Federal Register, Vol. 41, No. 139, Monday, July 19, 1976.

6. United Nations. Agreement Concerning the Adoption of Uniform Conditions of Approval and Reciprocal Recognition of Approval for Motor Vehicle Equipment and Parts. Addendum 12: Regulation No. 13, Uniform Provisions Concerning the Approval of Vehicles with Regard to Braking. Geneva, March 20, 1958.

7. European Communities Council Directive. On the Approximation of the Laws of Member States Relating to the Braking of Certain Motor Vehicles and Their Trailers (71/320/EEC), September 6, 1971.

8. Regulations for Braking Systems on Motor Vehicles and Trailers Which are Coupled to Vehicles (F-18). Sweden, December 29, 1971.

9. Schuring, D.J. Tire Parameter Determination. Final Report, Contract DOT-HS-4-00923, Calspan Corporation, December 1975.

10. Bernard, James E., et al. Vehicle-In-Use Limit Performance and Tire Factors: The Tire In Use. Final Report, Contract No. DOT-HS-031-3-693, Highway Safety Research Institute, Univ. of Michigan, March, 1975.

11. Ervin, R.D., et al. Vehicle Handling Performance. Final Report, Contract No. DOT-HS-031-1-159, Highway Safety Research Institute, Univ. of Michigan, November 1972.

12. Rice, Roy S. and Davis, James A. Vehicle Directional Control During Braking-in-a-Turn. Final Report, Control No. DOT-HS-4-00971, Calspan Corporation, July, 1975.

13. ISO Document 84. Proposal for Straight-Line and In-a-Turn Braking Test Procedures. Torino, Italy, June, 1975.

14. ISO Document 85. Straight-Line and In-A-Turn Braking Tests - Procedure Discussion and Analysis of the Experimental Results.

15. International Organization for Standardization. ISO/TC 22/SC 9 N 122. Italian Draft Proposal for an "In-a-Turn Braking Test Procedure." August 1977.

16. International Organization for Standardization. ISO/TC 22/SC 9 N 131. Results of Informal Group Meeting, The Hague, August 27, 1977.

17. ISO/TC 22/SC 9 N 143. Ad-hoc WG "Braking in a Turn" Open-Loop Test Procedure Draft. March, 1978.

18. ISO/TC 22/SC 9 N 150. Brief Minutes on the 8th Meeting Held in London. April 1978.

19. ISO/TC 22/SC 9 N 144. Ad-hoc WG "Braking in a Turn" Closed-Loop Test Procedure Draft. March 1978.

20. Boyer, R.C. and Enserink, E. Passenger Car Directional Control Test Program. Final Report, Contract DOT-HS-046-3-667, Ultrasystems, Inc., Phoenix, Arizona, December 1973.

21. Gilchrist, Arnold and Enserink, Bert. Passenger Car Braking Performance. Final Report, Contract DOT-HS-4-00932, Ultrasystems, Inc., Phoenix, Arizona, February 1976.

22. Ervin, R.D., et al. Improved Passenger Car Braking Performance. Final Report, Contract No. DOT-HS-6-01368, Highway Safety Research Institute, Univ. of Michigan, March 1978.

23. Bernard, James E. "Some Time-Saving Methods for the Digital Simulation of Highway Vehicles." Simulation, Vol. 21, No. 6, December 1973.

24. Goes, F. and Fischer, A. "Handling Performance Requirements of Automobiles--Discussed in the Context of the VW Golf." SAE Paper No. 741041, October 1974.

25. Bernard, J.E., Segel, L., and Wild, R.E. "Tire Shear Force Generation During Combined Steering and Braking Maneuvers." SAE Paper No. 770852, September 1977.

26. Tielking, J.T. Tire Traction Data Measured by the HSRI Mobile Tire Tester. Document 5, Highway Safety Research Institute, Univ. of Michigan, sponsored by the Motor Vehicle Manufacturers Association, March 1973.

27. Holmes, K.E. and Stone, R.D. Tyre Forces as Functions of Cornering and Braking Slip on Wet Road Surfaces. Road Research Laboratory Report No. LR 254, 1969.

APPENDIX A

SIMULATION DETAILS

This appendix contains a brief summary of the vehicle and tire models which were used in the computer simulation activities. Since these models have been described in detail in another report [10], only brief descriptions are given in this appendix, with the exception that changes from the original model are discussed in some detail. This appendix also presents tire and vehicle parameter data and discusses the sources and reliability of the data when appropriate.

A.1 The Vehicle Model

The vehicle model utilized for this study is a fourteen degree-of-freedom representation of a conventional passenger car with a solid rear axle and an independent front suspension. The various degrees of freedom are:

- body translation in the longitudinal, lateral, and vertical directions,
- body rotation about the pitch, yaw, and roll axes,
- vertical translation of the two front wheels,
- vertical and rolling motion of the rear axle, and
- the spin rotation of each wheel.

Several time-saving steps are utilized in implementing the dynamic equations, as discussed in reference [23]. Accordingly, the simulations are fairly economical to run, given the complexity of the model, as developed.

The steering system is described by a quasi-static model, which accounts for compliance in the system but not for any mass. The suspension rates are input in tabular form in order to account for the non-linear character of the bump stops, which are important when simulating limit maneuvers. The kinematic properties determined by suspension geometry are represented either by table look-ups or by coefficients, depending on the extent of the vehicle data available. Shock absorbers are assumed to be bilinear, that is, one rate for compression, and another for rebound.

Early in the study, the simulation was modified to accept arbitrary initial conditions. In this manner, braking-in-a-turn simulations become very efficient when one run is made to determine the response to a steer input and the final steady turn conditions are then used as initial conditions for the braking runs. This procedure cut the computer costs nearly in half, by cutting the braking-in-a-turn simulation times in half.

It was found that the computer program was inadequate for simulating braking performance as the vehicle slowed to a low speed, under many conditions, so the braking simulations were usually restricted to 1-1/2 to 2-1/2 seconds in duration. By that time, the vehicle reached a quasi steady state, any wheels that were going to lock-up had done so, and the longitudinal deceleration had settled to a state where it changed very slowly with time or remained constant. When results were needed right up to the condition of zero velocity, a separate program was used to "finish" the run. This was done by linearly regressing the deceleration time history for the final one second of the simulation, and then analytically integrating the regressed curve, using the velocity and stopping distance conditions at the end of the simulation as initial conditions for the analytic solution.

A.2 Sources of Vehicle Data

The large amount of parameter data required by the computer simulation program was obtained from a variety of sources, as discussed below.

General Motors provided chassis and inertial parameter data for a "1978 GM Intermediate Special Coupe" for a two-passenger load condition. These data were converted to the format needed by the HSRI simulation, and constituted the source of information on suspension geometry, steering compliance, inertias of the sprung mass, and the height of the c.g. Physical dimensions, weights, and spring rates were taken from the specifications of the Monte Carlo published by the MVMA. GAWR data were provided by GM, and the few remaining parameter items were estimated from measurements made on similar vehicles.

The Volkswagon Golf was selected as the representative European car

primarily because VW has published two papers which list many properties of the Golf (and/or its the American version, the Rabbit) [3, 24]. These papers provided the parameter values pertaining to suspension geometry, steering compliance, spring rates, roll stiffnesses, physical dimensions, and c.g. height. Weights of the base vehicle and of the various options, along with GAWR data, were provided by VW. The remaining parameter values were estimated from measurements made on similar vehicles.

The passenger car simulation and the VW Golf are not truly compatable, since the simulations assume a vehicle with a solid rear axle, whereas the Golf has an independent rear suspension. It was also noted that the resonant frequencies of the unsprung masses are much higher (about 15 Hz) for this vehicle than for most passenger cars, and would therefore require a smaller time step in the integration routine. In order to minimize the computational costs, the values of the unsprung masses were adjusted to permit use of the original time step, and the sprung mass parameter data were adjusted to maintain the correct fore/aft load distribution. Neither of these incompatabilities are significant in the context of the maneuvers which were simulated, but the errors which could arise from using the values given in this appendix should be considered if they will be used within a different context, such as a ride study.

A.3 The Tire Model

The mathematical model used to simulate the pneumatic tires was developed at HSRI for the purpose of providing accurate estimates of longitudinal and lateral tire forces over a range of slip angles and longitudinal slip ratios which occur during limit maneuvers. An advantage of the model is that very few tire parameters are needed, as the model is based on an analysis of the mechanical deformation of the tire when cornering and braking, instead of being a series of arbitrary mathematical functions which are fitted to measured data in the fashion of many other tire models.

The tire model does not predict any moments, but aligning torque is included in the simulation by considering the kingpin offset and a

constant mechanical trail. In addition, aligning torque from the tires can be input in tabular form. The model is fully described in reference [25].

A.4 Sources of Tire Data

The 1978 Monte Carlo is equipped with P205/70R-14 tires. This size corresponds to the older GR70-14 size designation. Laboratory measurements have been made by Calspan and published [9] for several tires of this type, but the utility of the data is limited because the testing did not cover simultaneous braking and steering, and the test surface was a steel belt instead of an actual road surface. Road tests of an FR70-14 tire were made by HSRI with a mobile tire tester, which covered several surface conditions and combined steering and braking [26], but these measurements were all made at one load. The tire parameters used in the simulations performed in this study were obtained by combining these two sources.

The HSRI data covered four surface conditions, namely wet and dry asphalt and wet and dry concrete. The wet and dry asphalt data were selected to represent the medium and the high friction surfaces needed for the simulations of non-test conditions, and the dry asphalt data were also used for simulating the open-loop ISO braking-in-a-turn tests. In both cases, the parameter values were selected by using a numerical minimization algorithm to "optimize" the match between the measured and predicted forces over a broad traction field of longitudinal slip ratios and slip angles. (It should be noted that agreement between the measured data and theory was not exact at the free-rolling, zero slip condition, as the agreement there was "traded off" to get a better match at other slip ratios.) The model predicts a rise in lateral force with slight braking, but in this case, the effect was not evident in the measurements, so to compensate, a lower cornering stiffness was used. It was found that good agreement was impossible for the wet asphalt data, so the minimization algorithm was used over a limited portion of the traction field which was considered to be most important, that is, low slip angles (0° - 4°) and low slip ratios (0% - 40%).

The Calspan data has an advantage in that great attention was paid to determining the variation in tire properties due to load changes. While the measurements were made on a steel surface instead of asphalt, it can be argued that the force-producing mechanisms in a pneumatic tire are very similar on different dry surfaces. The Calspan data were therefore utilized to introduce load sensitivities to the tire properties by normalizing the changes in C_α, C_s, μ_x, and μ_y to percentage changes, and then applying the percentage changes to the values derived from the HSRI data. The force producing mechanisms differ between wet and dry surfaces, so the Calspan data were not used to introduce load sensitivities to the wet asphalt data.

The third surface condition is a low friction surface, such as a polished surface with significant water depth. No measurements were found for the proper size and construction of tire on this type of surface, so all of the parameter values for the wet asphalt condition were used, except for the friction coefficients μ_x and μ_y. These coefficients were set at "typical" values published for a range of tires on wet, polished roads [27].

The VW Golf is equipped with 155 SR-13 tires, and no traction field measurements could be found for this tire. The tire is included in the Calspan library, however. Accordingly, the measurements published by Calspan were used to describe this tire. The parameters which are specific to the HSRI model were selected according to the recommendations made in reference [10] for radial tires. The friction coefficients, μ_x and μ_y, were set for dry and wet asphalt by assuming the same ratios between μ measured on the Calspan test belt and the μ as measured by HSRI for the FR70-14 tire. The values of μ_x and μ_y were set for the low friction surface to correspond with published measurements made with other tires [27], and were identical to the values used for the FR70-14 tire.

A.5 Vehicle and Tire Parameter Values

The parameter data used to describe the two vehicles are presented in Tables A.1 - A.5. The feedback gains used in the automatic steering

controller are presented in Table A.6. The units are: proportional feedback (GAINP), radian/ft; integral feedback (GAINI), radian/ft/sec; derivitive feedback (GAIND), radian-sec/ft. The turn radius was 535 ft., for the .2 g turn, and 268 ft., for the .4 g turn.

Tables A.7 - A.9 present the tire parameters extracted according to the above discussion. Tire forces which are predicted by the model from these parameter values are plotted as functions of longitudinal slip in Figures A.1 - A.8 and, when applicable, measured forces are also plotted to provide a comparison between the theory and the reality.

Table A.1. Vehicle Parameter Values for a Domestic Intermediate Sized Car Equipped with Many Options, and Lightly Loaded.

INPUT PARAMETER TABLE

SYMBOL	DESCRIPTION	INITIAL VALUE
INIT	KEY. INCLUDE INITIAL CONDITIONS IF .NE. 0	1
NBUMP	NUMBER OF BUMPS	0
A1	HORIZONTAL DISTANCE FROM CG TO MIDPOINT OF FRONT SUSPENSION (IN)	43.40
A2	HORIZONTAL DISTANCE FROM CG TO MIDPOINT OF REAR SUSPENSION (IN)	64.70
ALPHA1	STATIC DISTANCE, FRONT AXLE TO GROUND (IN)	11.50
ALPHA2	STATIC DISTANCE, REAR AXLE TO GROUND (IN)	11.50
AN1	TIRE PRESSURE DISTRIBUTION FUNCTION, FRONT	0.40
AN2	TIRE PRESSURE DISTRIBUTION FUNCTION, REAR	0.40
C1	VISCOUS DAMPING: BOUNCE ON FRONT AXLE (LB-SEC/IN)	3.00
C2	VISCOUS DAMPING: REBOUND ON FRONT AXLE (LB-SEC/IN)	6.00
C3	VISCOUS DAMPING: BOUNCE ON REAR AXLE (LB-SEC/IN)	4.00
C4	VISCOUS DAMPING: REBOUND ON REAR AXLE (LB-SEC/IN)	10.00
CALF1	LATERAL STIFFNESS, FRONT TIRE, ONE SIDE (LBS/DEG)	-1.00
CF1	MAXIMUM COULOMB FRICTION, FRONT SUSPENSION (LB)	50.00
CF2	MAXIMUM COULOMB FRICTION, REAR SUSPENSION (LB)	30.00
CGAMMA	CAMBER STIFFNESS, ONE SIDE (LBS/DEG)	10.00
DELTA1	STATIC VERTICAL DISTANCE, FRONT AXLE TO SPRUNG MASS CG (IN)	11.50
FA1	FRICTION REDUCTION PARAMETER, FRONT TIRES	0.002
FA2	FRICTION REDUCTION PARAMETER, REAR TIRES	0.002
G1	GRAVITY X COMPONENT	0.0
G2	GRAVITY Y COMPONENT	0.0
GR	STEERING GEAR RATIO	16.00
IXX	SPRUNG MASS ROLL MOMENT OF INERTIA (IN-LB-SEC**2)	5340.00
IYY	SPRUNG MASS PITCH MOMENT OF INERTIA (IN-LB-SEC**2)	23520.00
IZZ	SPRUNG MASS YAW MOMENT OF INERTIA (IN-LB-SEC**2)	25600.00
IXZ	SPRUNG MASS PITCH PLANE CROSS MOMENT (IN-LB-SEC**2)	300.00
JA2	ROLL MOMENT OF REAR AXLE (IN-LB-SEC**2)	350.00
JS1	POLAR MOMENT OF FRONT WHEEL, ONE SIDE (IN-LB-SEC**2)	10.00
JS2	POLAR MOMENT OF REAR WHEEL, ONE SIDE (IN-LB-SEC**2)	10.00
K1	SPRING RATE, FRONT SUSPENSION (LB/IN)	-1.00
K2	SPRING RATE, REAR SUSPENSION (LB/IN)	-1.00

Table A.1. (Cont.)

KPOFF	KINGPIN OFFSET(IN)	1.50
KSC	STEERING COLUMN SPRING RATE (IN-LB/RAD.)	1396.00
KSL	STEERING LINKAGE SPRING RATE, ONE SIDE (IN-LB/RAD.)	100000.00
KSW	STEERING TABLE KEY	4
KT1	SPRING RATE, FRONT TIRE, ONE SIDE (LB/IN)	1300.00
KT2	SPRING RATE, REAR TIRE, ONE SIDE (LB/IN)	1300.00
PW	WEIGHT OF PAYLOAD (LBS)	0.0
RCH1	ROLL CENTER HEIGHT, FRONT SUSPENSION (IN)	1.60
RCH2	ROLL CENTER HEIGHT, REAR SUSPENSION (IN)	15.30
ROLLF	FRONT AUXILIARY ROLL STIFFNESS (IN-LB/DEG)	4900.00
ROLLR	REAR AUXILIARY ROLL STIFFNESS (IN-LB/DEG)	900.00
RSCS	ROLL STEER COEFFICIENT AT STATIC EQUILIBRIUM (OVERSTEER IS POSITIVE)	-0.05
SY1	HORIZONTAL DISTANCE FROM BODY X-AXIS TO FRONT SUSPENSION (IN)	29.25
SY2	HORIZONTAL DISTANCE FROM BODY X-AXIS TO REAR SUSPENSION (IN)	18.50
TIMF	MAXIMUM REAL TIME FOR SIMULATION (SEC)	2.00
TRA1	FRONT HALF TRACK (IN)	29.25
TRA2	REAR HALF TRACK (IN)	28.90
TRAIL	MECHANICAL TRAIL(IN)	0.46
VEL	INITIAL VELOCITY (FPS)	52.00
WIND	TOTAL DRAG COEFFICIENT(LBS/(FT/SEC)**2)	0.02
W	SPRUNG WEIGHT OF CAR (LBS)	3288.00
WS1	WEIGHT OF FRONT SUSPENSION (LBS)	174.00
WS2	WEIGHT OF REAR SUSPENSION (LBS)	278.00

Table A.2. Vehicle Parameter Values for a Domestic Intermediate Sized Car Equipped with no Options, Loaded to the GVWR Condition.

INPUT PARAMETER TABLE

SYMBOL	DESCRIPTION	INITIAL VALUE
INIT	KEY. INCLUDE INITIAL CONDITIONS IF .NE. 0	1
NBUMP	NUMBER OF BUMPS	0
A1	HORIZONTAL DISTANCE FROM CG TO MIDPOINT OF FRONT SUSPENSION (IN)	45.90
A2	HORIZONTAL DISTANCE FROM CG TO MIDPOINT OF REAR SUSPENSION (IN)	62.20
ALPHA1	STATIC DISTANCE, FRONT AXLE TO GROUND (IN)	11.50
ALPHA2	STATIC DISTANCE, REAR AXLE TO GROUND (IN)	11.50
AN1	TIRE PRESSURE DISTRIBUTION FUNCTION, FRONT	0.27
AN2	TIRE PRESSURE DISTRIBUTION FUNCTION, REAR	0.27
C1	VISCOUS DAMPING: JOUNCE ON FRONT AXLE (LB-SEC/IN)	3.00
C2	VISCOUS DAMPING: REBOUND ON FRONT AXLE (LB-SEC/IN)	6.00
C3	VISCOUS DAMPING: JOUNCE ON REAR AXLE (LB-SEC/IN)	4.00
C4	VISCOUS DAMPING: REBOUND ON REAR AXLE (LB-SEC/IN)	10.00
CALF1	LATERAL STIFFNESS, FRONT TIRE, ONE SIDE (LBS/DEG)	-1.00
CF1	MAXIMUM COULOMB FRICTION, FRONT SUSPENSION (LB)	50.00
CF2	MAXIMUM COULOMB FRICTION, REAR SUSPENSION (LB)	30.00
CGAMMA	CAMBER STIFFNESS, ONE SIDE (LBS/DEG)	10.00
DELTA1	STATIC VERTICAL DISTANCE, FRONT AXLE TO SPRUNG MASS CG (IN)	11.50
FA1	FRICTION REDUCTION PARAMETER, FRONT TIRES	0.009
FA2	FRICTION REDUCTION PARAMETER, REAR TIRES	0.009
G1	GRAVITY X COMPONENT	0.0
G2	GRAVITY Y COMPONENT	0.0
GR	STEERING GEAR RATIO	16.00
IXX	SPRUNG MASS ROLL MOMENT OF INERTIA (IN-LB-SEC**2)	4650.00
IYY	SPRUNG MASS PITCH MOMENT OF INERTIA (IN-LB-SEC**2)	20500.00
IZZ	SPRUNG MASS YAW MOMENT OF INERTIA (IN-LB-SEC**2)	22200.00
IXZ	SPRUNG MASS PITCH PLANE CROSS MOMENT (IN-LB-SEC**2)	300.00
JA2	ROLL MOMENT OF REAR AXLE (IN-LB-SEC**2)	350.00
JS1	POLAR MOMENT OF FRONT WHEEL, ONE SIDE (IN-LB-SEC**2)	10.00
JS2	POLAR MOMENT OF REAR WHEEL, ONE SIDE (IN-LB-SEC**2)	10.00
K1	SPRING RATE, FRONT SUSPENSION (LB/IN)	-1.00
K2	SPRING RATE, REAR SUSPENSION (LB/IN)	-1.00

Table A.2. (Cont.)

KPOFF	KINGPIN OFFSET(IN)	1.50
KSC	STEERING COLUMN SPRING RATE (IN-LB/RAD.)	1396.00
KSL	STEERING LINKAGE SPRING RATE, ONE SIDE (IN-LB/RAD.)	10000.00
KSW	STEERING TABLE KEY	4
KT1	SPRING RATE, FRONT TIRE, ONE SIDE (LB/IN)	1300.00
KT2	SPRING RATE, REAR TIRE, ONE SIDE (LB/IN)	1300.00
PW	WEIGHT OF PAYLOAD (LBS)	877.00
PJ1	ROLL MOMENT OF INERTIA OF PAYLOAD (IN-LB-SEC**2)	0.0
PJ2	PITCH MOMENT OF INERTIA OF PAYLOAD (IN-LB-SEC**2)	0.0
PJ3	YAW MOMENT OF INERTIA OF PAYLOAD (IN-LB-SEC**2)	0.0
PX	HORIZONTAL DISTANCE FROM MIDPOINT OF REAR SUSPENSION TO PAYLOAD MASS CENTER (IN)	21.60
PZ	VERTICAL DISTANCE FROM GROUND TO PAYLOAD MASS CENTER (IN)	23.00
RCH1	ROLL CENTER HEIGHT, FRONT SUSPENSION (IN)	1.60
RCH2	ROLL CENTER HEIGHT, REAR SUSPENSION (IN)	15.30
ROLLF	FRONT AUXILIARY ROLL STIFFNESS (IN-LB/DEG)	4900.00
ROLLR	REAR AUXILIARY ROLL STIFFNESS (IN-LB/DEG)	900.00
RSCS	ROLL STEER COEFFICIENT AT STATIC EQUILIBRIUM (OVERSTEER IS POSITIVE)	-0.05
SY1	HORIZONTAL DISTANCE FROM BODY X-AXIS TO FRONT SUSPENSION (IN)	29.25
SY2	HORIZONTAL DISTANCE FROM BODY X-AXIS TO REAR SUSPENSION (IN)	18.50
TIMF	MAXIMUM REAL TIME FOR SIMULATION (SEC)	3.00
TRA1	FRONT HALF TRACK (IN)	29.25
TRA2	REAR HALF TRACK (IN)	28.90
TRAIL	MECHANICAL TRAIL(IN)	0.46
VEL	INITIAL VELOCITY (FPS)	58.70
WIND	TOTAL DRAG COEFFICIENT(LBS/(FT/SEC)**2)	0.02
W	SPRUNG WEIGHT OF CAR (LBS)	2982.00
WS1	WEIGHT OF FRONT SUSPENSION (LBS)	174.00
WS2	WEIGHT OF REAR SUSPENSION (LBS)	278.00

Table A.3. Suspension Characteristics of the Domestic Intermediate Car.

```
      SPRING COMPRESSION (IN) VS FORCE
     FRONT SUSPENSION  ...ONE SPRING ONLY
     NOTE:  BOTH FRONT SPRINGS ARE IDENTICAL
     REFERENCE SYSTEM: (0.0, -WS2/2.) AT THE REBOUND STOP,
     THEN INCREASINGLY POSITIVE FORCES FOR INCREASING
     COMPRESSIVE LOADS IN THE SPRING.
     NO. OF POINTS:  4
 -2.0000    -2087.0000
  1.7700      800.0000
  5.3900     1126.0000
 10.0000     3431.0000


      SPRING COMPRESSION (IN) VS FORCE
     REAR SUSPENSION  ...ONE SPRING ONLY
     NOTE:  BOTH REAR SPRINGS ARE IDENTICAL
     REFERENCE SYSTEM: (0.0, -WS1/2.) AT THE REBOUND STOP,
     THEN INCREASINGLY POSITIVE FORCES FOR INCREASING
     COMPRESSIVE LOADS IN THE SPRING.
     NO. OF POINTS:  4
 -2.0000    -2139.0000
  1.4000      700.0000
  6.4000     1200.0000
 10.0000     3000.0000

      SUSPENSION COMPRESSION (IN) VS TOE
    (FOR LEFT FRONT WHEEL, TOE FOLLOWS RIGHT HAND RULE.)
    ZERO COMPRESSION AT THE REBOUND STOP
    NO. OF POINTS: 2
    -7.350       -1.623
    12.650        1.863

      SUSPENSION COMPRESSION (IN) VS CAMBER (DEG)
      ZERO COMPRESSION AT THE REBOUND STOP
      NO. OF POINTS:  1
-10.0000        0.0
```

Table A.4. Vehicle Parameter Values of the European Subcompact Car, Equipped with Front End Option, for the Light and GVWR Loading Conditions.

INPUT PARAMETER TABLE

SYMBOL	DESCRIPTION	INITIAL VALUE
INIT	KEY. INCLUDE INITIAL CONDITIONS IF .NE. 0	0
NBUMP	NUMBER OF BUMPS	0
A1	HORIZONTAL DISTANCE FROM CG TO MIDPOINT OF FRONT SUSPENSION (IN)	31.87
A2	HORIZONTAL DISTANCE FROM CG TO MIDPOINT OF REAR SUSPENSION (IN)	62.63
ALPHA1	STATIC DISTANCE, FRONT AXLE TO GROUND (IN)	10.63
ALPHA2	STATIC DISTANCE, REAR AXLE TO GROUND (IN)	11.00
AN1	TIRE PRESSURE DISTRIBUTION FUNCTION, FRONT	0.0
AN2	TIRE PRESSURE DISTRIBUTION FUNCTION, REAR	0.0
C1	VISCOUS DAMPING: JOUNCE ON FRONT AXLE (LB-SEC/IN)	2.00
C2	VISCOUS DAMPING: REBOUND ON FRONT AXLE (LB-SEC/IN)	5.00
C3	VISCOUS DAMPING: JOUNCE ON REAR AXLE (LB-SEC/IN)	3.00
C4	VISCOUS DAMPING: REBOUND ON REAR AXLE (LB-SEC/IN)	8.00
CALF1	LATERAL STIFFNESS, FRONT TIRE, ONE SIDE (LBS/DEG)	-1.00
CF1	MAXIMUM COULOMB FRICTION, FRONT SUSPENSION (LB)	10.00
CF2	MAXIMUM COULOMB FRICTION, REAR SUSPENSION (LB)	10.00
CGAMMA	CAMBER STIFFNESS, ONE SIDE (LBS/DEG)	5.00
DELTA1	STATIC VERTICAL DISTANCE, FRONT AXLE TO SPRUNG MASS CG (IN)	10.27
FA1	FRICTION REDUCTION PARAMETER, FRONT TIRES	0.002
FA2	FRICTION REDUCTION PARAMETER, REAR TIRES	0.002
G1	GRAVITY X COMPONENT	0.0
G2	GRAVITY Y COMPONENT	0.0
G3	STEERING GEAR RATIO	18.70
IXX	SPRUNG MASS ROLL MOMENT OF INERTIA (IN-LB-SEC**2)	1795.00
IYY	SPRUNG MASS PITCH MOMENT OF INERTIA (IN-LB-SEC**2)	7300.00
IZZ	SPRUNG MASS YAW MOMENT OF INERTIA (IN-LB-SEC**2)	7547.00
IXZ	SPRUNG MASS PITCH PLANE CROSS MOMENT (IN-LB-SEC**2)	120.00
JA2	ROLL MOMENT OF REAR AXLE (IN-LB-SEC**2)	500.00
JS1	POLAR MOMENT OF FRONT WHEEL, ONE SIDE (IN-LB-SEC**2)	6.00
JS2	POLAR MOMENT OF REAR WHEEL, ONE SIDE (IN-LB-SEC**2)	6.00
K1	SPRING RATE, FRONT SUSPENSION (LB/IN)	-1.00
K2	SPRING RATE, REAR SUSPENSION (LB/IN)	-1.00

Table A.4. (Cont.)

KPOFF	KINGPIN OFFSET(IN)	-1.50
KSC	STEERING COLUMN SPRING RATE (IN-LB/RAD.)	1243.00
KSI	STEERING LINKAGE SPRING RATE, ONE SIDE (IN-LB/RAD.)	200000.00
KSW	STEERING TABLE KEY	1
KT1	SPRING RATE, FRONT TIRE, ONE SIDE (LB/IN)	1000.00
KT2	SPRING RATE, REAR TIRE, ONE SIDE (LB/IN)	1000.00
PW	WEIGHT OF PAYLOAD (LBS)	0.0
RCH1	ROLL CENTER HEIGHT, FRONT SUSPENSION (IN)	1.30
RCH2	ROLL CENTER HEIGHT, REAR SUSPENSION (IN)	0.0
ROLLF	FRONT AUXILIARY ROLL STIFFNESS (IN-LB/DEG)	0.0
ROLLR	REAR AUXILIARY ROLL STIFFNESS (IN-LB/DEG)	1200.00
RSCS	ROLL STEER COEFFICIENT AT STATIC EQUILIBRIUM (OVERSTEER IS POSITIVE)	0.05
SY1	HORIZONTAL DISTANCE FROM BODY X-AXIS TO FRONT SUSPENSION (IN)	27.35
SY2	HORIZONTAL DISTANCE FROM BODY X-AXIS TO REAR SUSPENSION (IN)	22.25
TIME	MAXIMUM REAL TIME FOR SIMULATION (SEC)	2.00
TRA1	FRONT HALF TRACK (IN)	27.35
TRA2	REAR HALF TRACK (IN)	22.25
TRAIL	MECHANICAL TRAIL(IN)	1.00
VEL	INITIAL VELOCITY (FPS)	58.70
WIND	TOTAL DRAG COEFFICIENT(LBS/(FT/SEC)**2)	0.02
W	SPRUNG WEIGHT OF CAR (LBS)	1785.00
WS1	WEIGHT OF FRONT SUSPENSION (LBS)	150.00
WS2	WEIGHT OF REAR SUSPENSION (LBS)	150.00

Payload Data for the GVWR Condition

PW	WEIGHT OF PAYLOAD (LBS)	671.00
PJ1	ROLL MOMENT OF INERTIA OF PAYLOAD (IN-LB-SEC**2)	0.0
PJ2	PITCH MOMENT OF INERTIA OF PAYLOAD (IN-LB-SEC**2)	0.0
PJ3	YAW MOMENT OF INERTIA OF PAYLOAD (IN-LB-SEC**2)	0.0
PX	HORIZONTAL DISTANCE FROM MIDPOINT OF REAR SUSPENSION TO PAYLOAD MASS CENTER (IN)	17.03
PZ	VERTICAL DISTANCE FROM GROUND TO PAYLOAD MASS CENTER (IN)	22.54

Table A.5. Suspension Characteristics of the European Subcompact Car.

SPRING COMPRESSION (IN) VS FORCE
FRONT SUSPENSION ...ONE SPRING ONLY
NOTE: BOTH FRONT SPRINGS ARE IDENTICAL
REFERENCE SYSTEM: (0.0, -WS2/2.) AT THE REBOUND STOP, THEN INCREASINGLY POSITIVE FORCES FOR INCREASING COMPRESSIVE LOADS IN THE SPRING.
NO. OF POINTS: 8

0.0	-165.0000
0.1000	0.0
0.3000	331.0000
3.3000	571.0000
4.8500	765.0000
5.8000	949.0000
6.0000	1166.0000
6.5000	1850.0000

SPRING COMPRESSION (IN) VS FORCE
REAR SUSPENSION ...ONE SPRING ONLY
NOTE: BOTH REAR SPRINGS ARE IDENTICAL
REFERENCE SYSTEM: (0.0, -WS1/2.) AT THE REBOUND STOP, THEN INCREASINGLY POSITIVE FORCES FOR INCREASING COMPRESSIVE LOADS IN THE SPRING.
NO. OF POINTS: 8

0.0	-47.5000
0.3000	29.0000
0.7500	157.0000
3.2000	314.0000
4.7000	457.0000
6.5000	714.0000
7.7000	1060.0000
7.8000	1260.0000

SUSPENSION COMPRESSION (IN) VS TOE
(FOR LEFT FRONT WHEEL, TOE FOLLOWS RIGHT HAND RULE.)
ZERO COMPRESSION AT THE REBOUND STOP
NO. OF POINTS: 7

0.200	0.333
1.000	0.300
2.400	0.170
3.000	0.050
3.900	-0.133
4.800	-0.400
5.800	-0.870

SUSPENSION COMPRESSION (IN) VS CAMBER (DEG)
ZERO COMPRESSION AT THE REBOUND STOP
NO. OF POINTS: 4

0.3000	1.8800
2.4000	0.5000
3.9000	-0.2500
6.0000	-0.5000

Table A.6. Automatic Controller Parameter Values for the Two Passenger Cars.

CONTROLLER VARIABLES:	CL= 10.0000
	GAINP= 2.0000
	GAINI= 0.0
	GAIND= 0.0200
	RCONST= 535.0000
	STL= 8.0000 DEG

European Car

CONTROLLER VARIABLES:	CL= 15.0000
	GAINP= 2.0000
	GAINI= 0.0
	GAIND= 0.0500
	RCONST= 535.0000
	STL= 8.0000 DEG

Domestic Car

Table A.7. Tire Parameter Values Used for the Domestic Car on Dry Asphalt.

VERTICAL LOAD VS LATERAL STIFFNESS (LBS/DEG)

AM = 0.396
FA = 0.002
NO. OF POINTS: 6

LOAD	STIFFNESS	CA1	CA2
0.0	134.0000	0.0001	100.0000
690.0000	134.0000	0.0001	100.0000
1034.0000	170.0000	0.0001	100.0000
1374.0000	185.0000	0.0001	100.0000
1720.0000	185.0000	0.0001	100.0000
2065.0000	174.0000	0.0001	100.0000

VERTICAL LOAD VS LONGITUDINAL STIFFNESS (LBS)

NO. OF POINTS: 5

0.0	16300.0000
1029.0000	16300.0000
1368.0000	20400.0000
1716.0000	19200.0000
2060.0000	26757.0000

VERTICAL LOAD VS MUZERO

NO.OF.POINTS: 5

0.0	1.1200	1.0200
800.0000	1.1200	1.0200
1368.0000	1.0420	0.9490
1716.0000	0.9980	0.9090
2060.0000	0.8990	0.8190

Table A.8. Tire Parameter Values Used for the European Car on Dry Asphalt.

VERTICAL LOAD VS LATERAL STIFFNESS (LBS/DEG)

AN = 0.001
FA = 0.002
NO. OF POINTS: 6

LOAD	STIFFNESS	CA1	CA2
0.0	120.0000	0.0	0.0
384.0000	120.0000	0.0	0.0
588.0000	127.0000	0.0	0.0
793.0000	130.0000	0.0	0.0
994.0000	119.0000	0.0	0.0
1195.0000	92.0000	0.0	0.0

VERTICAL LOAD VS LONGITUDINAL STIFFNESS (LBS)

NO. OF POINTS: 5

0.0	10526.0000
598.0000	10526.0000
801.0000	21372.0000
1003.0000	12223.0000
1203.0000	21855.0000

VERTICAL LOAD VS MUZERO

NO.OF.POINTS: 6

0.0	1.0200	1.2400
384.0000	1.0200	1.2400
588.0000	0.9600	1.1700
793.0000	0.9000	1.1200
994.0000	0.8500	1.0600
1195.0000	0.8300	1.0000

Table A.9. Tire Parameter Values Used for the Wet Road Surface.

Car Source	Surface	μ_x	μ_y	C_s	C_α	a/2ℓ	FA	CA1	CA2
Domestic	Wet Asphalt	.72	1.82	8820	166	.27	.009	4.1	12.
	Wet, Polished Surface	.45	.45	8820	166	.27	.009	4.1	12.
European	Wet Asphalt	.65	1.64	10000	125	0	.009	4.	12.
	Wet, Polished Surface	.45	.45	10000	125	0	.009	4.	12.

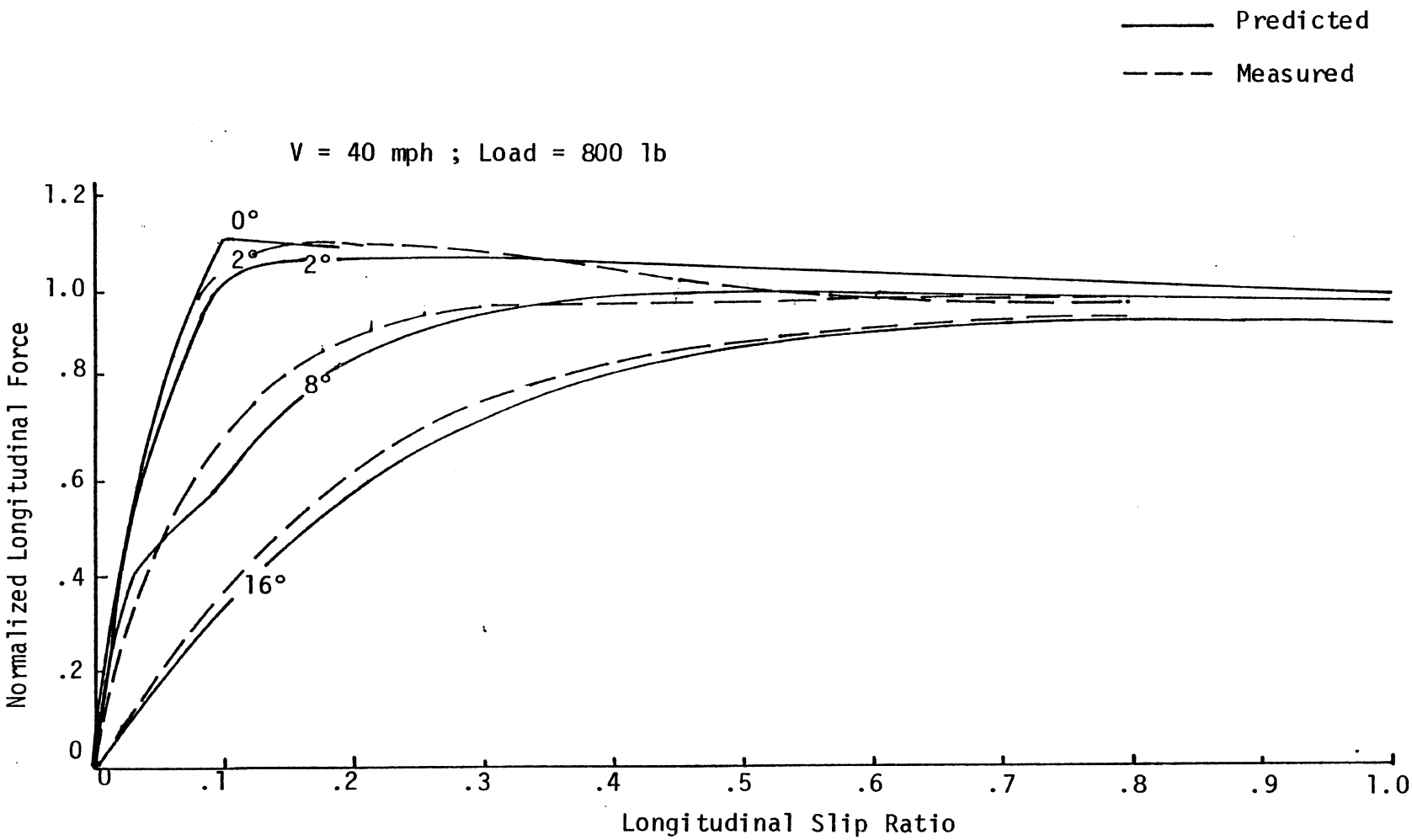

Figure A.1. Predicted and measured longitudinal force generated by the FR70-14 Tire on Dry Asphalt.

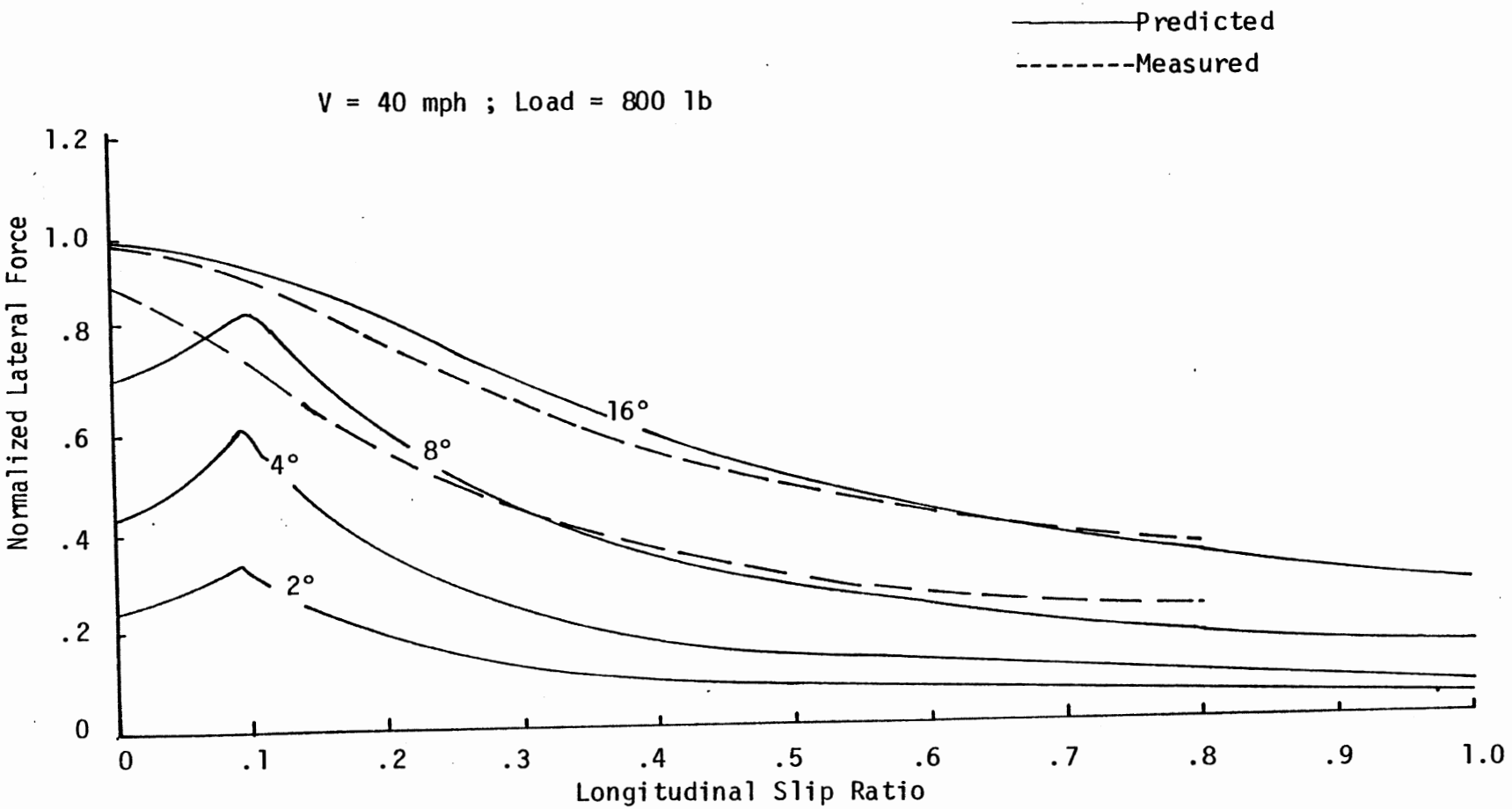

Figure A.2. Predicted and measured lateral force generated by the FR70-14 Tire on Dry Asphalt.

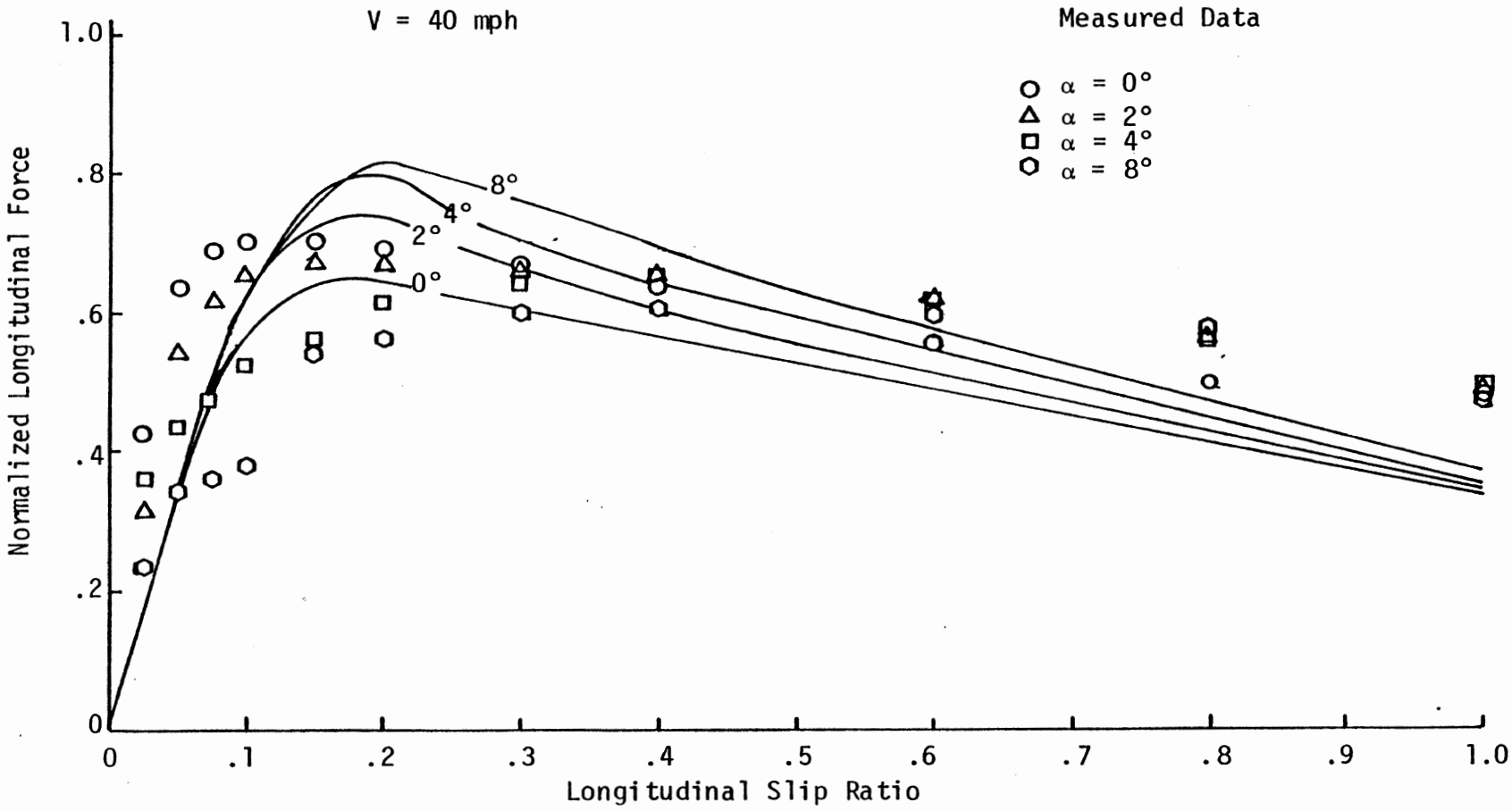

Figure A.3. Predicted and measured longitudinal force generated by the FR70-14 tire on wet asphalt.

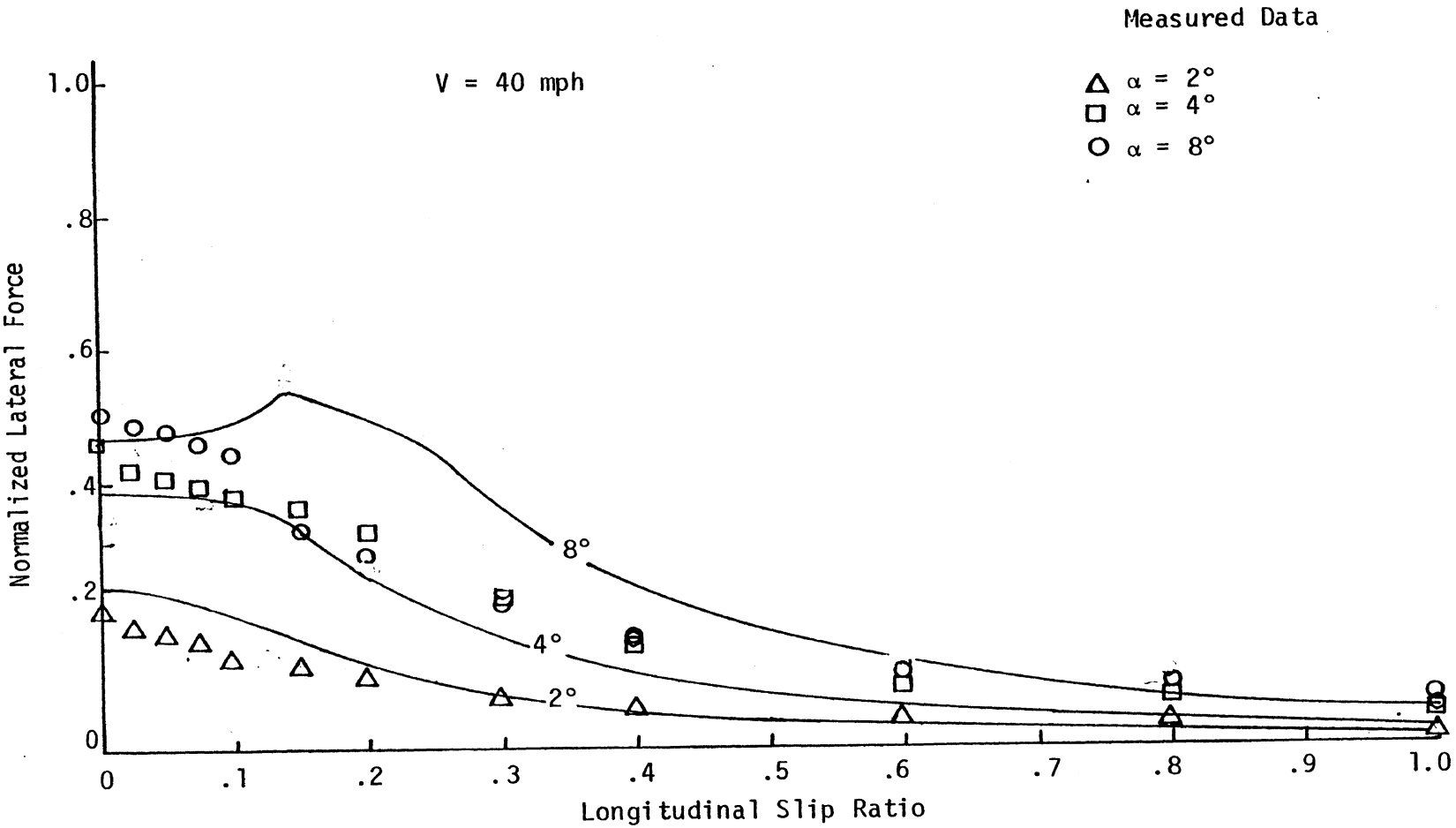

Figure A.4. Predicted and measured lateral force generated by the FR70-14 tire on wet asphalt.

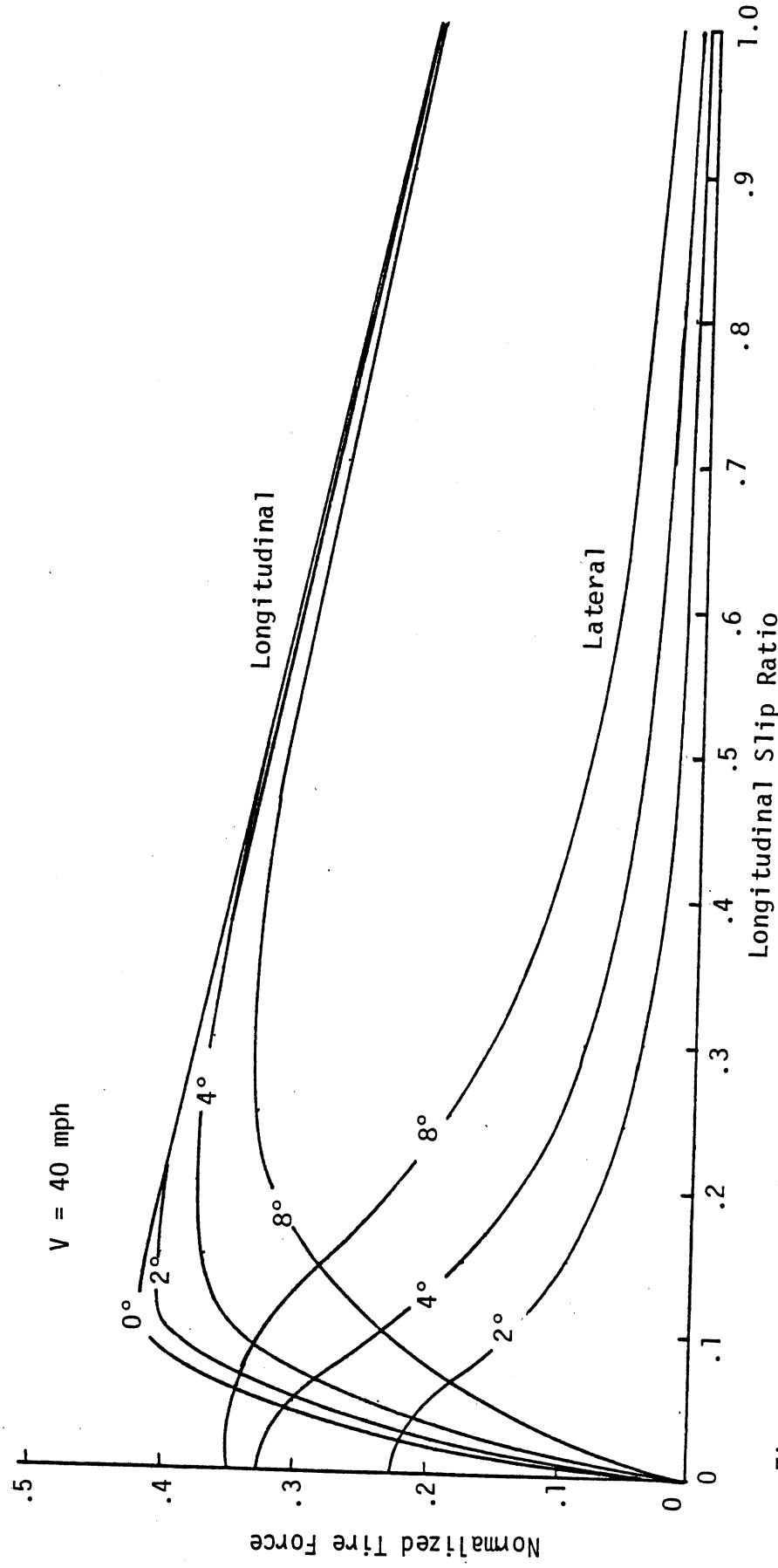

Figure A.5. Predicted tire forces generated by the FR70-14 tire on a wet, polished surface.

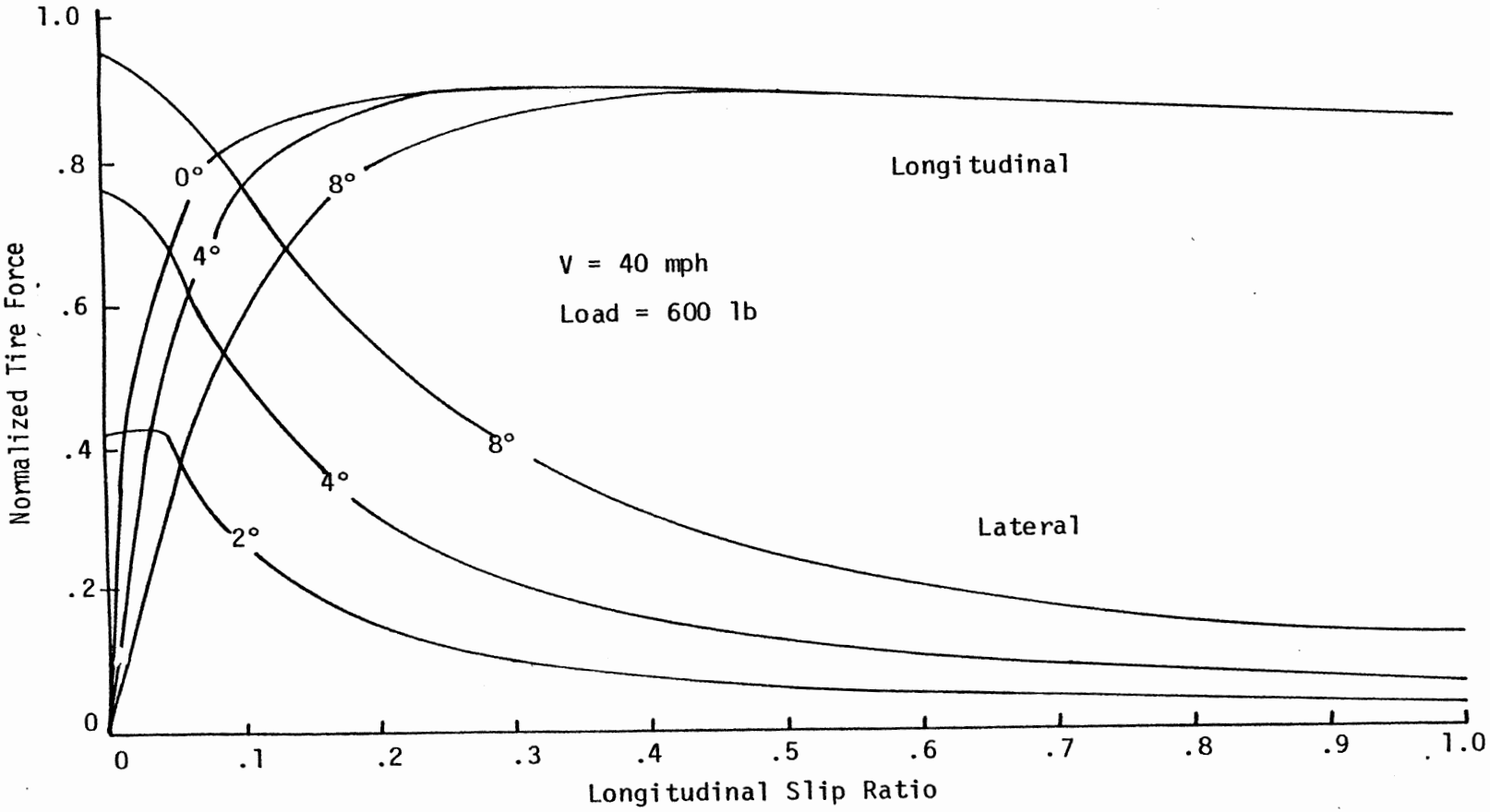

Figure A.6. Predicted tire forces generated by the 155 SR-13 tire on dry asphalt.

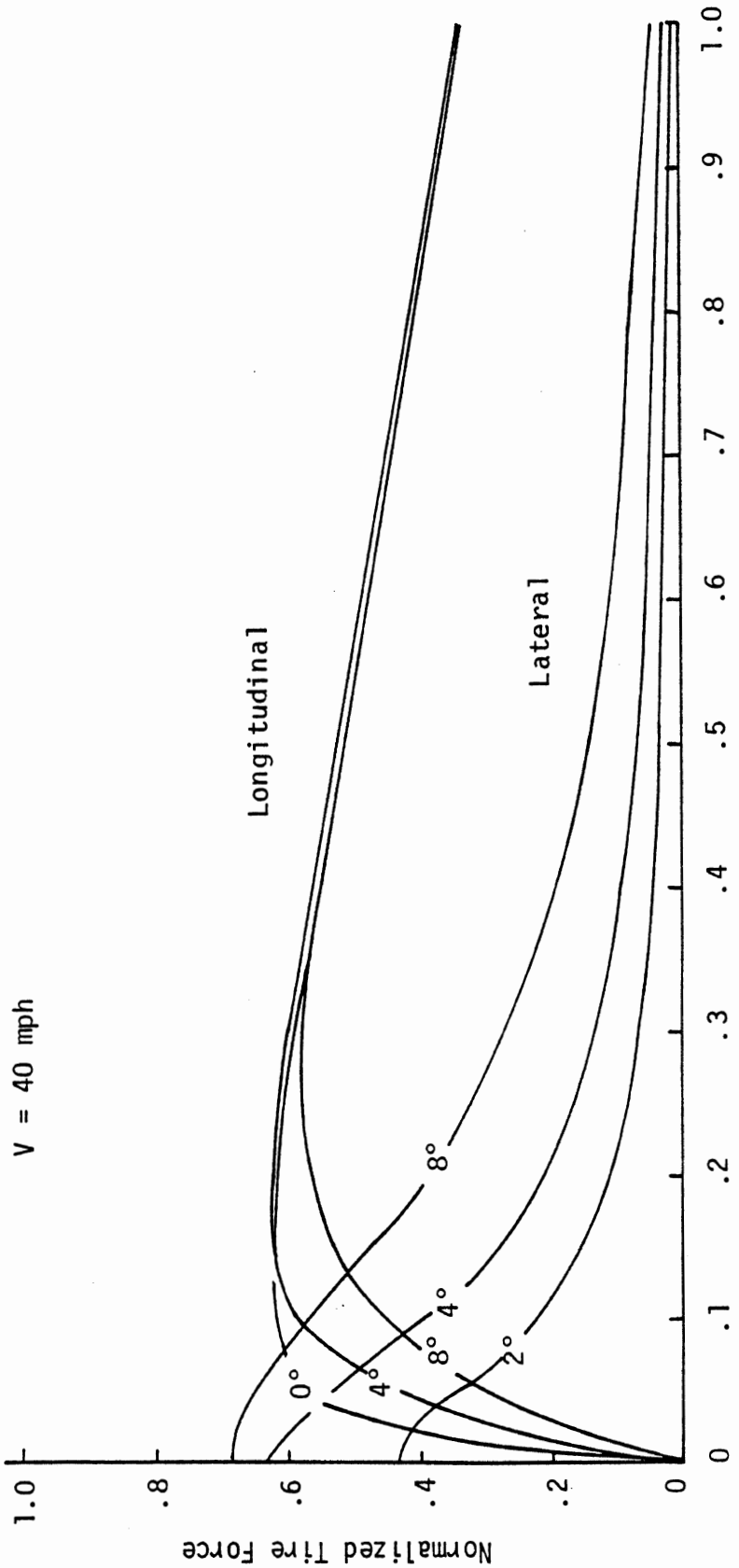

Figure A.7. Predicted tire forces generated by the 155 SR-13 tire on wet asphalt.

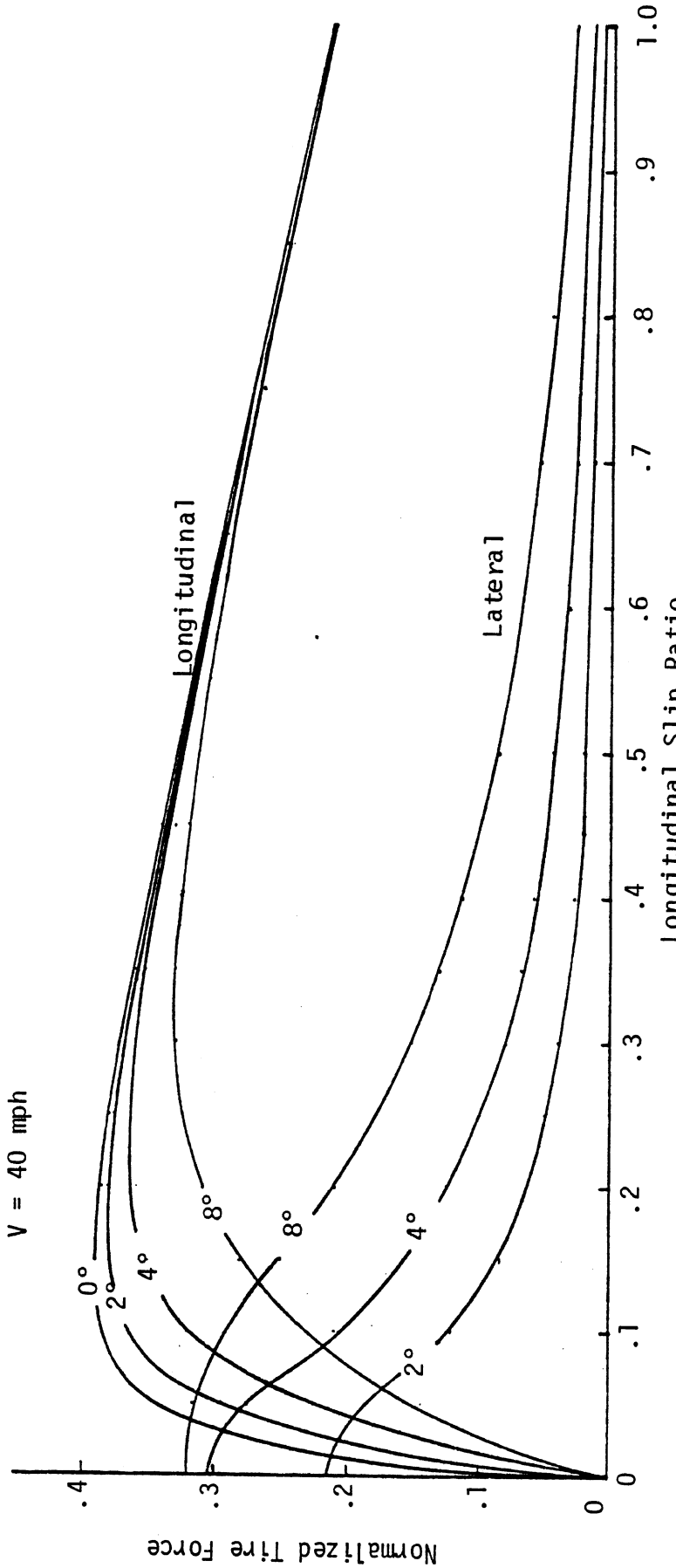

Figure A.8. Predicted tire forces generated by the 155SR-13 tire on a wet, polished surface.

APPENDIX B

SPEED VS. DISTANCE PLOTS, OBTAINED FROM COMPUTER SIMULATIONS OF BRAKING UNDER CONDITIONS NOT ADDRESSED IN THE VARIOUS REGULATIONS

This appendix contains speed vs. distance plots for the limit braking runs made for each combination of surface/vehicle/load/proportioning, simulated as described in section three of this report. These results were obtained with the models and input data described and presented in Appendix A.

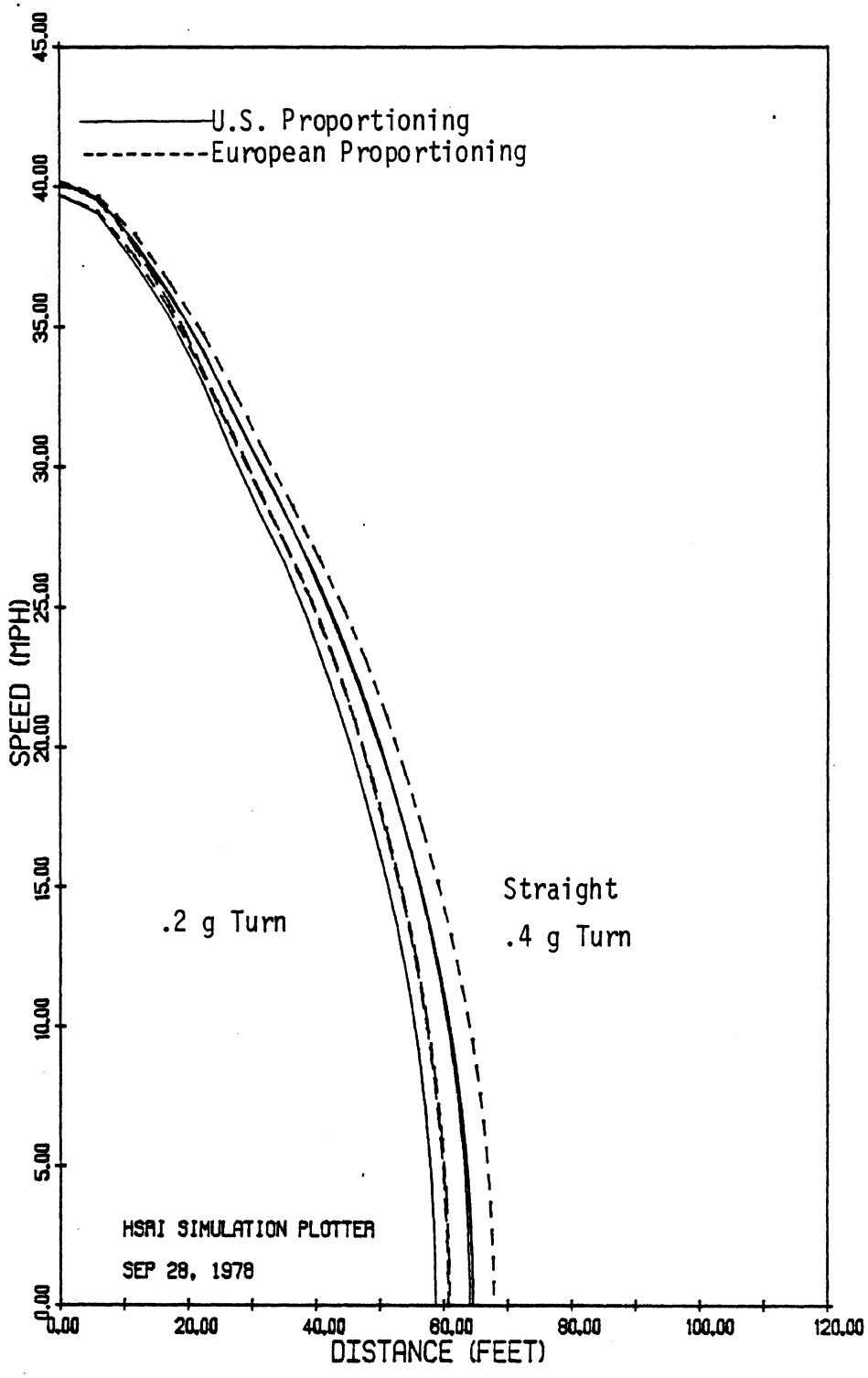

Figure B.1. Speed vs. distance curves for the domestic intermediate, lightly loaded, on the high friction surface.

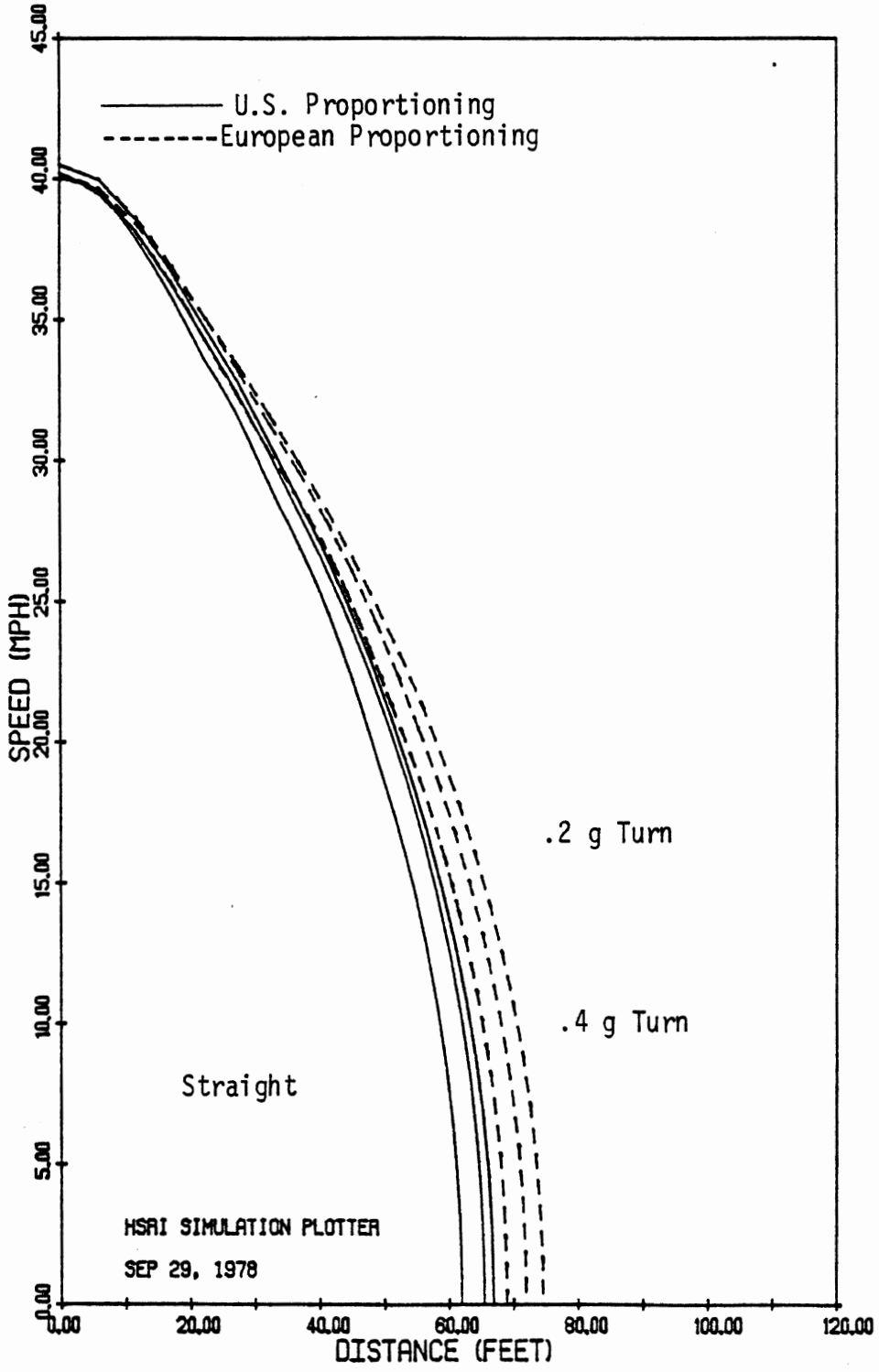

Figure B.2. Speed vs. distance curves for the domestic intermediate, loaded to GVWR, on the high friction surface.

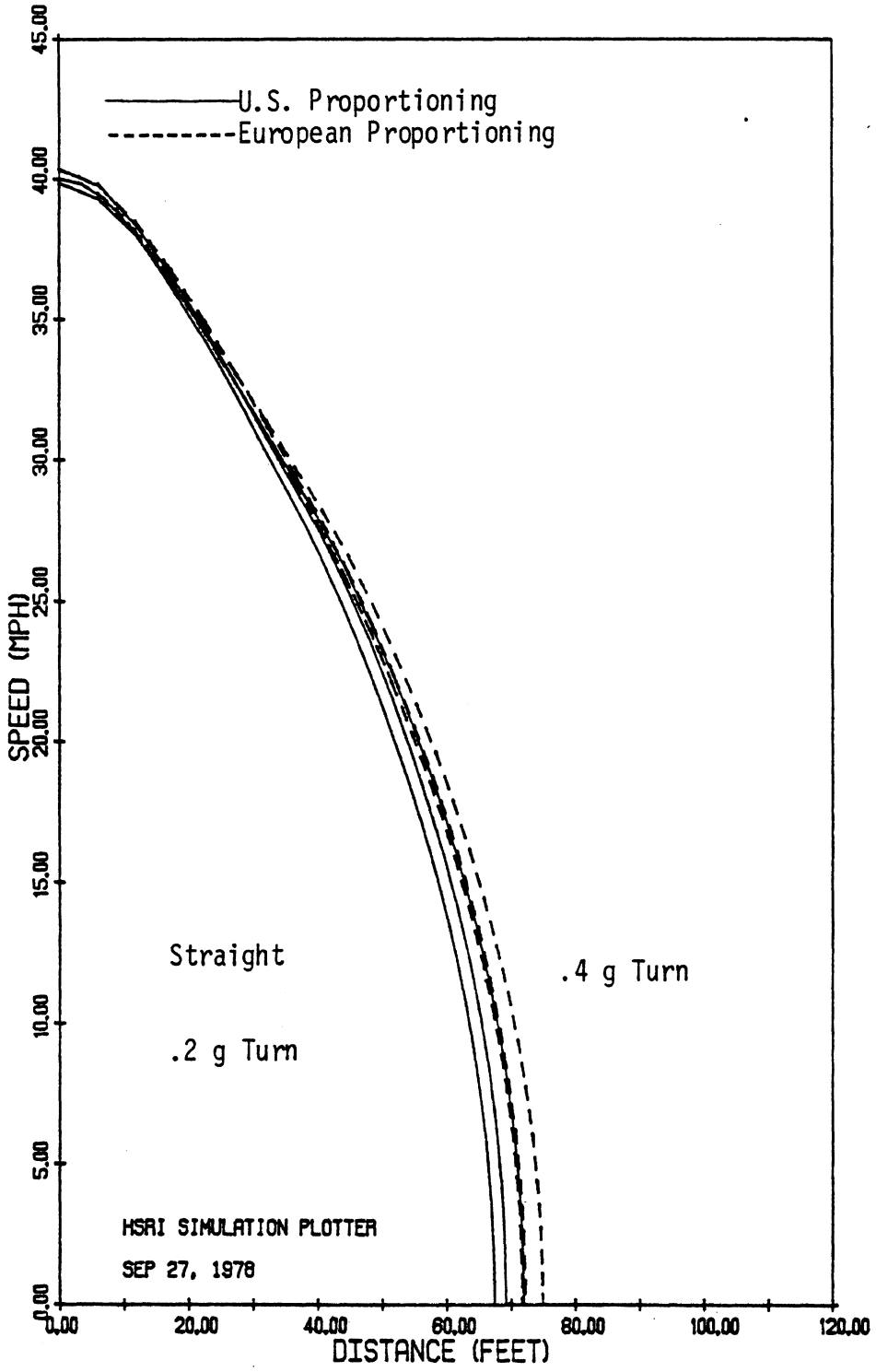

Figure B.3. Speed vs. distance curves for the European subcompact, lightly loaded, on the high friction surface.

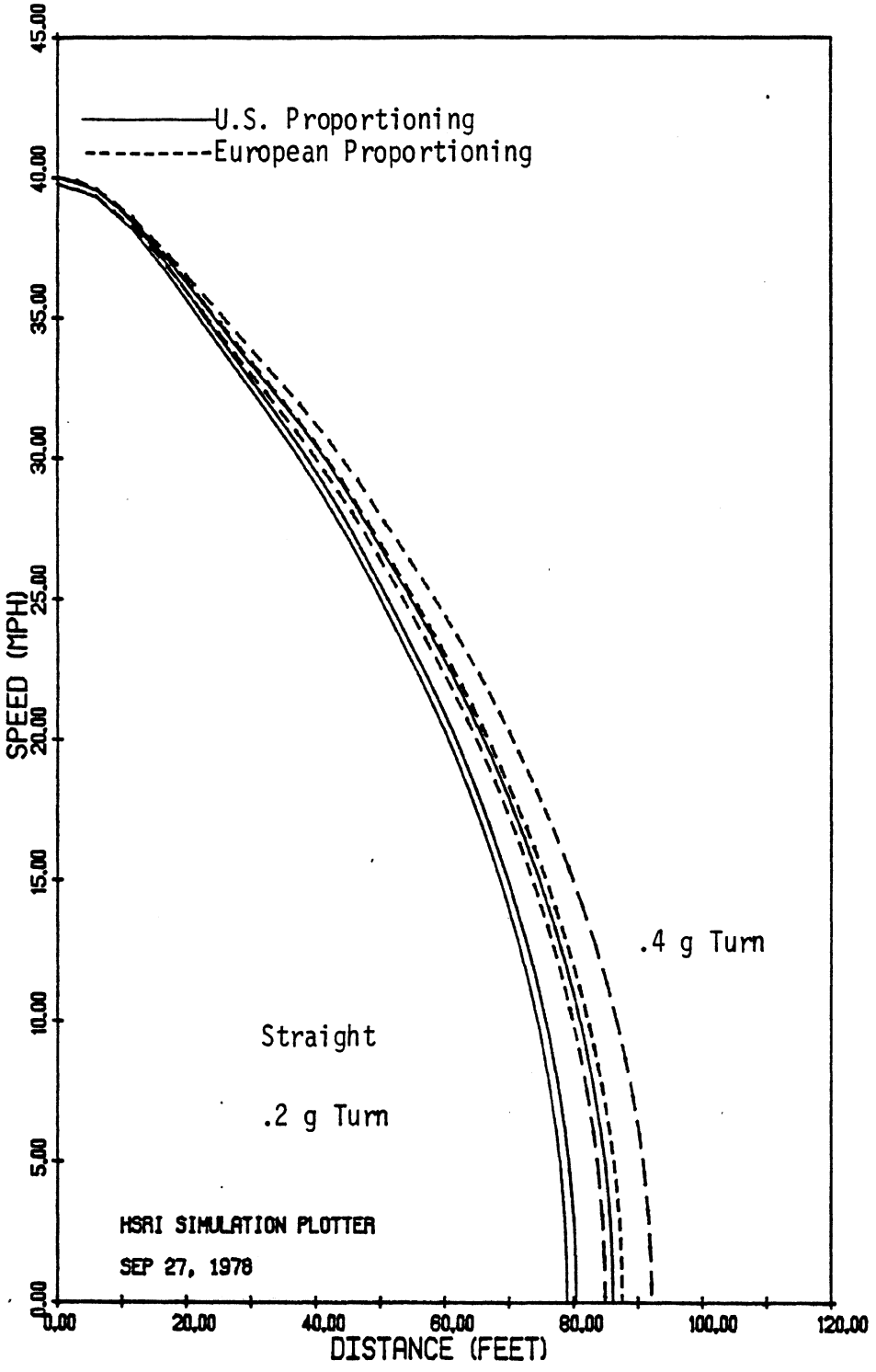

Figure B.4. Speed vs. distance curves for the European subcompact, loaded at GVWR, on the high friction surface.

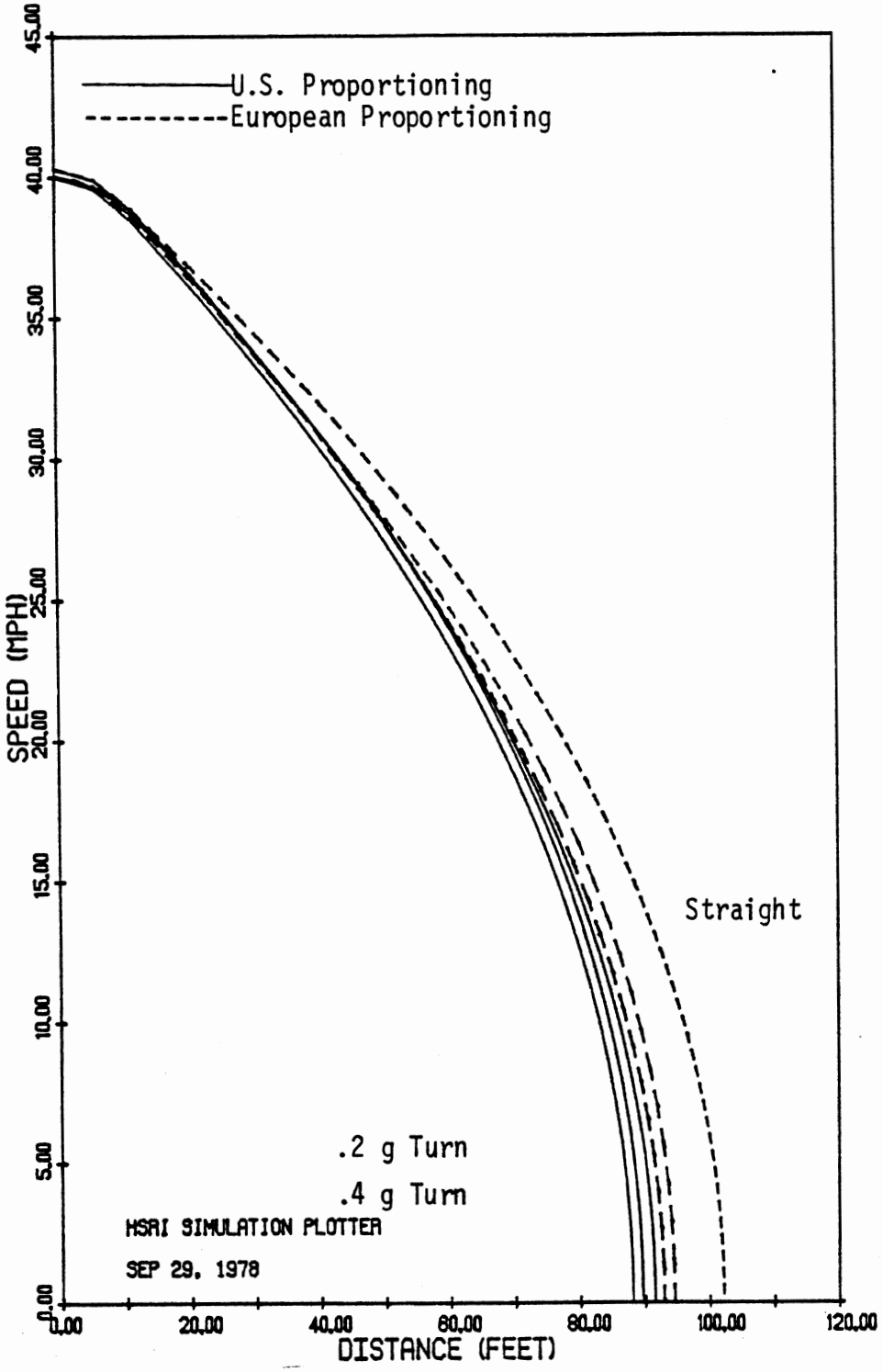

Figure B.5. Speed vs. distance curves for the domestic intermediate, lightly loaded, on the medium friction surface.

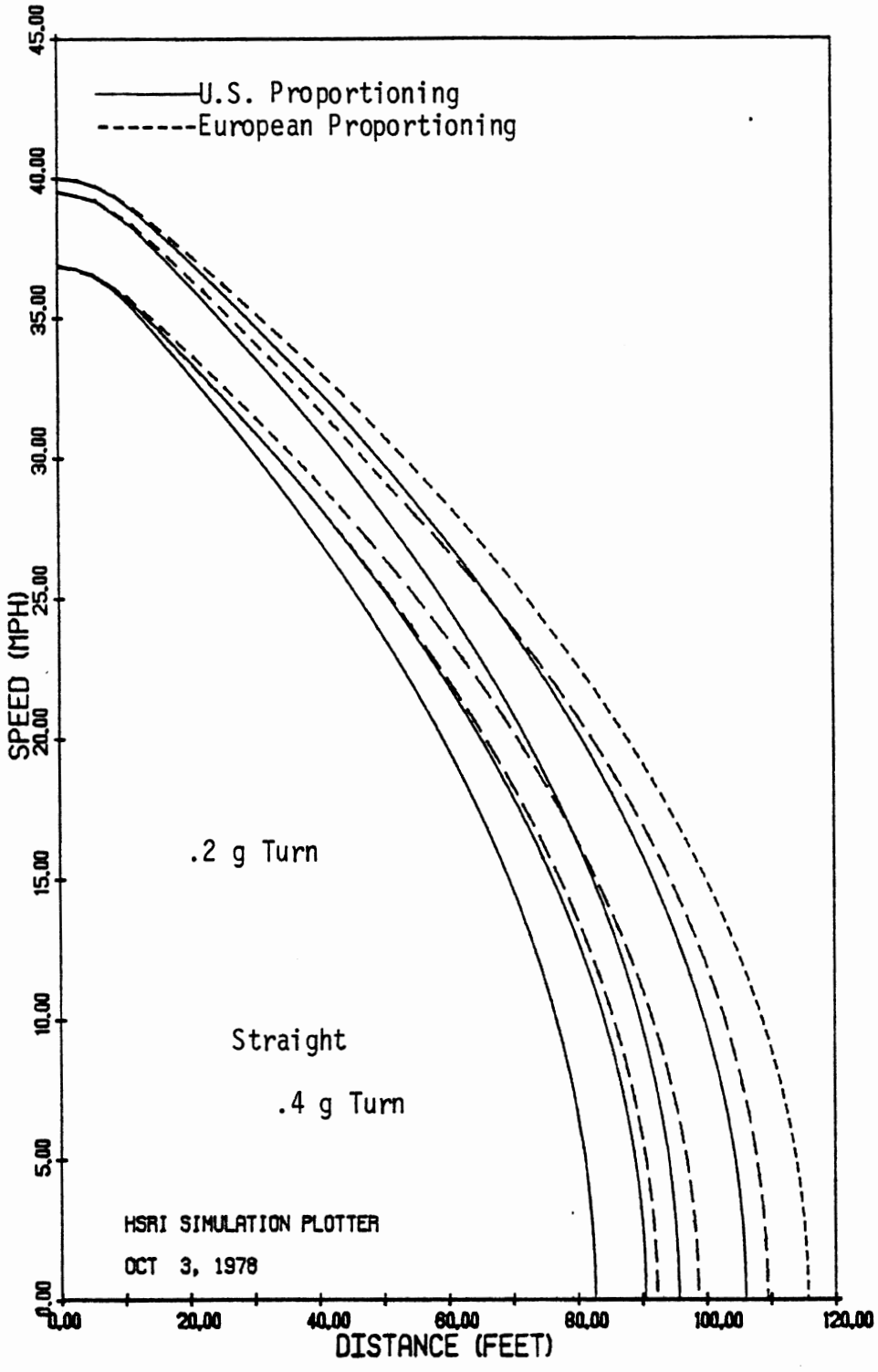

Figure B.6. Speed vs. distance curves for the domestic intermediate, loaded at GVWR, on the medium friction surface.

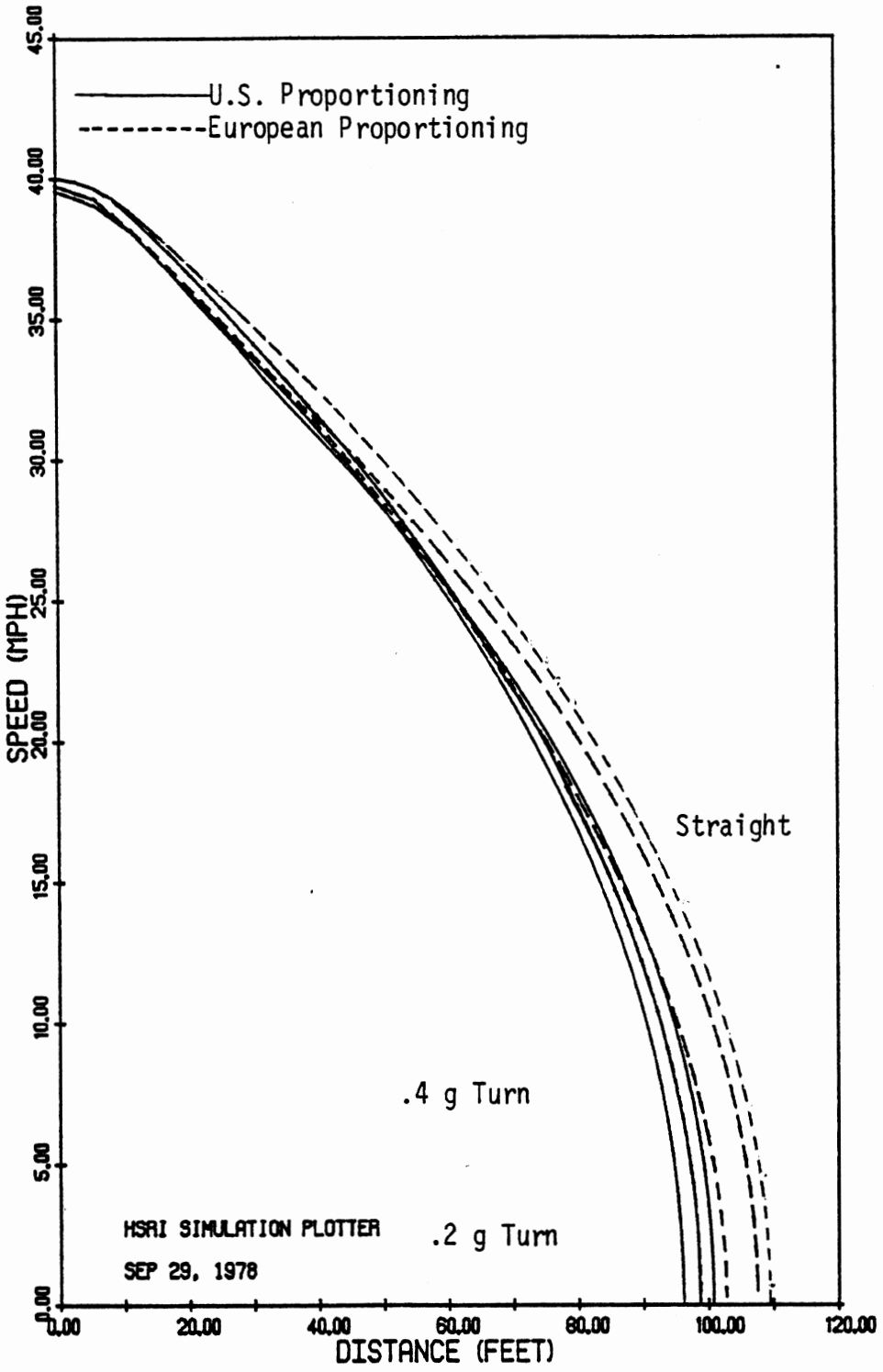

Figure B.7. Speed vs. distance curves for the European subcompact, lightly loaded, on the medium friction surface.

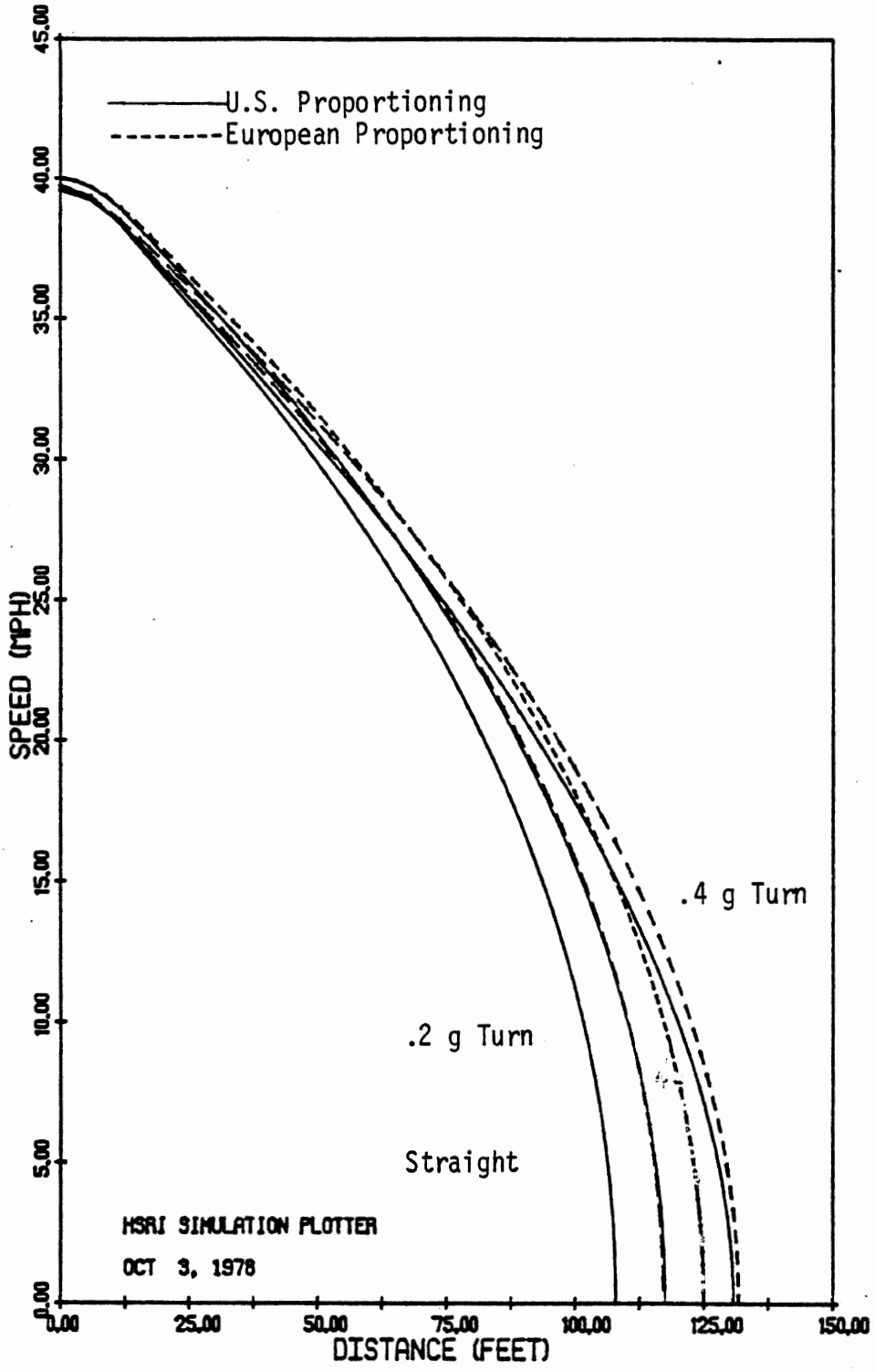

Figure B.8. Speed vs. distance curves for the European subcompact, loaded at GVWR, on the medium friction surface.

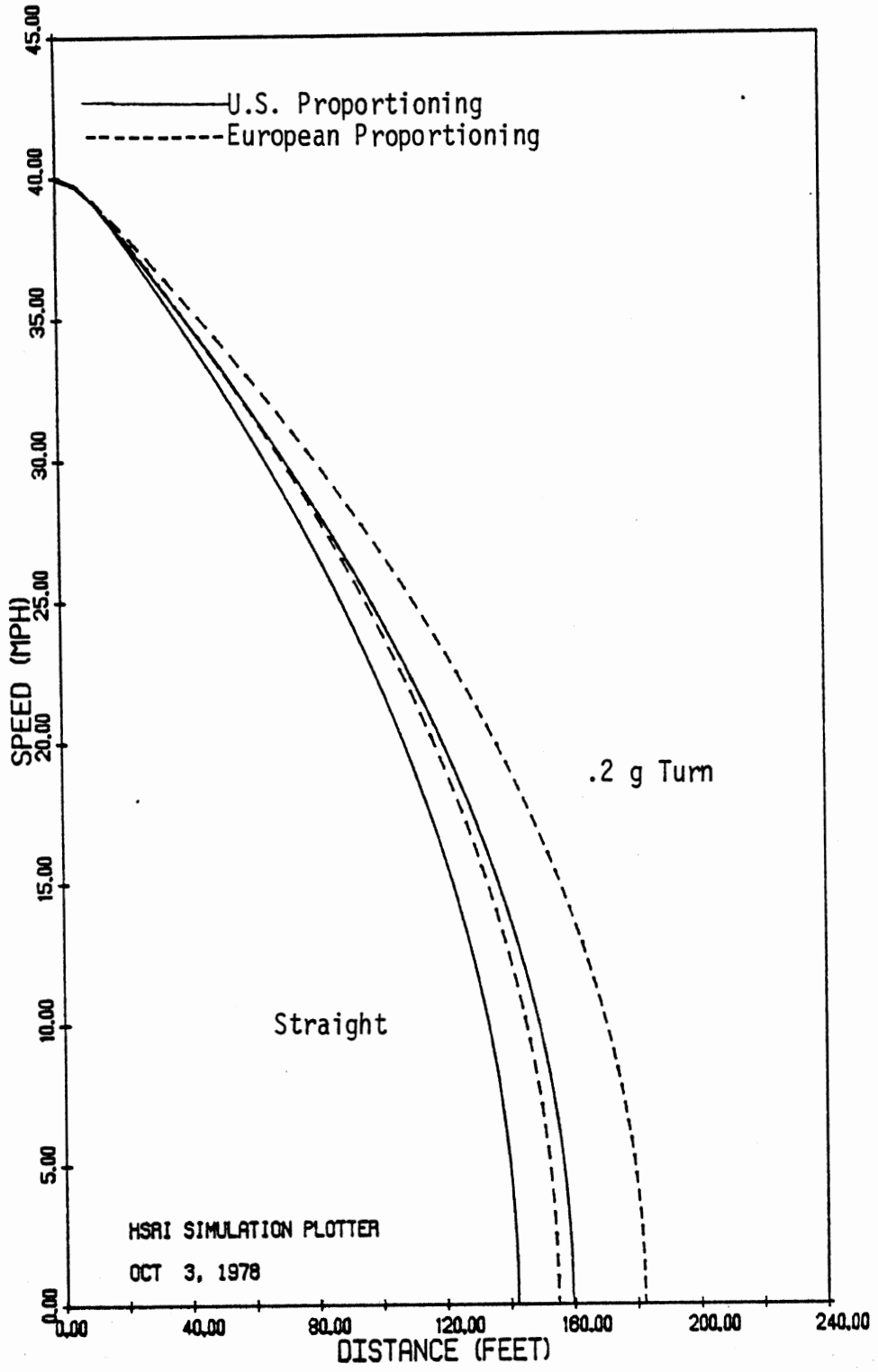

Figure B.9. Speed vs. distance curves for the domestic intermediate, lightly loaded, on the low friction surface.

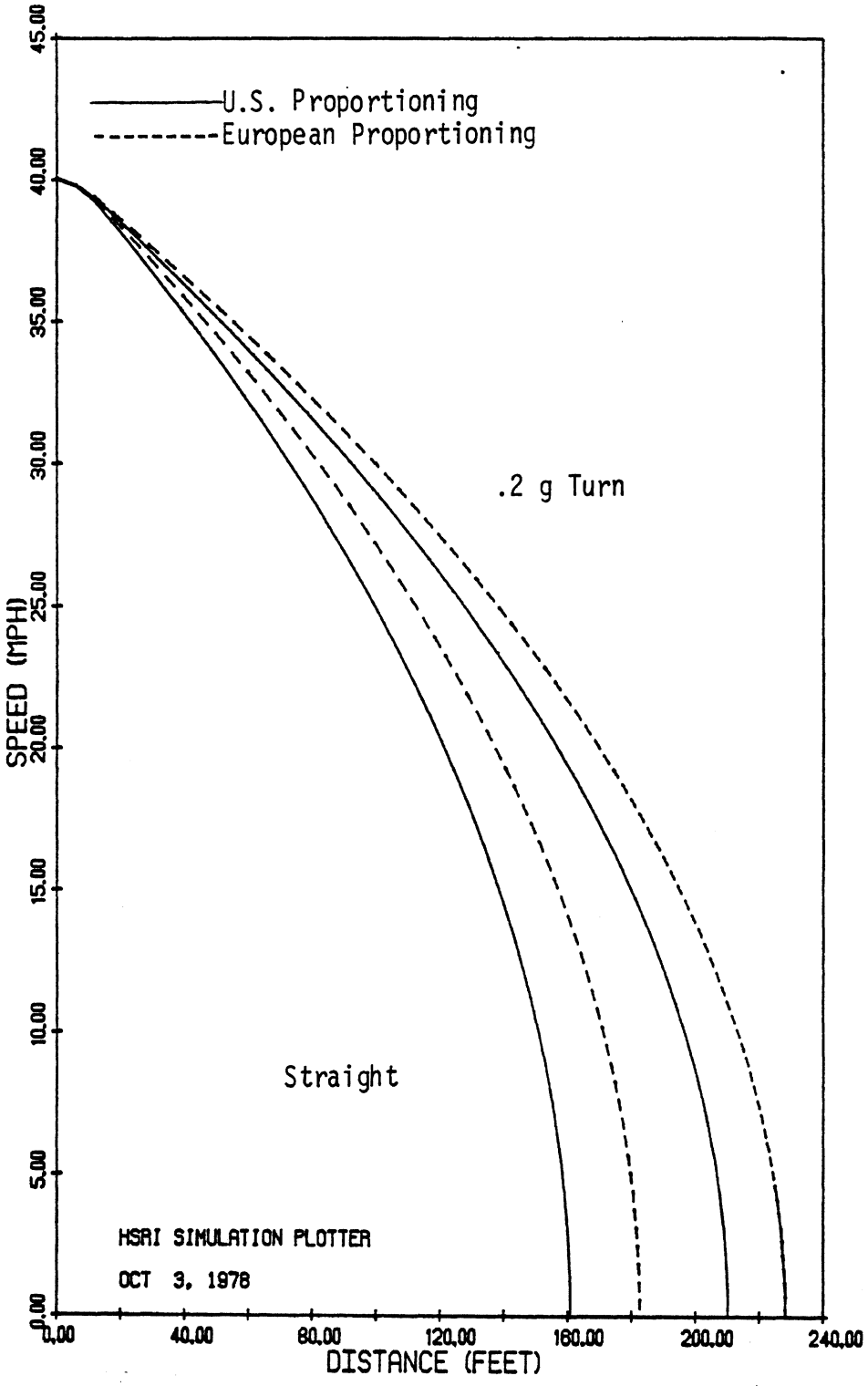

Figure B.10. Speed vs. distance curves for the domestic intermediate, loaded at GVWR, on the low friction surface.

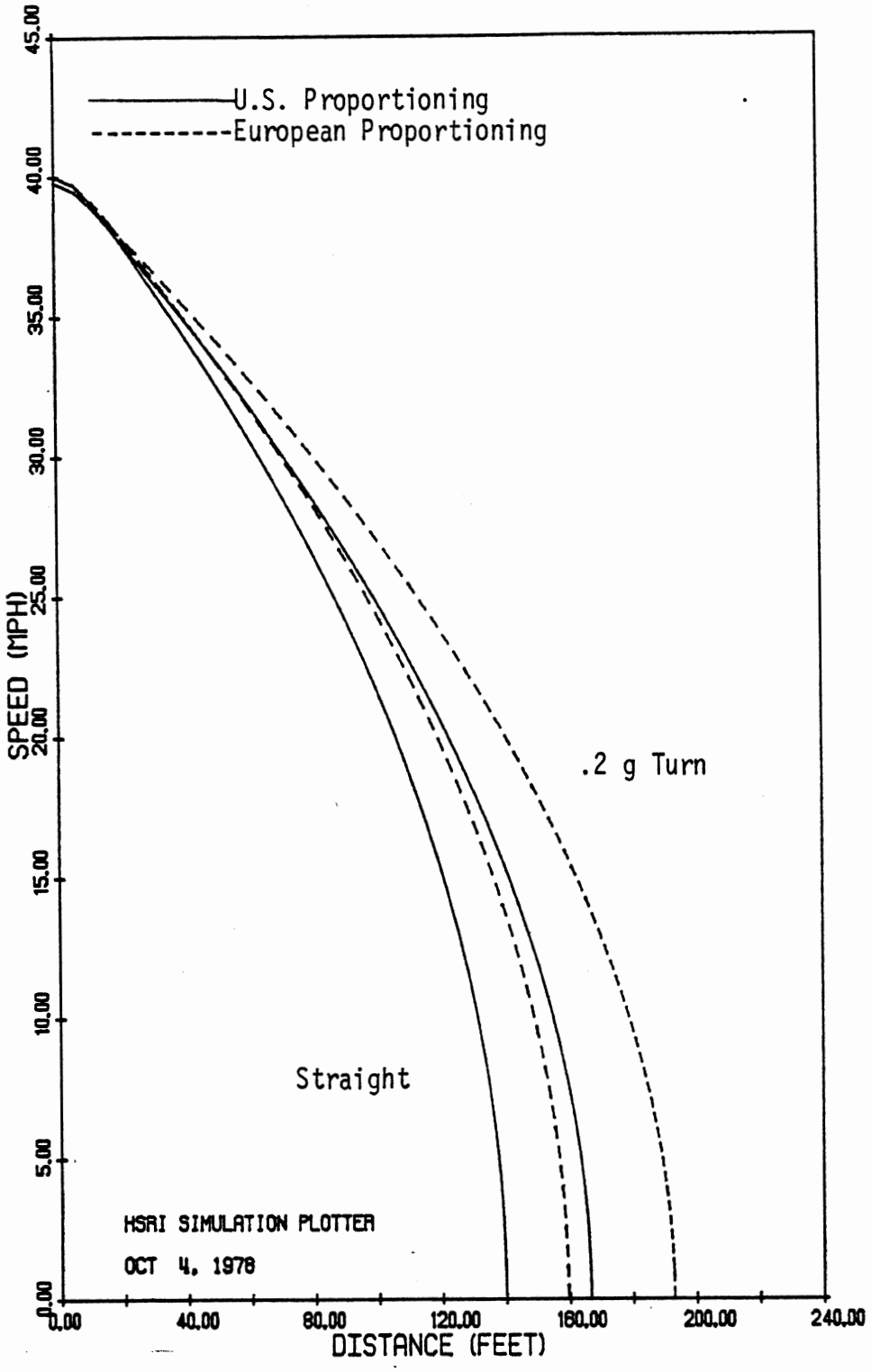

Figure B.11. Speed vs. distance curves for the European subcompact, lightly loaded, on the low friction surface.

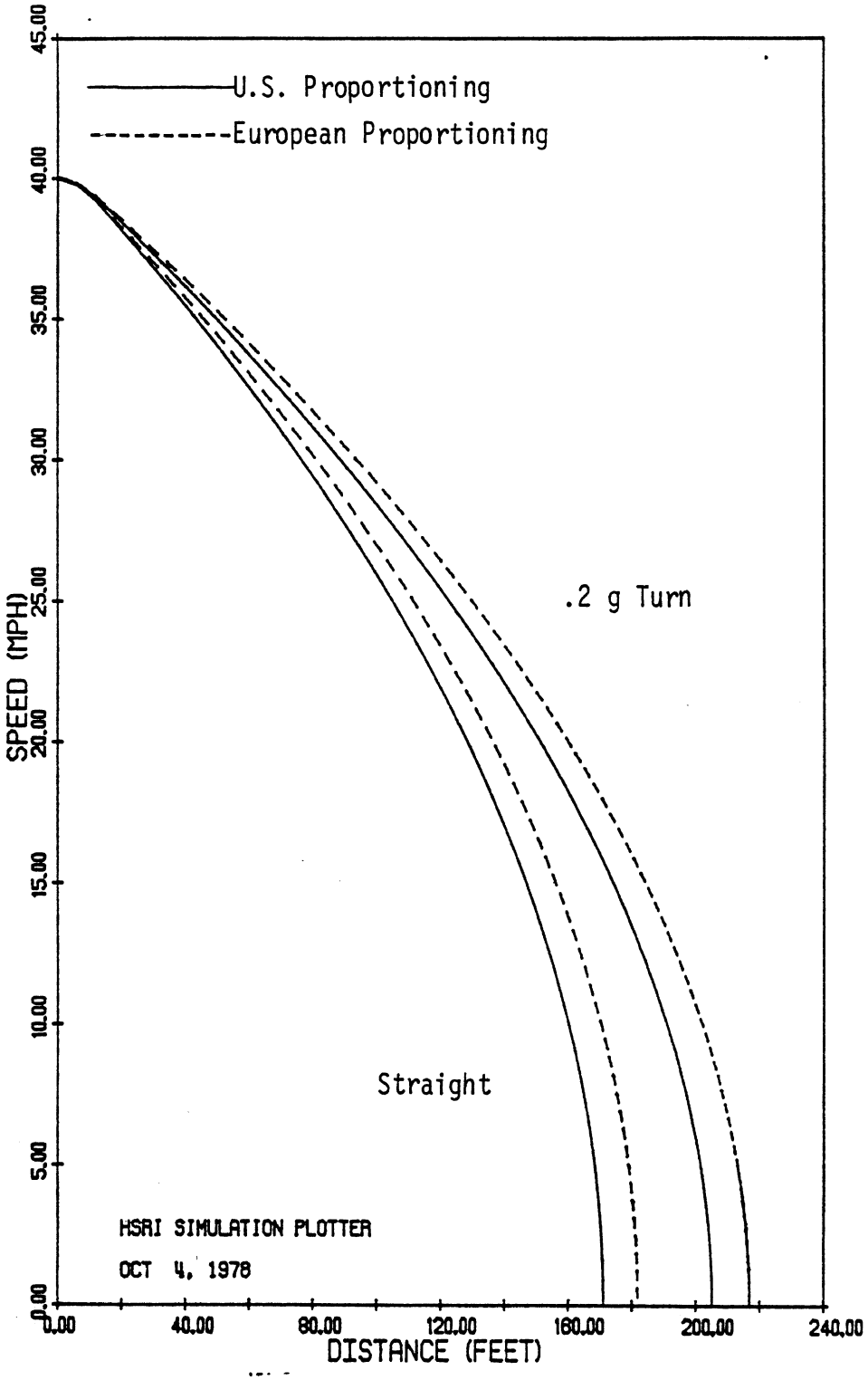

Figure B.12. Speed vs. distance curves for the European subcompact, loaded to GVWR, on the low friction surface.

APPENDIX C

RESULTS OF THE OPEN-LOOP BRAKING IN A TURN SIMULATIONS

This appendix contains the complete results of the open-loop braking in a turn simulations. Tables C.1 through C.16 present various performance indices for eight different vehicle/load initial radius conditions. The tabulated variables are discussed in Section 4.3. One of these indices, normalized path curvature averaged over one second ($R_o\tilde{\rho}$), is used to prepare the plots shown in Figures C.1 through C.8. These plots are also discussed in Section 4.3.

Prop. (%)	Pressure (psi)	$\tilde{A}_x$ (g's)	A_xs.s. (g's)	$\tilde{A}_y$ (g's)	A_y(1) (g's)	$\tilde{r}$ (deg/sec)	r(1) (deg/sec)	$\tilde{\beta}$ (deg)	β(1) (deg)
70	250	.47	.51	.27	.21	9.0	8.7	- .7	- .3
	300	.55	.60	.26	.20	8.9	8.6	- .7	- .1
	350	.64	.69	.23	.16	7.5	6.3	- .8	.1
	400	.70	.76	.20	.09	6.2	3.5	- .9	.0
	450	.76	.82	.14	.02	3.7	-1.0	- .9	- .2
	500	.78	.85	.09	.01	2.1	-3.3	-1.3	- .4
80	300	.49	.53	.26	.20	8.7	8.6	- .7	- .2
	350	.56	.61	.22	.16	6.9	6.3	- .6	- .0
	400	.62	.67	.15	.04	4.2	1.3	- .5	.0
	450	.65	.69	.10	-.01	2.2	- .4	- .5	- .3
90	300	.44	.48	.26	.20	8.6	8.4	- .7	- .3
	350	.51	.55	.21	.14	6.7	5.2	- .6	- .2
	400	.55	.60	.13	.01	3.6	.3	- .5	- .0
	450	.56	.60	.09	-.01	1.9	- .1	- .4	0.0

Table C.1 Unweighted braking in a turn numerics for the European car, at GVWR loading, with R_o = 100 m (A_y = .3 g).

Prop. (%)	Pressure (psi)	A_x s.s. (g's)	$\frac{\tilde{A}_y \cdot R_o}{\tilde{V}^2}$	$\frac{A_y(1) \cdot R_o}{V(1)^2}$	$\frac{\tilde{r} \cdot R_o}{\tilde{V}}$	$\frac{r(1) \cdot R_o}{V(1)}$	$R_o\tilde{\rho}$	$R_o\rho(1)$
70	250	.51	1.14	1.31	1.04	1.21	1.13	1.30
	300	.60	1.18	1.40	1.06	1.29	1.18	1.40
	350	.69	1.08	1.34	.91	1.01	1.03	1.46
	400	.76	.96	.86	.77	.60	.87	1.05
	450	.82	.68	.17	.47	-.18	.50	.19
	500	.85	.50	.06	.26	-.60	.24	.14
	600	.86	.46	.50	.52	.41	.14	.11
80	300	.53	1.12	1.29	1.01	.82	1.10	1.29
	350	.61	.98	1.19	.83	.95	.92	1.25
	400	.67	.69	.31	.51	.20	.56	.32
	450	.69	.47	-.06	.27	-.06	.30	-.10
90	300	.48	1.08	1.10	.98	1.14	1.06	1.22
	350	.55	.91	.90	.78	.75	.85	.88
	400	.60	.60	.10	.42	.05	.47	.11
	450	.60	.42	-.04	.22	-.01	.26	-.06

Table C.2 Normalized braking in a turn numerics for the European car, at GVWR loading, with R_o = 100 m (A_y = .3 g).

Prop. (%)	Pressure (psi)	$\tilde{A}_x$ (g's)	A_xs.s. (g's)	$\tilde{A}_y$ (g's)	$A_y(1)$ (g's)	$\tilde{r}$ (deg/sec)	r(1) (deg/sec)	$\tilde{\beta}$ (deg)	$\beta(1)$ (deg)
70	300	.56	.60	.39	.25	16.1	12.0	-1.5	.5
	350	.63	.69	.36	.22	15.2	9.8	-1.8	-.3
	400	.68	.76	.30	.19	12.0	7.8	-1.7	.2
	450	.74	.82	.25	.15	9.1	3.3	-1.7	-.0
	500	.78	.86	.18	0.00	5.0	-3.5	-2.1	-.3
80	300	.50	.53	.36	.22	14.3	13.4	- .8	.6
	350	.56	.61	.30	.15	11.4	9.2	- .8	.5
	400	.61	.67	.25	.11	9.0	5.7	- .8	.5
	450	.65	.70	.20	-.01	6.5	-.4	- .9	-.1
	500	.67	.72	.16	0.00	4.5	-.5	-1.0	-.1
90	300	.45	.48	.36	.24	14.0	13.2	- .8	.4
	350	.50	.55	.29	.14	10.7	7.8	- .8	.3
	400	.54	.60	.24	.07	8.2	3.9	- .7	.3
	450	.56	.61	.18	0.00	5.6	-.2	- .8	-.1

Table C.3 Unweighted braking in a turn numerics for the European car, at GVWR loading, with R_o = 40 m (A_y = .5 g).

Prop. (%)	Pressure (psi)	A_x s.s. (g's)	$\frac{\tilde{A}_y \cdot R_o}{\tilde{V}^2}$	$\frac{A_y(1) \cdot R_o}{V(1)^2}$	$\frac{\tilde{r} \cdot R_o}{\tilde{V}}$	$\frac{r(1) \cdot R_o}{V(1)}$	$R_o\tilde{\rho}$	$R_o\rho(1)$
70	300	.60	1.14	1.36	.98	.98	1.14	1.42
	350	.69	1.09	1.44	.95	.88	1.05	1.32
	400	.76	.95	1.41	.76	.75	.89	1.45
	450	.82	.81	1.33	.59	.34	.66	1.02
	500	.86	.59	-.02	.33	-.38	.33	.08
80	300	.53	1.01	1.04	.85	1.02	.99	1.09
	350	.61	.88	.85	.69	.75	.81	.91
	400	.67	.77	.68	.56	.50	.66	.78
	450	.70	.61	-.04	.41	-.04	.42	-.07
	500	.72	.51	-.03	.29	-.04	.30	-.10
90	300	.48	.96	1.02	.81	.96	.94	1.04
	350	.55	.80	.66	.64	.60	.73	.68
	400	.60	.68	.36	.49	.31	.56	.38
	450	.61	.53	-.01	.34	-.02	.36	-.02

Table C.4 Normalized braking in a turn numerics for the European car, at GVWR loading, with R_o = 40 m (A_y = .5 g).

Prop. (%)	Pressure (psi)	$\tilde{A}_x$ (g's)	A_xs.s. (g's)	$\tilde{A}_y$ (g's)	$A_y(1)$ (g's)	$\tilde{r}$ (deg/sec)	r(1) (deg/sec)	$\tilde{\beta}$ (deg)	β(1) (deg)
70	200	.49	.54	.29	.27	11.1	10.9	-.3	-.2
	250	.58	.63	.29	.24	11.0	10.2	-.2	.1
	300	.67	.73	.27	.20	10.3	8.6	-.3	.3
	350	.74	.83	.28	.25	12.3	-.7	-1.8	-1.9
	400	.80	.90	.17	.17	12.7	14.0	-3.0	-8.4
80	200	.44	.48	.26	.21	9.2	8.7	.1	.4
	250	.54	.58	.28	.21	10.0	8.9	0.0	.5
	300	.63	.69	.27	.23	10.5	9.9	-.2	.1
	350	.71	.79	.21	.12	7.8	4.9	-.2	.2
	400	.76	.85	.12	0.00	4.4	.5	.5	-.2
	450	.78	.87	.09	.01	3.2	-5.0	-1.0	-.7
90	250	.48	.52	.27	.21	9.4	9.1	.1	.5
	300	.57	.62	.25	.19	8.8	8.3	.1	.5
	350	.65	.72	.19	.11	6.6	5.1	.1	.4
	400	.68	.74	.10	0.00	3.4	-.0	-.1	-.0

Table C.5 Unweighted braking in a turn numerics for the European car, lightly loaded, with R_o = 100 m (A_y = .3 g).

Prop. (%)	Pressure (psi)	A_x s.s. (g's)	$\frac{\tilde{A}_y \cdot R_o}{\tilde{V}^2}$	$\frac{A_y(1) \cdot R_o}{V(1)^2}$	$\frac{\tilde{r} \cdot R_o}{\tilde{V}}$	$\frac{r(1) \cdot R_o}{V(1)}$	$R_o\tilde{\rho}$	$R_o\rho(1)$
70	200	.54	1.28	1.71	1.30	1.54	1.31	1.70
	250	.63	1.32	1.81	1.32	1.55	1.38	1.80
	300	.73	1.30	1.73	1.27	1.41	1.36	1.81
	350	.83	1.38	2.50	1.55	-.13	1.38	2.19
	400	.90	.85	1.95	1.64	2.60	.54	.27
80	200	.48	1.11	1.25	1.06	1.18	1.12	1.26
	250	.58	1.23	1.48	1.18	1.30	1.27	1.50
	300	.69	1.28	1.89	1.27	1.58	1.34	1.92
	350	.79	1.02	1.10	.98	.84	1.01	1.10
	400	.85	.63	.03	.56	.08	.47	.05
	450	.87	.47	.06	.40	-.91	.22	-.03
90	250	.52	1.15	1.36	1.10	1.28	1.17	1.38
	300	.62	1.11	1.37	1.05	1.25	1.13	1.40
	350	.72	.88	.91	.81	.82	.85	.94
	400	.74	.51	0.00	.43	0.00	.35	-.03

Table C.6 Normalized braking in a turn numerics for the European car, lightly loaded, with R_o = 100 m (A_y = .3 g).

Prop. (%)	Pressure (psi)	$\tilde{A}_x$ (g's)	A_xs.s. (g's)	$\tilde{A}_y$ (g's)	$A_y(1)$ (g's)	$\tilde{r}$ (deg/sec)	r(1) (deg/sec)	$\tilde{\beta}$ (deg)	$\beta(1)$ (deg)
70	200	.47	.52	.42	.31	19.2	16.9	.2	1.0
	250	.56	.63	.39	.26	18.2	15.7	.3	1.4
	300	.66	.73	.36	.21	16.5	13.3	.3	1.8
	350	.73	.82	.32	.14	15.3	4.5	- .8	.6
	400	.80	.90	.23	.22	18.2	16.2	-3.7	-9.8
80	200	.44	.48	.43	.35	19.5	17.0	.2	.9
	250	.53	.59	.41	.30	18.7	16.7	.2	1.2
	300	.62	.69	.36	.25	16.7	14.6	.3	1.5
	350	.70	.79	.28	.13	12.7	7.6	.1	1.1
	400	.75	.86	.19	.01	8.7	1.4	- .3	- .4
	450	.78	.88	.14	.01	5.7	-4.5	-1.2	- .5
90	250	.49	.52	.39	.27	17.3	14.8	.5	1.6
	300	.57	.62	.35	.22	15.6	13.2	.5	1.8
	350	.64	.71	.26	.13	11.7	7.7	.3	1.2
	400	.68	.75	.18	0.00	7.8	.3	- .0	0.0
	450	.70	.76	.13	0.00	5.3	- .5	- .3	- .1

Table C.7 Unweighted braking in a turn numerics for the European car, lightly loaded, with R_o = 40 m (A_y = .5 g).

Prop. (%)	Pressure (psi)	A_x s.s. (g's)	$\frac{\tilde{A}_y \cdot R_o}{\tilde{V}^2}$	$\frac{A_y(1) \cdot R_o}{V(1)^2}$	$\frac{\tilde{r} \cdot R_o}{\tilde{V}}$	$\frac{r(1) \cdot R_o}{V(1)}$	$R_o\tilde{\rho}$	$R_o\rho(1)$
70	200	.52	1.16	1.41	1.13	1.26	1.19	1.43
	250	.63	1.15	1.45	1.11	1.30	1.21	1.56
	300	.73	1.10	1.42	1.05	1.24	1.18	1.70
	350	.82	1.03	1.18	.99	.46	1.05	1.31
	400	.90	.80	2.26	1.21	1.83	.51	.44
80	200	.48	1.16	1.46	1.13	1.23	1.19	1.44
	250	.59	1.16	1.50	1.13	1.32	1.21	1.57
	300	.69	1.09	1.56	1.04	1.28	1.15	1.77
	350	.79	.88	.97	.81	.74	.87	1.09
	400	.86	.62	.05	.57	.15	.45	-.03
	450	.88	.48	.07	.38	-.49	.23	.04
90	250	.52	1.09	1.25	1.02	1.12	1.12	1.32
	300	.62	1.03	1.25	.96	1.09	1.07	1.42
	350	.71	.81	.83	.73	.70	.77	.92
	400	.75	.56	0.00	.50	.03	.40	-.04
	450	.76	.43	-.03	.34	-.05	.23	-.07

Table C.8 Normalized braking in a turn numerics for the European car, lightly loaded, with R_o = 40 m (A_y = .5 g).

Prop. (%)	Pressure (psi)	$\tilde{A}_x$ (g's)	A_xs.s. (g's)	$\tilde{A}_y$ (g's)	A_y(1) (g's)	$\tilde{r}$ (deg/sec)	r(1) (deg/sec)	$\tilde{\beta}$ (deg)	β(1) (deg)
60	300	.48	.53	.27	.23	9.6	8.4	-1.4	-1.0
	400	.63	.69	.28	.24	10.2	8.1	-1.6	-1.2
	500	.76	.84	.27	.34	12.2	12.2	-2.7	-3.9
	600	.87	.95	.22	.29	13.5	22.6	-3.6	-8.1
	700	.90	.99	.15	.12	8.0	9.4	-3.1	-6.1
70	300	.42	.46	.28	.24	9.4	8.5	-1.4	-1.1
	400	.55	.60	.27	.21	9.4	7.7	-1.4	- .9
	500	.68	.74	.25	.19	8.7	6.8	-1.4	- .8
	600	.79	.87	.18	.08	5.6	2.1	-1.3	- .5
	700	.86	.95	.12	.01	2.8	2.3	-1.2	- .4
	800	.88	.97	.10	.01	1.4	-3.1	-1.3	- .2
80	400	.48	.52	.27	.22	9.2	7.9	-1.3	-1.0
	500	.60	.65	.24	.18	8.2	6.9	-1.3	- .7
	600	.69	.76	.15	.03	3.7	1.2	- .9	- .0
	700	.74	.79	.11	-.01	2.0	-1.0	- .8	- .1
	800	.76	.81	.09	-.02	1.0	-1.0	- .8	.0

Table C.9 Unweighted braking in a turn numerics for the domestic car, at GVWR loading, with R_o = 100 m (A_y = .3 g).

Prop. (%)	Pressure (psi)	$A_{xs.s.}$ (g's)	$\frac{\tilde{A}_y \cdot R_o}{\tilde{V}^2}$	$\frac{A_y(1) \cdot R_o}{V(1)^2}$	$\frac{\tilde{r} \cdot R_o}{V^2}$	$\frac{r(1) \cdot R_o}{V(1)}$	$R_o\tilde{\rho}$	$R_o\rho(1)$
60	300	.53	1.19	1.48	1.12	1.18	1.17	1.40
	400	.69	1.30	1.97	1.24	1.29	1.30	1.82
	500	.84	1.38	3.53	1.55	2.20	1.36	2.80
	600	.95	1.19	3.64	1.77	4.49	1.04	1.89
	700	.99	.79	1.72	1.10	1.95	.45	.34
70	300	.46	1.16	1.38	1.08	1.14	1.13	1.32
	400	.60	1.19	1.47	1.12	1.14	1.17	1.41
	500	.74	1.20	1.67	1.07	1.12	1.20	1.58
	600	.87	.94	.88	.72	.39	.84	.86
	700	.95	.66	.08	.37	.46	.45	.04
	800	.97	.55	.08	.18	-.63	.31	.13
80	400	.52	1.16	1.39	1.07	1.11	1.13	1.33
	500	.65	1.12	1.40	.99	1.06	1.09	1.32
	600	.76	.72	.31	.46	.20	.60	.38
	700	.79	.54	-.12	.25	-.18	.38	-.14
	800	.81	.45	-.16	.13	-.17	.26	-.17

Table C.10. Normalized braking-in-a-turn numerics for the domestic car, at GVWR loading, for R_o = 100 m. (A_y = .3 g).

Prop. (%)	Pressure (psi)	$\tilde{A}_x$ (g's)	A_xs.s. (g's)	$\tilde{A}_y$ (g's)	A_y(1) (g's)	$\tilde{r}$ (deg/sec)	r(1) (deg/sec)	$\tilde{\beta}$ (deg)	β(1) (deg)
60	300	.50	.53	.44	.32	18.5	14.3	-2.2	- .9
	400	.65	.70	.43	.42	21.5	22.3	-3.1	-3.9
	500	.76	.84	.38	.29	17.8	10.8	-3.6	-2.9
	600	.86	.96	.33	.37	21.0	26.1	-5.8	-10.9
	700	.90	1.00	.25	.22	16.6	16.7	-6.4	-12.5
70	400	.56	.60	.40	.26	16.7	12.7	-1.9	- .4
	500	.68	.74	.34	.22	13.6	8.8	-2.0	- .2
	600	.77	.86	.29	.11	10.8	5.0	-2.0	.0
	700	.86	.97	.25	.04	8.8	-2.6	-3.0	-1.7
	800	.88	.99	.20	.04	5.6	-5.6	-3.3	-1.9
80	400	.50	.53	.40	.27	16.1	13.2	-2.0	- .5
	500	.60	.65	.31	.18	11.5	9.4	-1.5	.2
	600	.68	.75	.26	.08	8.9	5.1	-1.5	.3
	700	.73	.80	.21	.00	6.0	-1.1	-1.6	- .3
	800	.76	.83	.17	-.01	3.8	-1.4	-1.6	- .3
	1000	.83	.90	.15	-.01	2.7	-2.0	-1.9	- .4

Table C.11 Unweighted braking in a turn numerics for the domestic car, at GVWR loading, with R_o = 40 m (A_y = .5 g).

Prop. (%)	Pressure (psi)	A_x s.s. (g's)	$\frac{\tilde{A}_y \cdot R_o}{\tilde{V}^2}$	$\frac{A_y(1) \cdot R_o}{V(1)^2}$	$\frac{\tilde{r} \cdot R_o}{\tilde{V}}$	$\frac{r(1) \cdot R_o}{V(1)}$	$R_o\tilde{\rho}$	$R_o\rho(1)$
60	300	.50	1.22	1.53	1.10	1.10	1.22	1.51
	400	.65	1.33	2.82	1.35	2.03	1.36	2.50
	500	.76	1.25	2.60	1.17	1.15	1.25	2.10
	600	.86	1.17	4.50	1.43	3.23	1.02	2.18
	700	.90	.92	3.16	1.15	2.21	.44	.30
70	400	.56	1.16	1.43	1.02	1.04	1.17	1.41
	500	.68	1.09	1.61	.87	.83	.90	1.18
	600	.77	.96	1.00	.71	.54	.75	.62
	700	.86	.86	.47	.60	-.32	.63	.26
	800	.88	.70	.51	.39	-.73	.41	.24
80	400	.50	1.11	1.27	.96	1.01	1.09	1.26
	500	.60	.94	1.08	.71	.81	.90	1.18
	600	.68	.83	.58	.57	.48	.74	.62
	700	.73	.68	-.03	.39	-.11	.47	-.05
	800	.76	.58	-.11	.25	-.15	.34	-.11
	1000	.83	.52	-.14	.18	-.24	.28	-.13

Table C.12 Normalized braking in a turn numerics for the domestic car, at GVWR loading, with R_o = 40 m (A_y = .5 g).

Prop. (%)	Pressure (psi)	$\tilde{A}_x$ (g's)	A_xs.s. (g's)	$\tilde{A}_y$ (g's)	$A_y(1)$ (g's)	$\tilde{r}$ (deg/sec)	r(1) (deg/sec)	$\tilde{\beta}$ (deg)	β(1) (deg)
60	300	.54	.60	.31	.36	13.1	15.6	-1.5	-2.3
	400	.67	.74	.29	.30	12.1	12.1	-1.4	-1.6
	500	.82	.94	.30	.48	20.4	36.4	-4.2	-11.4
	600	.89	.98	.19	.23	15.5	14.8	-4.6	-12.1
70	300	.48	.51	.27	.23	9.7	8.7	- .7	- .3
	400	.62	.68	.30	.31	12.2	13.6	-1.3	-1.7
	500	.74	.83	.28	.29	11.7	11.7	-1.5	-1.7
	600	.86	.98	.19	.20	10.0	2.5	-2.5	-5.1
	650	.89	1.01	.16	.13	10.0	6.7	-3.0	-6.9
80	400	.55	.60	.26	.20	9.4	8.1	- .7	- .2
	500	.68	.74	.26	.18	9.3	7.1	- .8	- .1
	600	.77	.87	.16	.00	5.5	-3.0	- .9	- .3
	700	.83	.95	.10	-.02	2.3	0	-1.0	- .1

Table C.13 Unweighted braking in a turn numerics for the domestic car, lightly loaded, with R_o = 100 m (A_y = .3 g).

Prop. (%)	Pressure (psi)	A_x s.s. (g's)	$\frac{\tilde{A}_y \cdot R_o}{\tilde{V}^2}$	$\frac{A_y(1) \cdot R_o}{V(1)^2}$	$\frac{\tilde{r} \cdot R_o}{\tilde{V}}$	$\frac{r(1) \cdot R_o}{V(1)}$	$R_o\tilde{\rho}$	$R_o\rho(1)$
60	300	.60	1.40	2.54	1.56	2.30	1.44	2.33
	400	.74	1.40	2.59	1.49	2.00	1.46	2.38
	500	.94	1.53	5.39	2.62	6.83	1.49	3.57
	600	.98	1.03	2.99	2.04	2.99	.53	.35
70	300	.51	1.18	1.43	1.13	1.22	1.18	1.41
	400	.68	1.39	2.46	1.48	2.14	1.43	2.28
	500	.83	1.39	2.94	1.48	2.07	1.45	2.73
	600	.98	1.00	2.49	1.31	.50	.69	.01
	650	1.01	.85	1.81	1.32	1.37	.46	-.32
80	400	.60	1.18	1.45	1.12	1.20	1.19	1.44
	500	.74	1.25	1.57	1.15	1.18	1.26	1.58
	600	.87	.84	.03	.70	-.55	.68	.00
	700	.95	.54	-.30	.30	.00	.31	-.23

Table C.14 Normalized braking in a turn numerics for the domestic car, lightly loaded, with R_o = 100 m (A_y = .3 g).

Prop. (%)	Pressure (psi)	$\tilde{A}_x$ (g's)	A_xs.s. (g's)	$\tilde{A}_y$ (g's)	$A_y(1)$ (g's)	$\tilde{r}$ (deg/sec)	r(1) (deg/sec)	$\tilde{\beta}$ (deg)	$\beta(1)$ (deg)
60	300	.54	.59	.45	.43	23.1	22.6	-1.6	-1.6
	400	.66	.74	.41	.31	20.9	17.4	-1.2	- .3
	500	.83	.93	.34	.49	27.8	36.8	-4.7	-12.2
	600	.89	.98	.28	.30	24.5	21.6	-6.0	-17.0
	700	.91	.99	.20	.23	14.8	5.2	-6.2	-12.6
70	300	.50	.54	.46	.44	22.8	23.6	-1.4	-1.6
	400	.62	.68	.44	.40	22.8	21.4	-1.7	-1.4
	500	.74	.83	.36	.32	18.6	12.9	-1.6	-1.0
	600	.84	.96	.28	.12	16.0	7.3	-2.7	-5.0
	700	.89	.99	.19	.20	12.1	.1	-4.6	-8.5
80	300	.44	.47	.42	.31	19.3	16.4	- .6	.5
	400	.57	.61	.43	.36	21.0	18.7	-1.1	- .3
	500	.69	.75	.37	.31	17.9	13.0	-1.4	- .4
	600	.78	.91	.26	.07	13.0	-2.0	-1.5	-12.6
	700	.83	.92	.18	-.01	6.9	-5.5	-2.1	-1.0
	800	.85	.94	.17	.02	6.6	-6.7	-2.4	-1.4

Table C.15 Unweighted braking in a turn numerics for the domestic car, lightly loaded, with R_o = 40 m (A_y = .5 g).

Prop. (%)	Pressure (psi)	A_x s.s. (g's)	$\frac{\tilde{A}_y \cdot R_o}{\tilde{V}^2}$	$\frac{A_y(1) \cdot R_o}{V(1)^2}$	$\frac{\tilde{r} \cdot R_o}{\tilde{V}}$	$\frac{r(1) \cdot R_o}{V(1)}$	$R_o\tilde{\rho}$	$R_o\rho(1)$
60	300	.59	1.35	2.33	1.42	1.85	1.43	2.21
	400	.74	1.35	2.32	1.35	1.68	1.47	2.28
	500	.93	1.22	5.77	1.91	4.44	2.43	3.16
	600	.98	1.05	4.16	1.73	2.85	.48	-.63
	700	.49	.76	3.61	1.07	.73	.17	-.28
70	300	.54	1.32	2.18	1.38	1.84	1.38	2.08
	400	.68	1.41	2.62	1.45	1.93	1.50	2.52
	500	.83	1.24	2.95	1.24	1.39	1.36	2.73
	600	.96	1.00	1.49	1.11	.92	.78	-.03
	700	.99	.72	3.04	.86	.00	.27	.59
80	300	.47	1.17	1.37	1.14	1.21	1.25	1.47
	400	.61	1.31	2.12	1.31	1.59	1.39	2.08
	500	.75	1.22	2.45	1.17	1.29	1.27	2.18
	600	.91	.91	.77	.88	-.23	.83	.66
	700	.92	.66	-.12	.48	-.68	.38	-.27
	800	.94	.63	.21	.46	-.87	.33	-.06

Table C.16 Normalized braking in a turn numerics for the domestic car, lightly loaded, with R_o = 40 m (A_y = .5 g).

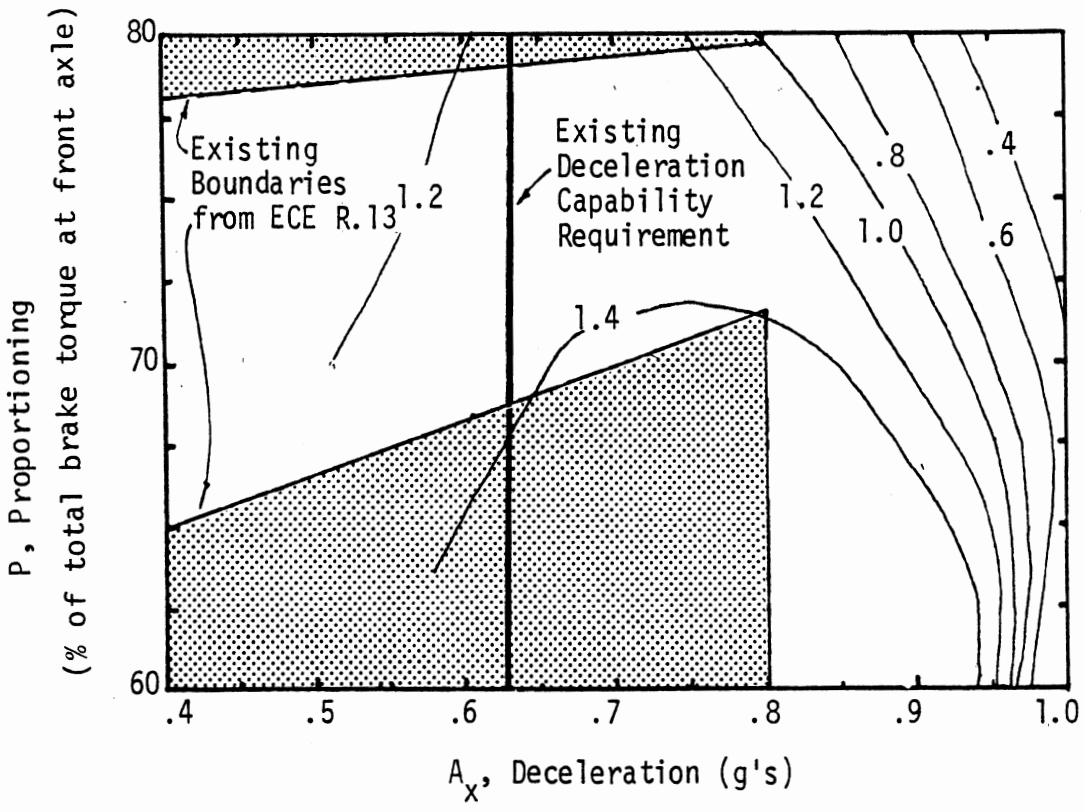

Figure C.1. Lines of constant normalized path curvature for the domestic car, lightly loaded, braking in a turn, with an initial lateral acceleration of .3 g's.

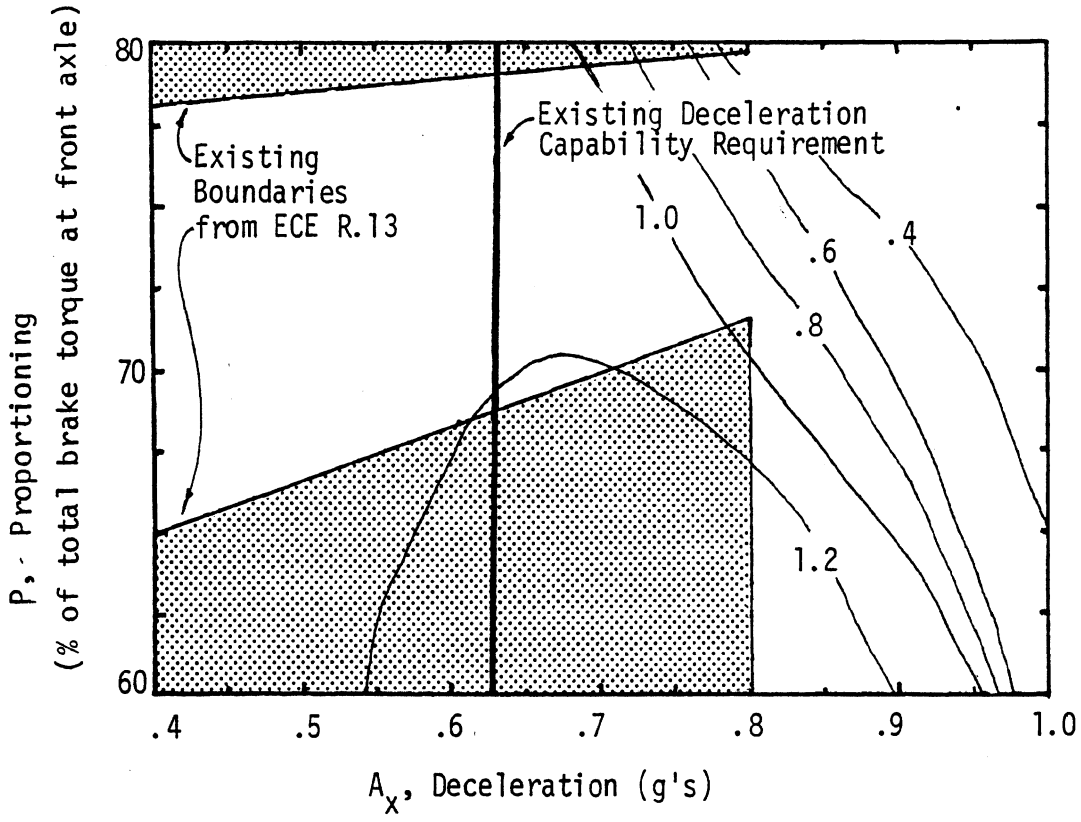

Figure C.2. Lines of constant normalized path curvature for the domestic car, loaded to the GVWR condition, braking in a turn with an initial lateral acceleration of .3 g's.

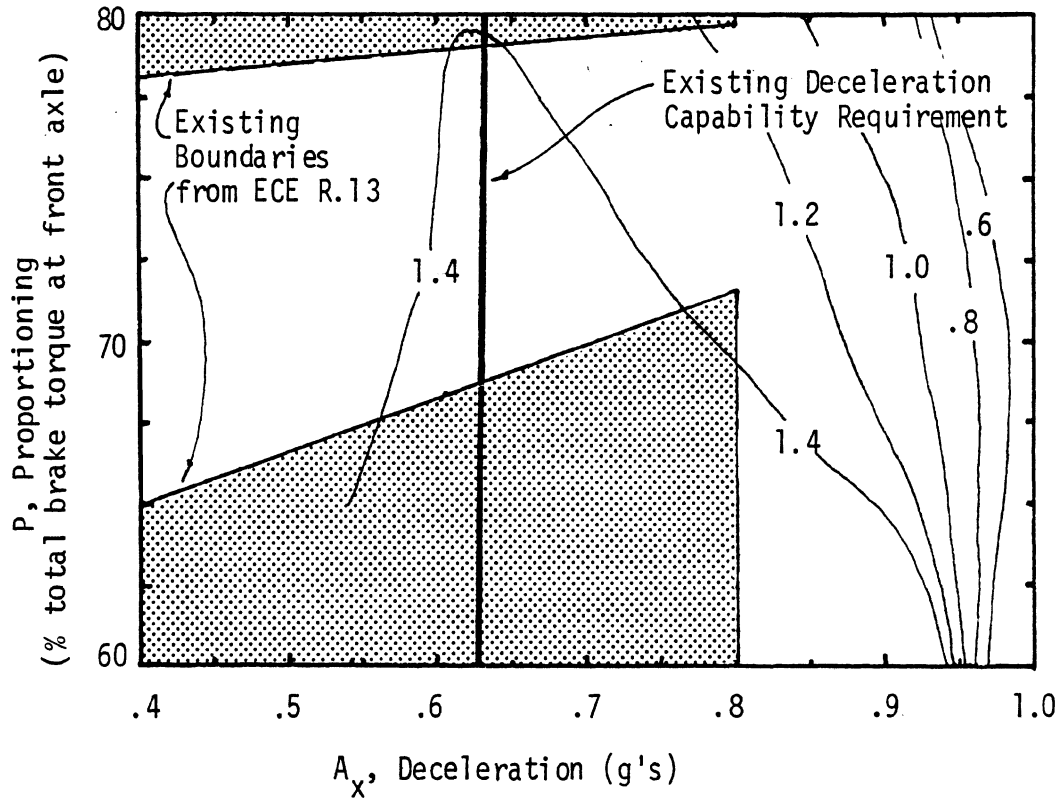

Figure C.3. Lines of constant normalized path curvature for the domestic car, lightly loaded, braking in a turn with an initial lateral acceleration of .5 g's.

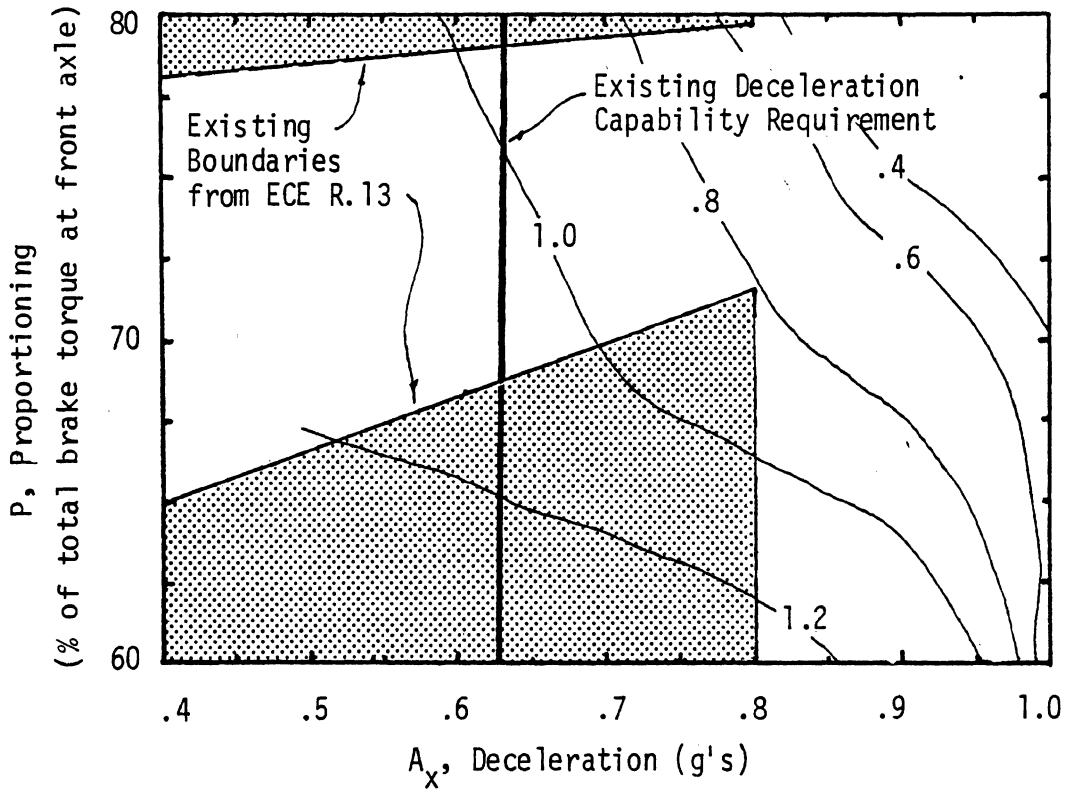

Figure C.4. Lines of constant normalized path curvature for the domestic car, loaded to the GVWR condition, braking in a turn with an initial lateral acceleration of .5 g's.

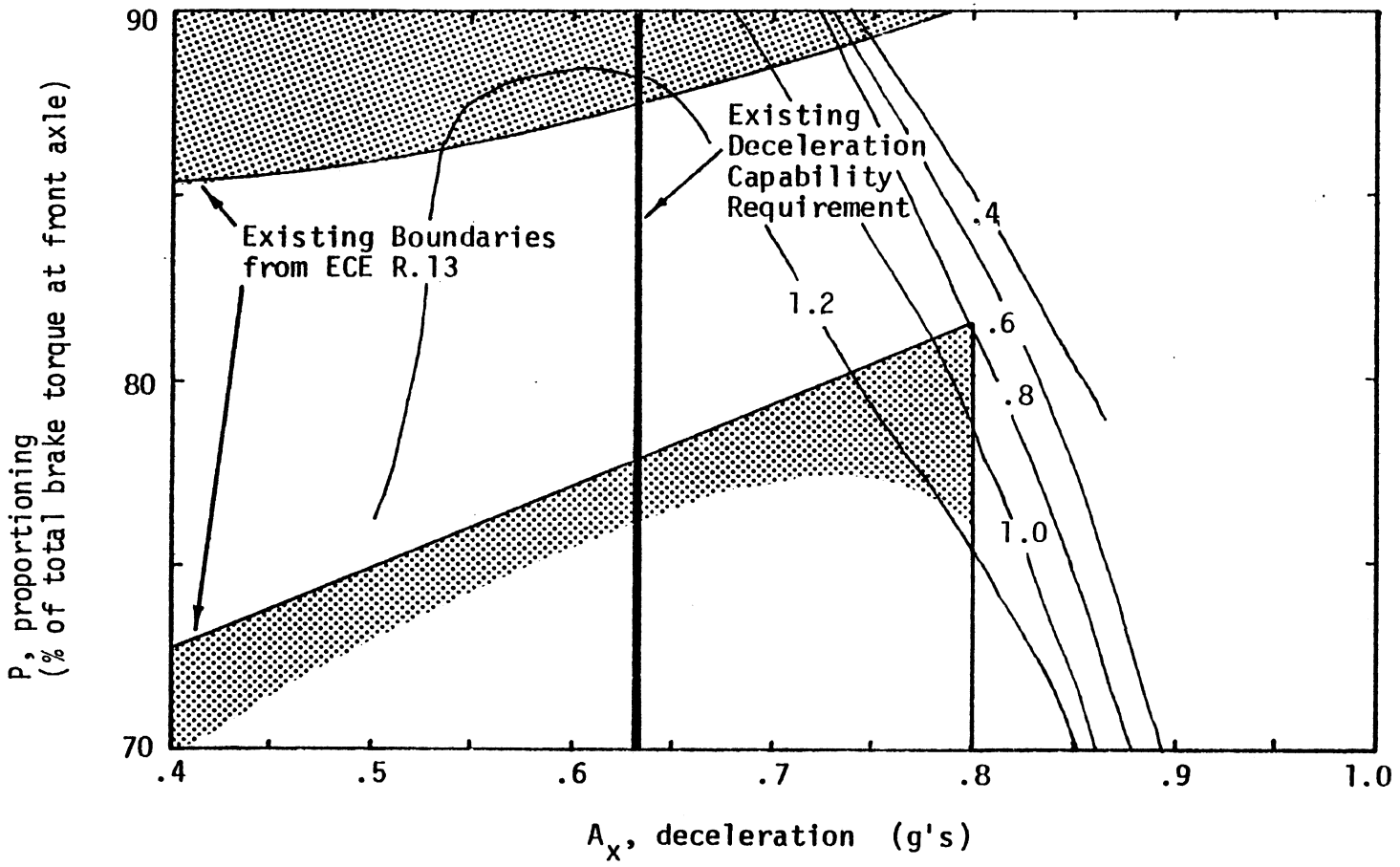

Figure C.5. Lines of normalized path curvature for the European car, lightly loaded, braking in a turn with an initial lateral acceleration of .3 g's.

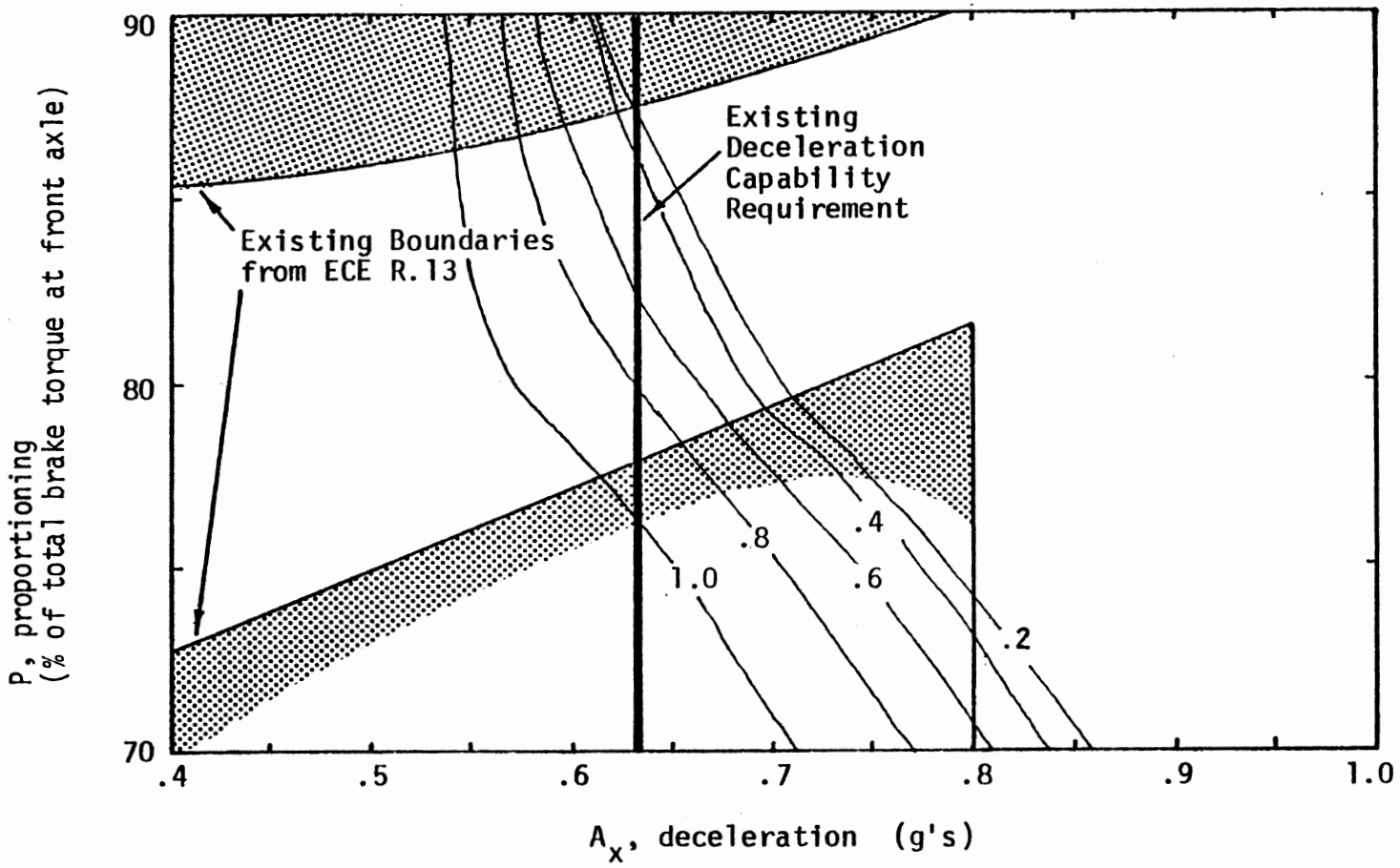

Figure C.6. Lines of constant normalized path curvature for the European car, loaded to the GVWR condition, braking in a turn with an initial lateral acceleration of .3 g's.

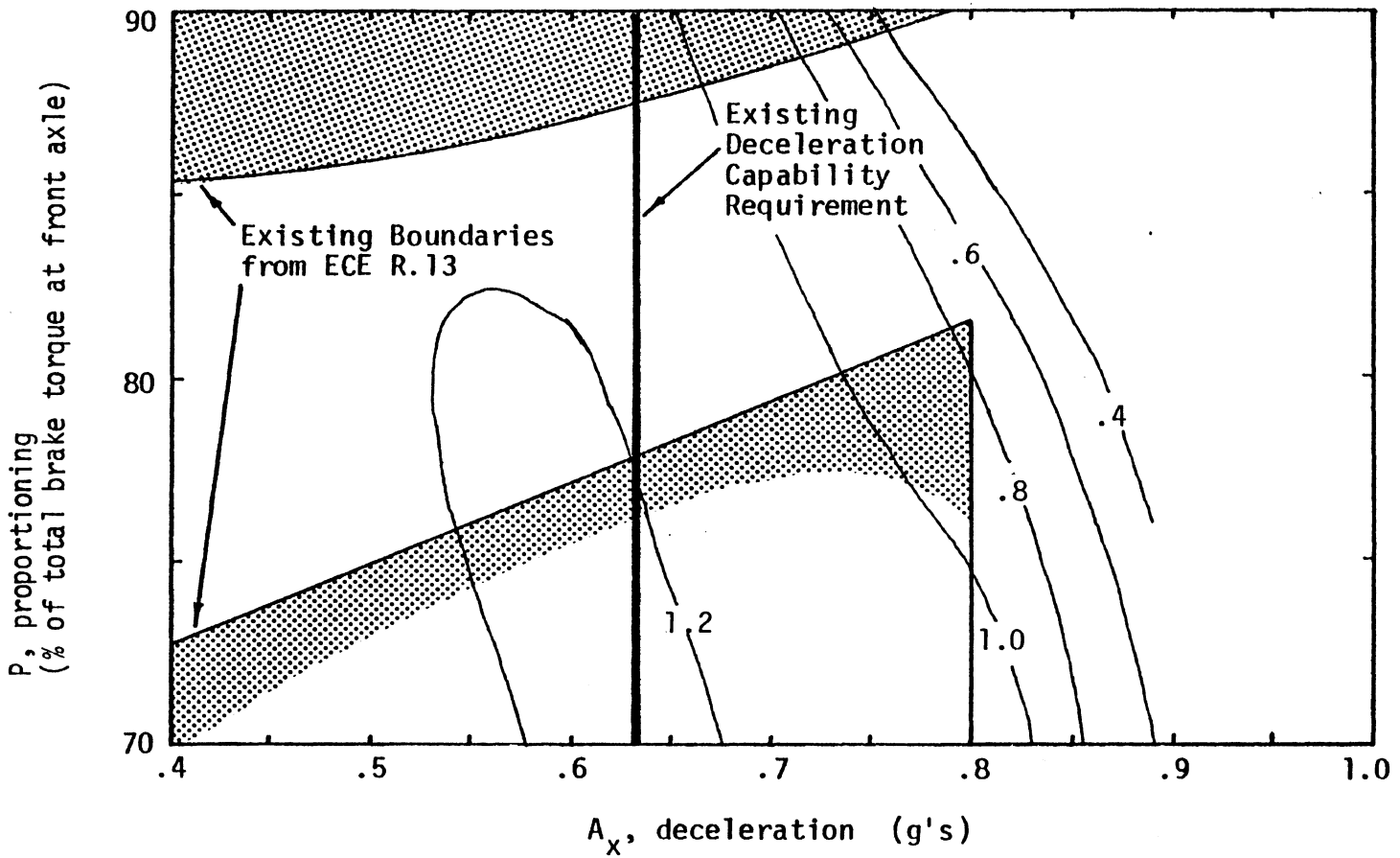

Figure C.7. Lines of constant normalized path curvature for the European car, lightly loaded, braking in a turn with an initial lateral acceleration of .5 g's.

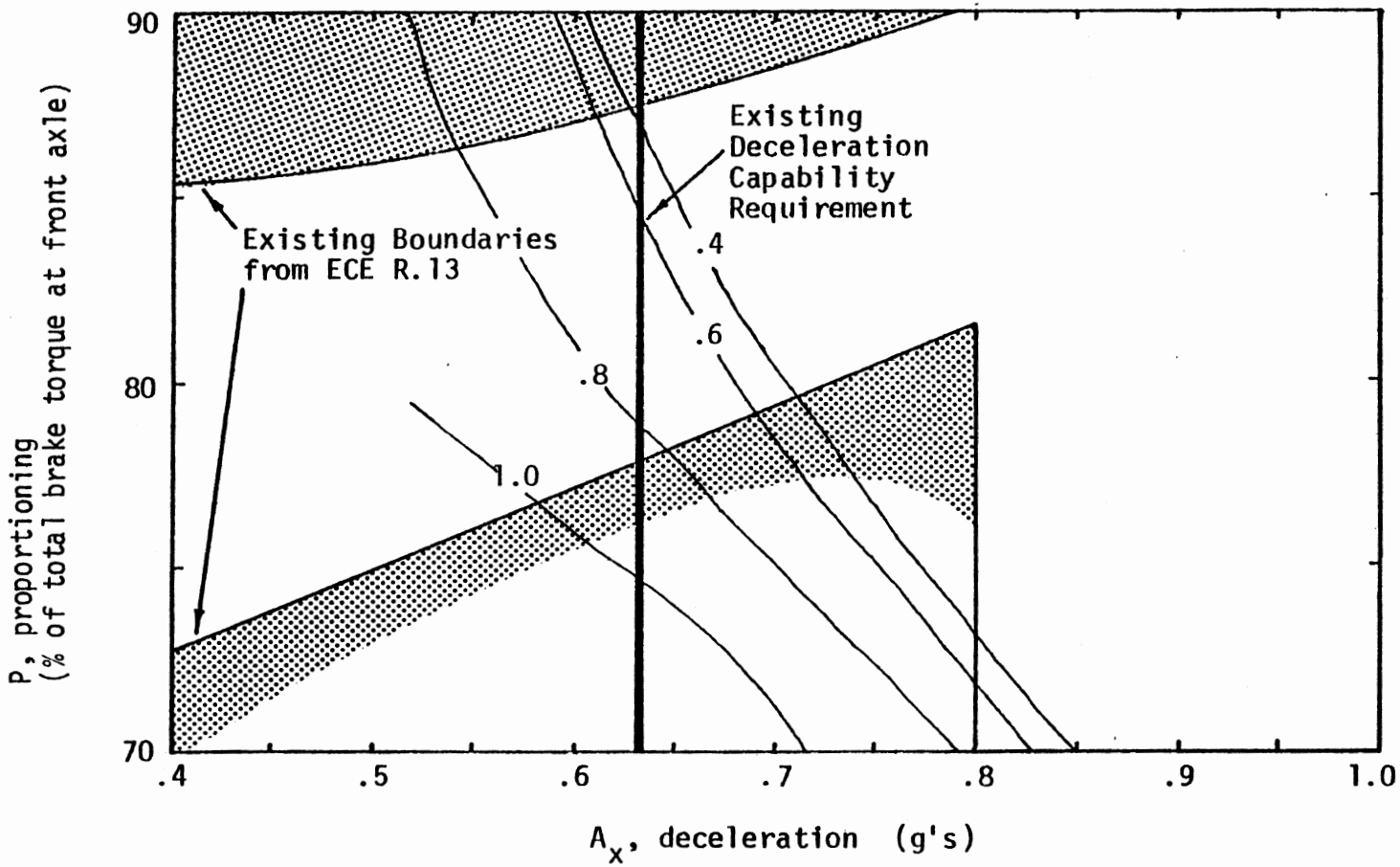

Figure C.8. Lines of constant normalized path curvature for the European car, loaded to the GVWR condition, braking in a turn with an initial lateral acceleration of .5 g's.